1139

1572

R and D CENTER

LABORATORY

TECHNICAL REPORT

NO. 13087

DEVELOPMENT OF SEALS OF HIGH-TEMPERATURE AND HIGH EFFECTIVENESS HEAT EXCHANGERS USED IN ADVANCED TURBINE ENGINES

CONTRACT NUMBER DAA E07-83-C-R122

DECEMBER 1984

by L. Davis
Allison Gas Turbine Division
P. O. Box 420
Indianapolis, IN 46206-0420
Allison Report No. EDR 11999

Approved for Public Release:
Distribution Unlimited

U.S. ARMY TANK-AUTOMOTIVE COMMAND
RESEARCH AND DEVELOPMENT CENTER
Warren, Michigan 48090 48397-5000

REPORT DOCUMENTATION PAGE

1a. REPORT SECURITY CLASSIFICATION: Unclassified	1b. RESTRICTIVE MARKINGS: None
2a. SECURITY CLASSIFICATION AUTHORITY	3. DISTRIBUTION/AVAILABILITY OF REPORT: Approved for Public Release: Distribution Unlimited
2b. DECLASSIFICATION/DOWNGRADING SCHEDULE	
4. PERFORMING ORGANIZATION REPORT NUMBER(S): EDR 11999	5. MONITORING ORGANIZATION REPORT NUMBER(S): 13087
6a. NAME OF PERFORMING ORGANIZATION: Allison Gas Turbine Division; 6b. OFFICE SYMBOL (If applicable): N/A	7a. NAME OF MONITORING ORGANIZATION: US Army Tank-Automotive Command
6c. ADDRESS (City, State and ZIP Code): P.O. Box 894, Indianapolis, IN 46206	7b. ADDRESS (City, State and ZIP Code): Warren, Michigan 48090
8a. NAME OF FUNDING/SPONSORING ORGANIZATION: US Army Tank-Automotive Command; 8b. OFFICE SYMBOL (If applicable): AMSTA-RGRT	9. PROCUREMENT INSTRUMENT IDENTIFICATION NUMBER: N/A
8c. ADDRESS (City, State and ZIP Code): Warren, Michigan 48090	10. SOURCE OF FUNDING NOS.

PROGRAM ELEMENT NO.	PROJECT NO.	TASK NO.	WORK UNIT NO.
	N/A	N/A	N/A

11. TITLE (Include Security Classification): Development of Seals of High Temperature and High Effectiveness (cont)

12. PERSONAL AUTHOR(S): L.C. Davis

13a. TYPE OF REPORT	13b. TIME COVERED	14. DATE OF REPORT (Yr., Mo., Day)	15 PAGE COUNT
Final	FROM 9/22/83 TO 9/22/84	1984 December	114

16. SUPPLEMENTARY NOTATION: Contract No. DAAE07-83-R-R007

17. COSATI CODES		
FIELD	GROUP	SUB. GR.
N/A	N/A	N/A

18. SUBJECT TERMS (Continue on reverse if necessary and identify by block number): High pressure, high temperature regenerator disk and seals, Ceramic seals, extruded matrix

19. ABSTRACT (Continue on reverse if necessary and identify by block number)

This analysis predicts that the selected extruded ceramic regenerator disk and seals can withstand the 9:1 engine compression ratio and the 2000°F inlet gas temperature with acceptable life and leakage while providing a minimum engine plus fuel volume. Some materials development is required for 2000°F operation and for cyclic operation above 2150°F, whereas little new technology would be required at 1800°F operation.

A conceptual layout drawing, materials list, and development plan are included.

20. DISTRIBUTION/AVAILABILITY OF ABSTRACT	21. ABSTRACT SECURITY CLASSIFICATION	
UNCLASSIFIED/UNLIMITED ☒ SAME AS RPT. ☐ DTIC USERS ☐	Unclassified	
22a. NAME OF RESPONSIBLE INDIVIDUAL: Harry Koontz	22b. TELEPHONE NUMBER (Include Area Code): 313-574-5834	22c. OFFICE SYMBOL: AMSTA-RGRT

DD FORM 1473, 83 APR — EDITION OF 1 JAN 73 IS OBSOLETE.

Title (cont): Heat Exchangers Used in Advanced Turbine Engines

PREFACE

Contributors to this report are Bob Pecha, disk stress; Ron Clark, seal stress; Naveen Rau, seal cooling; and Tony Jackman, development plan.

THIS PAGE LEFT BLANK INTENTIONALLY

TABLE OF CONTENTS

THIS PAGE LEFT BLANK INTENTIONALLY

LIST OF ILLUSTRATIONS

LIST OF ILLUSTRATIONS (CONTINUED)

LIST OF ILLUSTRATIONS (CONTINUED)

THIS PAGE LEFT BLANK INTENTIONALLY

1.0. INTRODUCTION AND OBJECTIVES

The objective of this program was to make a preliminary design of a rotating regenerator for a 1500 hp turbine engine operating at about a 9:1 pressure ratio and at 2000°F regenerator inlet temperature. Major concerns addressed in this program were:

- o the ability of an extruded ceramic regenerator disk to withstand the specified high pressure and temperature
- o the ability of regenerator seals to withstand the specified high pressure and temperature with acceptable leakage and wear
- o the selection of a design for minimum engine plus fuel volume

Specific goals were as follows:

- o regenerator system
  2000-hr life
  minimum maintenance
  maximum fuel economy at low power
  compatible materials

- o regenerator seals
  minimum leakage and carryover
  minimum clamping load

- o regenerator disk
  low thermal expansion and conductivity
  high thermal and chemical stability
  high strength
  optimum drive speed

Work on this program was also to result in material recommendations and a development plan.

2.0. REGENERATOR DISK

2.1. Matrix Selection and Disk Size

An extruded triangular ceramic matrix was selected to meet the high pressure requirement because of the inherent high strength of the truss-like structure. Figure 2-1 shows the geometry of this matrix. The matrix would be produced by Corning Glass Works, and it would have the following dimensions:

- o 3.5 mils wall thickness
- o 1500 passages per $in.^2$
- o 1800 ft^2/ft^3 surface area
- o 0.715 open area fraction
- o 0.019 in. hydraulic diameter

Blocks of this matrix would be cemented together to form a disk 32 in. in diameter and 2.5 in. thick. The blocks might be rectangular or, if suitable tooling were perfected, they might be pie-shaped to permit preferential orientation of the triangular matrix for strength. Disk diameter, thickness, and matrix dimensions were selected in Allison's Advanced Integrated Propulsion System (AIPS) program. Figure 2-2 shows that minimum engine plus fuel volume

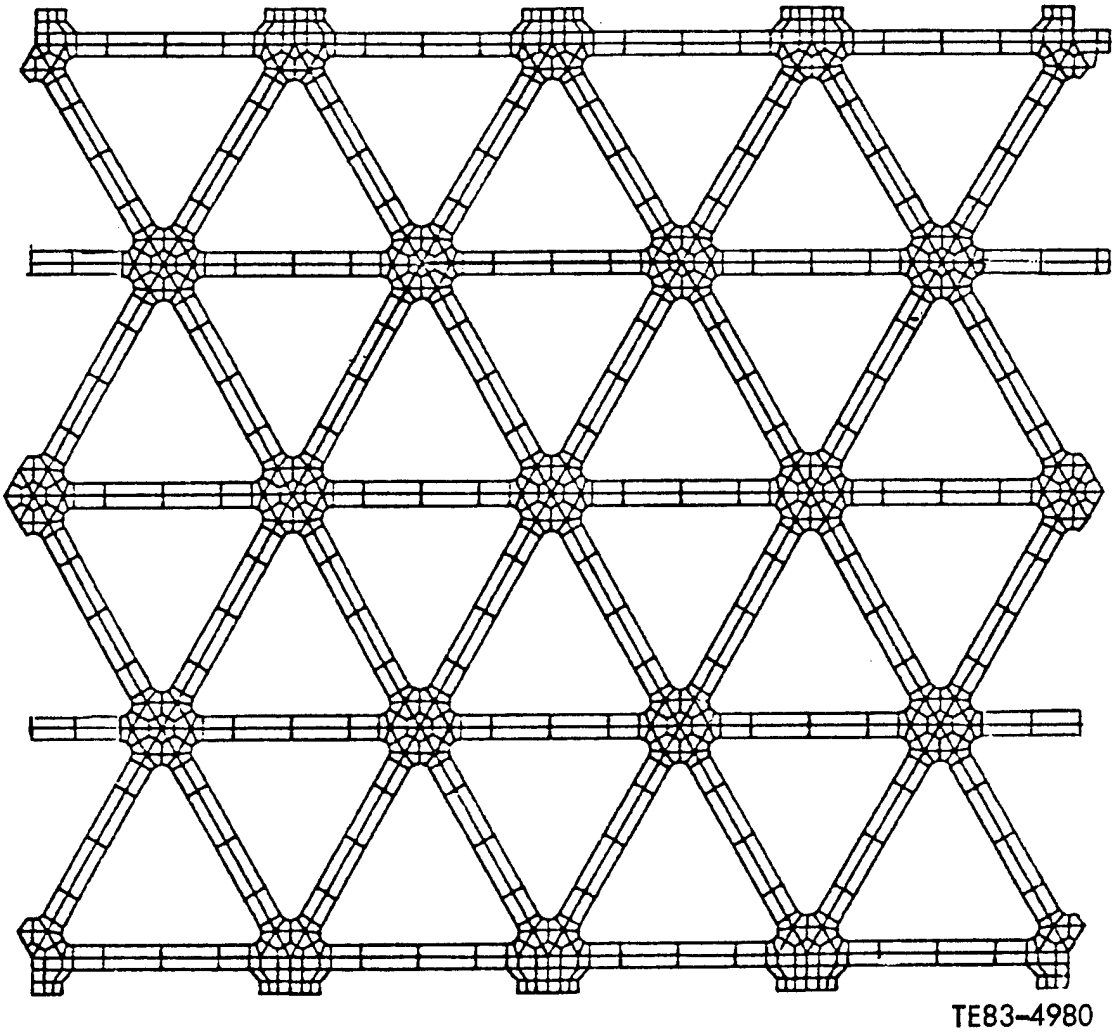

Figure 2-1. Micro Model of 3.5 Mil Extruded Matrix.

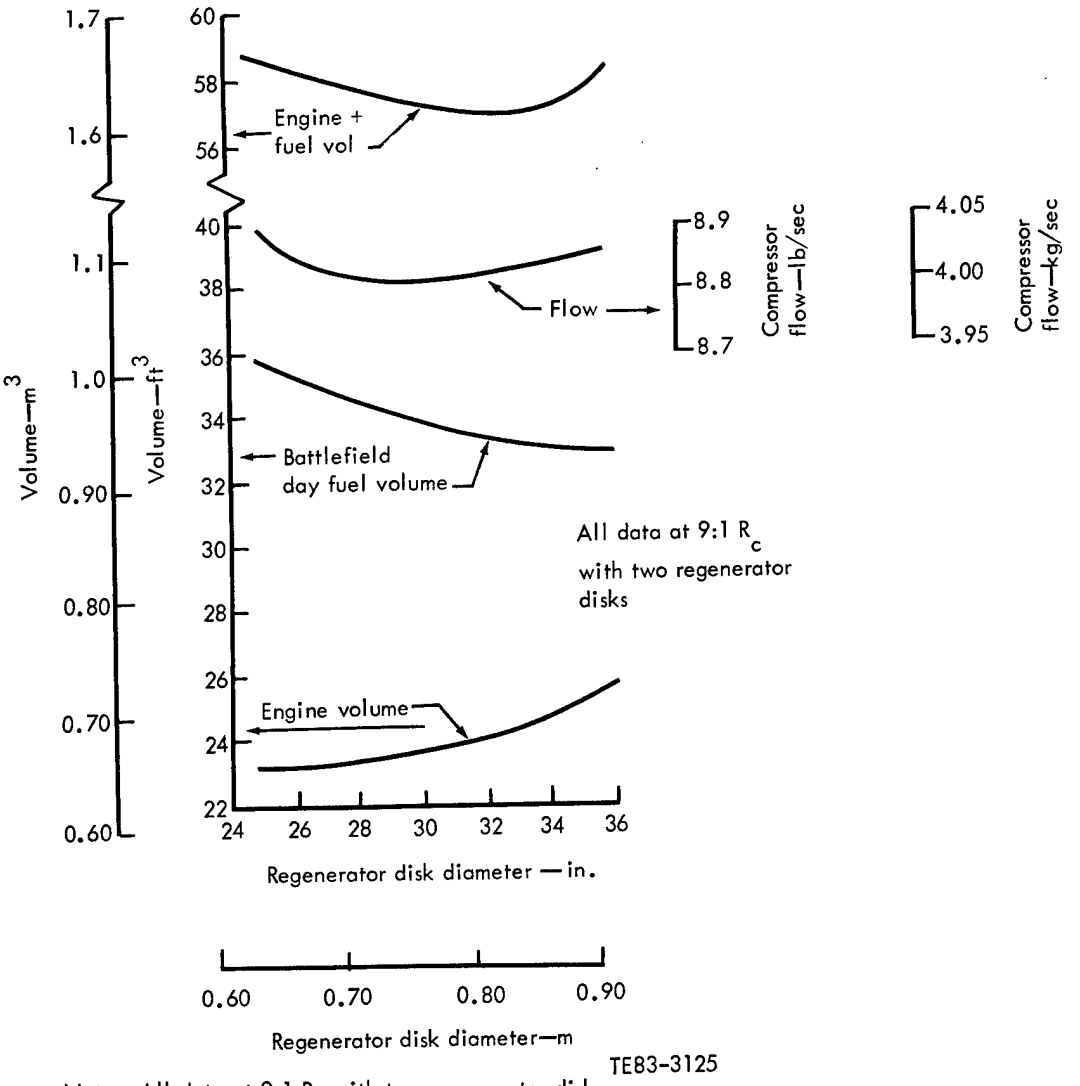

Note: All data at 9:1 R_c with two regenerator disks

Figure 2-2. Relationship of Disk Diameter to Engine Plus Fuel Volume

is achieved with a 32-in. diameter disk. Figure 2-3 shows the effect of varying disk thickness and matrix passage hydraulic diameter. For this evaluation, all matrix dimensions were scaled proportionally and thus maintain a constant open area fraction of 0.715 and produce a changing surface area per unit volume. Although a 3-in. thick disk with approximately a 0.017-in. hydraulic diameter produced minimum specific fuel consumption (SFC), minimum engine plus fuel volume was achieved with the 2-in. thick disk and 0.013-in. hydraulic diameter. The 2-in. thickness with the large 32-in. diameter was judged to present a problem with machining forces, therefore a 2.5-in. thickness was chosen. A hydraulic diameter of 0.019 in. and 3.5 mil wall were chosen for initial development to provide lower risk without significant performance loss.

NGK of Japan has extruded magnesium aluminum silicate (MAS) to these dimensions giving confidence that Corning can extrude their preferred aluminum silicate (AS) to the same dimensions. The selected 3.5 mil matrix results in only 0.6 ft^3 greater engine plus fuel volume than the 2.5 mil matrix and has much less risk..

2.2. Disk Strength

Allison tests show that neither Corning nor NGK regenerator matrix materials now available have adequate strength for the TACOM-AIPS high-pressure and high-temperature requirements. Corning wrapped AS (code 9461) matrix has good basic material strength and fair resistance to thermal cycles, but the wrap process produces a physically weak matrix. NGK extruded MAS matrix is physically strong, but the basic MAS material is unacceptably porous, very weak, and has poor resistance to thermal cycles. New materials without these problems are being developed by both companies.

An analytical prediction of the strength of an extruded AS matrix and the matrix's adequacy to resist AIPS high pressure and high temperature will provide considerable confidence that the desired matrix can be developed. AS code 9461 material would have adequate thermal cyclic life for initial engine development. The procedure used for predicting the strength of an extruded AS matrix was as follows:

(1) Weibull modulus and probability of survival of wrapped AS matrix in radial compression was established from test data.

(2) Weibull characteristic strength of basic AS material was determined using a micro model of wrapped matrix.

(3) Compressive stress in an extruded AS matrix for the same probability of failure was determined using a micro model of the desired extruded matrix. Effective elastic moduli for stress analysis of a complete regenerator disk were also determined from the micro model.

(4) Stress in the complete disk of extruded AS matrix was then determined with the appropriate high-pressure, high-temperature, and drive and seal loads for comparison with the previously established limits. The previously calculated effective moduli are used treating the disk as a continuous material.

Median strength and elastic modulus predicted by a micro model for an extruded 3.5 mil wall AS matrix are listed in Table 2-1. The micro model is shown in Figure 2-1. Intrinsic AS material strength was obtained from a micro model for

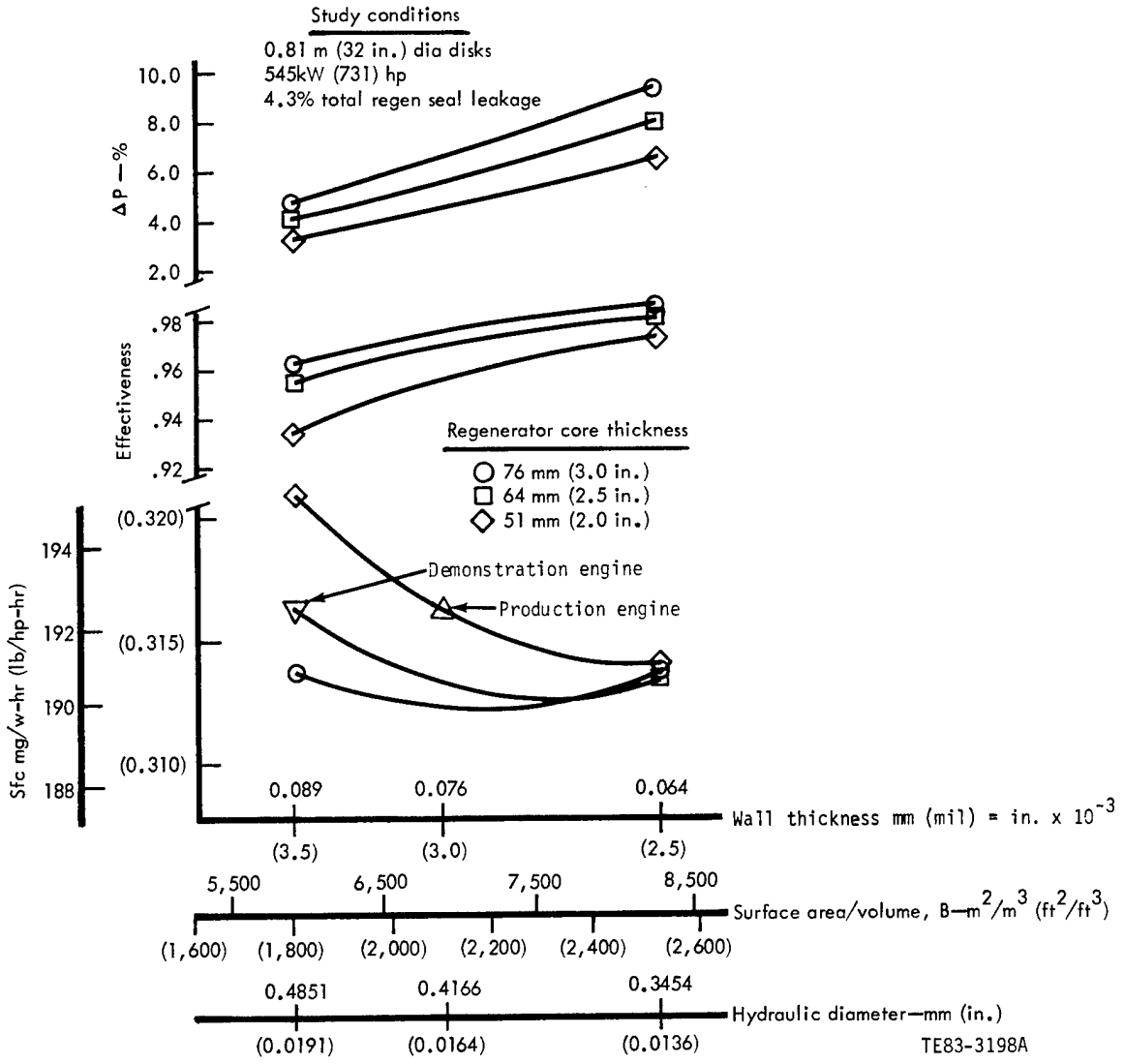

Figure 2-3. Effect of Varying Disk Thickness and Matrix Passage Hydraulic Diameter

the wrapped AS matrix, which was used in the Ceramic Applications in Turbine Engines (CATE) program and is shown in Figure 2-4. Table 2-1 compares a measured radial compressive strength of 86.6 lb/in.^{2} for 2.6 mil wall wrapped AS material to a calculated strength of 1224 lb/in.^{2} for the 3.5 mil wall extruded AS, and shows an improvement factor of 14 due to the perfect truss-like structure and thicker wall. The radial direction is defined as being perpendicular to one of three sets of mutually parallel walls while the tangential direction is parallel to one such set. The predicted 1224 lb/in.^{2} radial compressive strength of extruded AS seems extraordinarily high; however, NGK 5.1 mil wall MAS, despite being weakened by very high porosity, still measures 200 lb/in.^{2}, making the prediction more plausible for a dense material. The wrapped matrix has been used successfully at 4:1 pressure ratio, hence the extruded matrix likely will prove adequate at 9:1. Weibull probability analysis was applied to the test data on the wrapped matrix and was included in the predicted strength for the extruded matrix. Moduli calculated by micro model for a 3.5 mil wrapped matrix are also shown in Table 2-1 for comparison.

2.3. Disk Stress

The properties determined from the micro model and listed in Table 2-1 are termed bulk properties and will be used in the disk model shown in Figure 2-5 to determine bulk stresses so that the detailed matrix need not be modeled for an entire disk that would be prohibitive.

Pressures, mechanical loads, and temperatures for the 100% speed and full power were established and applied to the nodes and elements that make up the finite element computer model. Seal friction loads measured on the industrial gas turbine (IGT) 404 were modified for the difference in pressure and disk size. Figure 2-6 shows a plot of tangential force in pounds per inch of seal versus angular position for the rim seal and for a typical radial location on the crossarm seal on the hot side of the disk. The forces on the cold side are much smaller since the coefficient of friction of the seals on the cold side is 0.05 as compared with 0.40 on the hot side. The differential pressures acting on the disk are shown in Figure 2-7 for the radial and tangential directions and in Figure 2-8 for the axial direction. The pressure drop at the rim seal is applied to the model in two steps to simulate the pressure distribution in the seal along its radial width. The force due to the pressure drop across the crossarm seal is, in the model, assumed to be distributed over 10 deg of circumferential distance.

At 100% speed, full power, the regenerator inlet temperature is 662°F and the exhaust gas temperature is 1450°F. The regenerator temperature varies with the angular position as it is exposed alternately to hot exhaust gas and cold inlet air. A good approximation of the effective thermal gradient as it affects stress is a circumferentially averaged thermal distribution. This is shown in Figure 2-9. In the stress analysis, the temperatures that have been calculated with their circumferential variation will be applied.

Two operating conditions were considered in the analysis: 100% speed, full power, with a 9:1 pressure ratio, a 1450°F gas temperature and a 662°F air temperature; and 51% speed with a 2:1 pressure ratio, a 2000°F gas temperature and a 239°F air temperature. The 100% speed high pressure case was more

Table 2-1. Comparison of Mechanical Properties of Extruded and Wrapped Aluminum Silicate (AS) Matrices

Median strength--lb/in.^{2}

	TACOM extruded 3.5 mil	CATE wrapped 2.6 mil	Strength ratio, TACOM/CATE
Radial compressive	1224	86.6 (test data)	14.1
Tangential compressive	2065	1104 (calculated)	1.9
Shear (T_{rt})	327	148 (calculated)	2.2

Elastic modulus--lb/in. x 10^6

	Extruded 3.5 mil	Wrapped 3.5 mil
Radial compressive	0.228	0.0282
Tangential compressive	0.273	0.306
Axial compressive	0.546	0.5778
Shear (G_{rt})	0.0782	0.0443

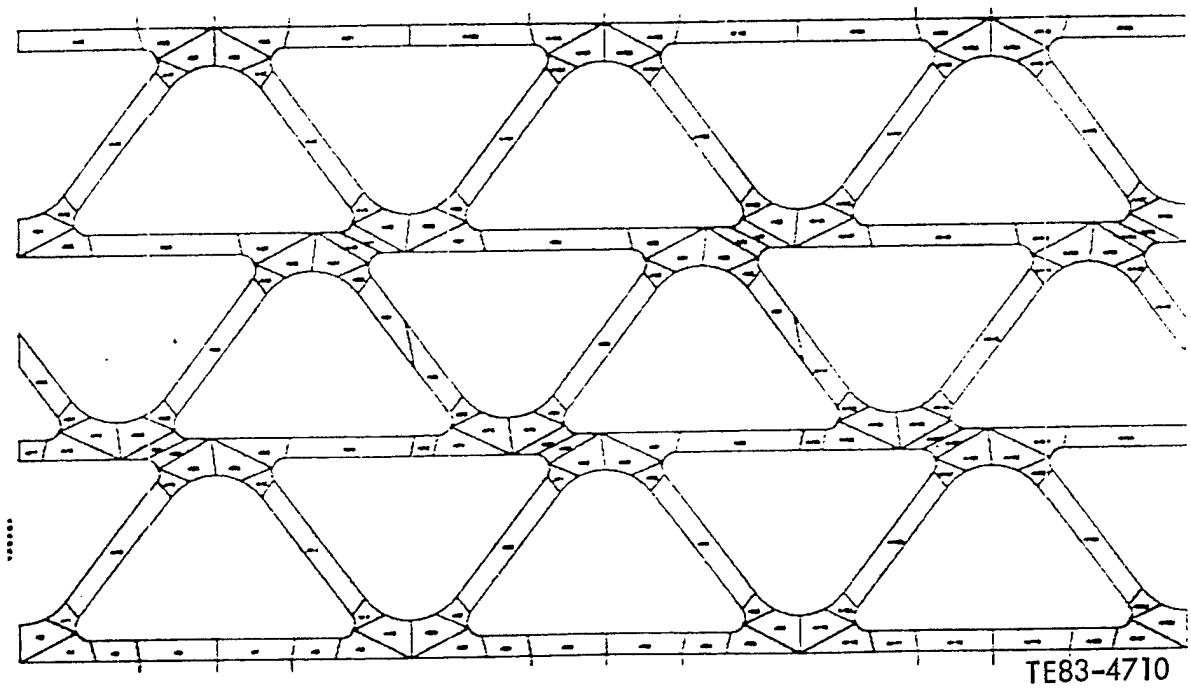

Figure 2-4. Micro Model for Wrapped AS Matrix.

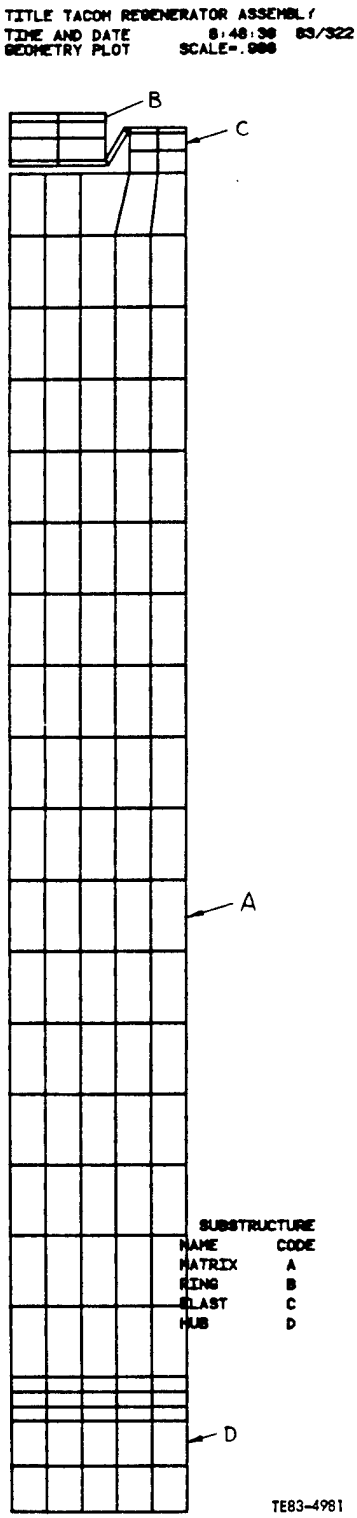

Figure 2-5. Finite Element Model of Proposed Regenerator Disk

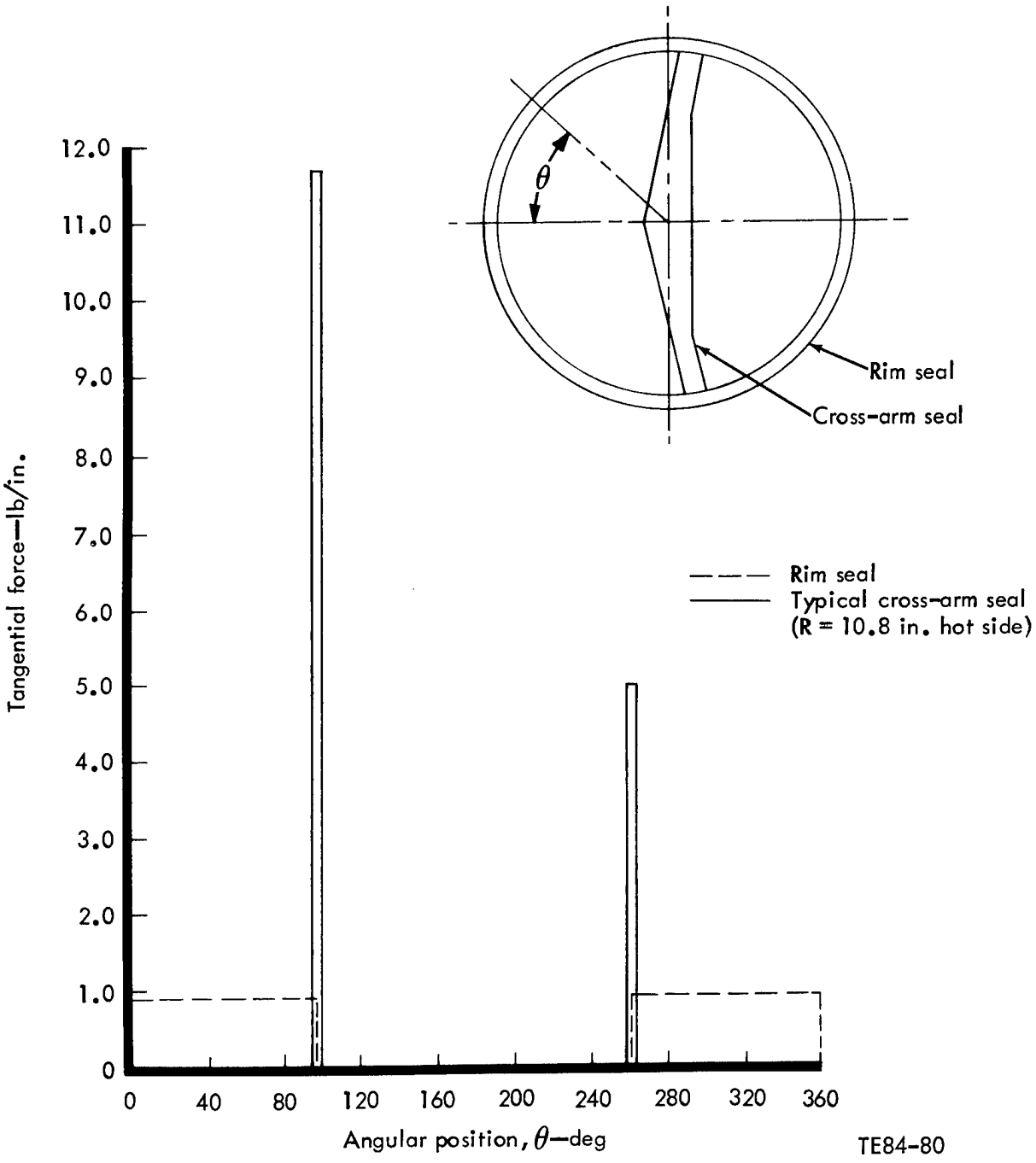

Figure 2-6. Tangential Seal Friction Force Versus Angular Position

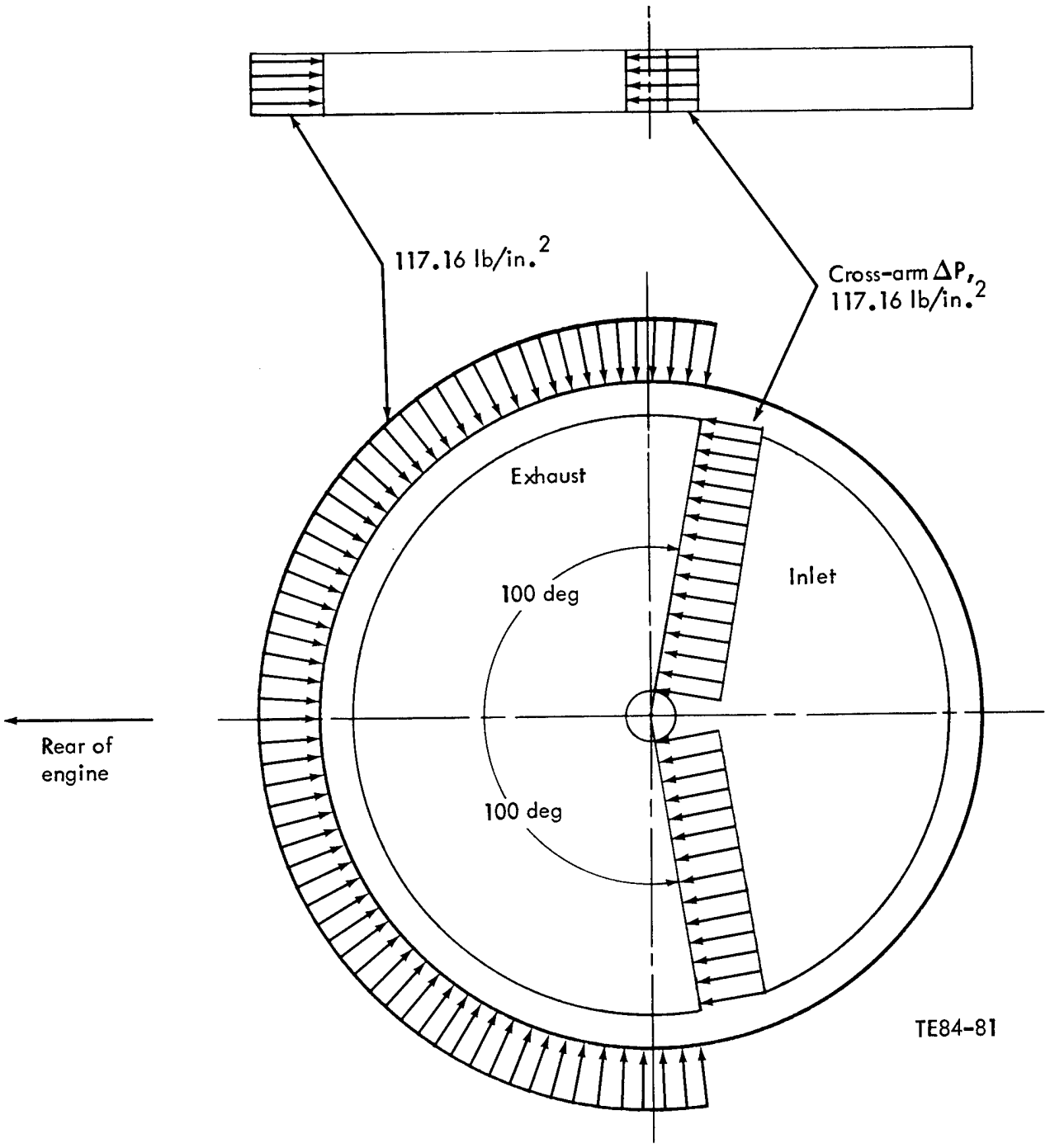

Figure 2-7. Radial and Tangential Differential Pressure on Regenerator

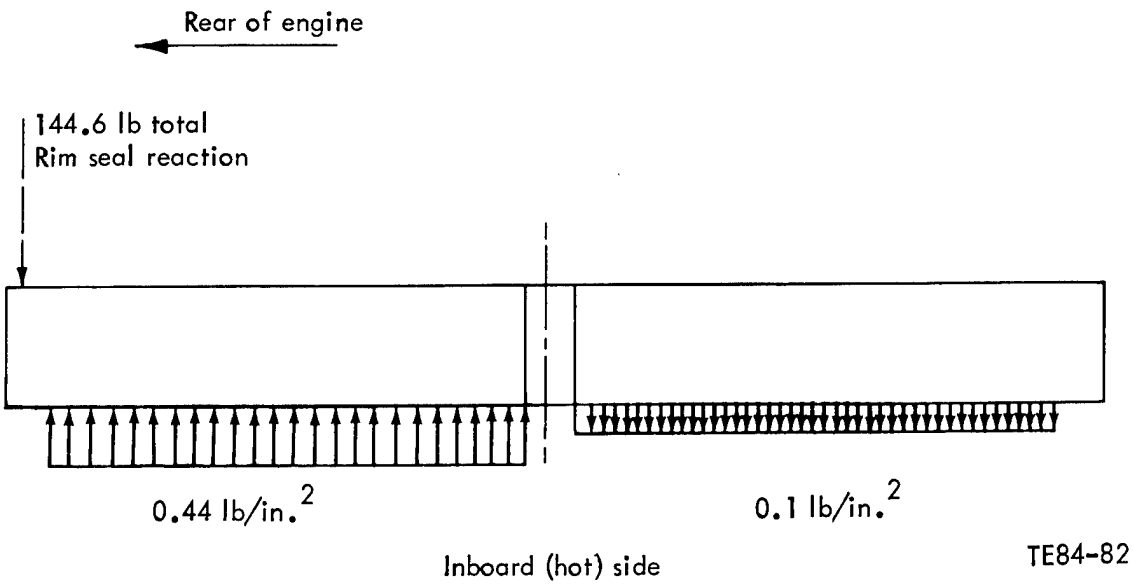

Figure 2-8. Axial Differential Pressure on Left-Hand Regenerator Viewed from Above.

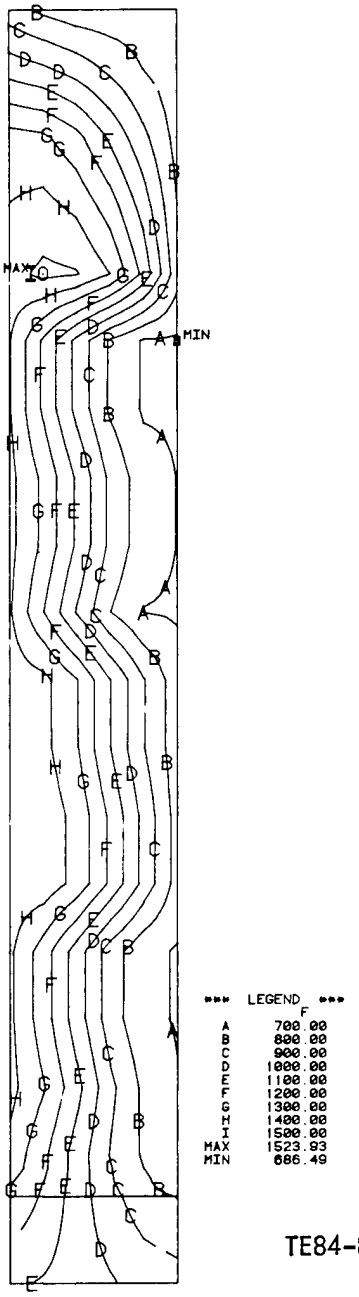

Figure 2-9. Circumferentially Averaged Temperatures for 100% Speed at Full Power

severe. It should be remembered that these are the bulk stresses of the assumed continuous material of the model and not the detailed stresses in the actual matrix, which are much higher.

Since the 32-in. diameter disk cannot be extruded in one piece, it will be made of a number of extruded blocks bonded together. This analysis assumed that the blocks are pie-shaped, having a small angle on their sides and bonded together in a manner that approaches an axisymmetric disk; that is, one set of parallel walls were considered normal to the disk radius in the middle of each segment.

Peak stresses for all loads acting on the disk at 100% speed, full power, are shown in Table 2-2. They are compared with those of the IGT 404 (CATE) regenerator.

The variation of the peak stresses with circumferential position is shown in Figure 2-10. The peak radial stress, 197 lb/in.^{2} compression at the hub, occurs in a radial plane 10 deg counterclockwise of the rearward horizontal centerline (θ = 350 deg). Ninety-five percent of the cause is pressure. The stress distribution in this plane is shown in Figure 2-11. The peak tangential stress and shear stress are 80% and 62% due to pressure, respectively, and occur in radial planes at θ = 60 deg and θ = 30 deg, respectively. The stress distributions are shown in Figures 2-12 and 2-13.

The ratio of extruded to wrapped matrix strength is 14.1 for radial, 1.9 for tangential, and 2.2 for shear. Since the increase in strength is greater than the increase in stress, as shown in the preceding table, the TACOM disk can be expected to be more durable than the IGT 404 (CATE) regenerator disk, which was satisfactory. We believe that actual strength/stress ratios will be even more favorable than the analysis predicts because no allowance has been made for known, prevalent, thin and distorted walls in the wrapped CATE matrix, which tends to reduce the predicted inherent material strength.

The analysis predicts that the selected extruded disk would have more than adequate strength to survive all imposed conditions. Dr. Robert Katz, Chief, Ceramics Research Division, Army Materials and Mechanics Research Center, was advised of these conclusions during his visit of 22 March 1984. Allison report TDR AD0400-034 covers details of the disk stress analysis.

2.4. Disk Cyclic Thermal Resistance

Although Corning AS ceramic has been shown to be adequate for 2000°F steady-state operation, we expect it would have limited life for cyclic operation. Allison has developed a laboratory test that simulates the temperature spikes, above steady-state levels, that occur during engine accelerations. Cyclic exposure causes loss in hot face strength depending on the peak temperature and number of cycles. Figure 2-14 shows how Corning AS loses strength with cyclic exposure. Momentary inlet gas temperature peaks of 2150°F could be tolerated with acceptable life. Normally, peaks of 2300°F would be expected with steady-state operation at 2000°F, which would limit disk life to 1000 cycles or about 50 hr for a typical duty cycle. An 1800°F steady-state limit would hold peaks to 2100°F and result in adequate life. Another option would be to schedule the fuel control for a slower initial acceleration rate during initial development resulting in about a six-second acceleration instead of a four-second one. Within the next two years, suppliers expect to develop material that will tolerate 2200°F steady-state and 2300°F peaks.

Table 2-2. Peak Stresses, 100% Speed, Full Power

	Radial stress-- $lb/in.^2$	Tangential stress-- $lb/in.^2$	Shear stress-- $lb/in.^2$
TACOM (extruded)	197	187	52
CATE (wrapped)	48	170	32
Stress ratio (TACOM/CATE)	4.1	1.1	1.6
Strength ratio (TACOM/CATE)	14.1	1.9	2.2

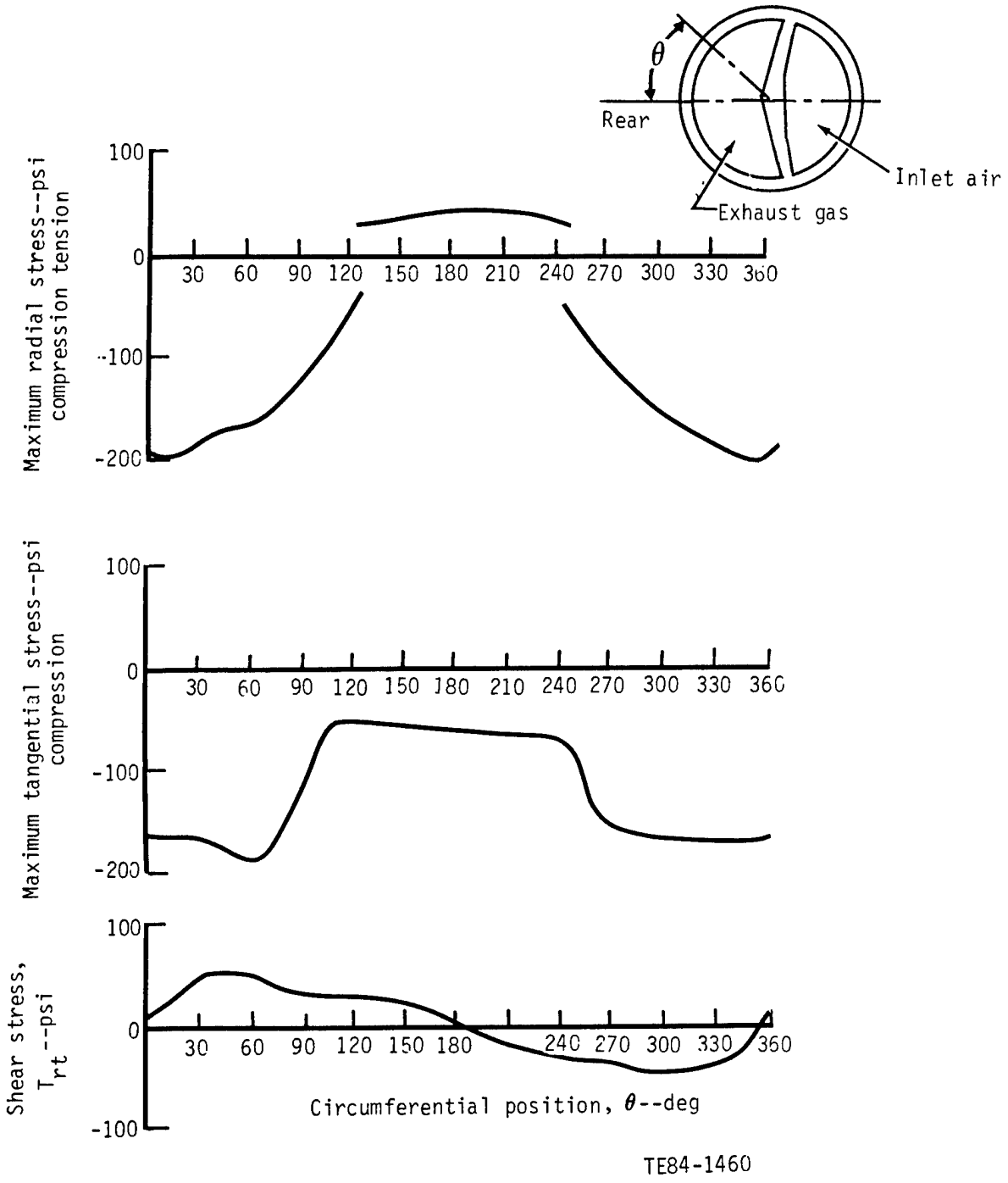

Figure 2-10. Peak Stress Due to All Loads Versus Circumferential Position at 100% Speed, Full Power

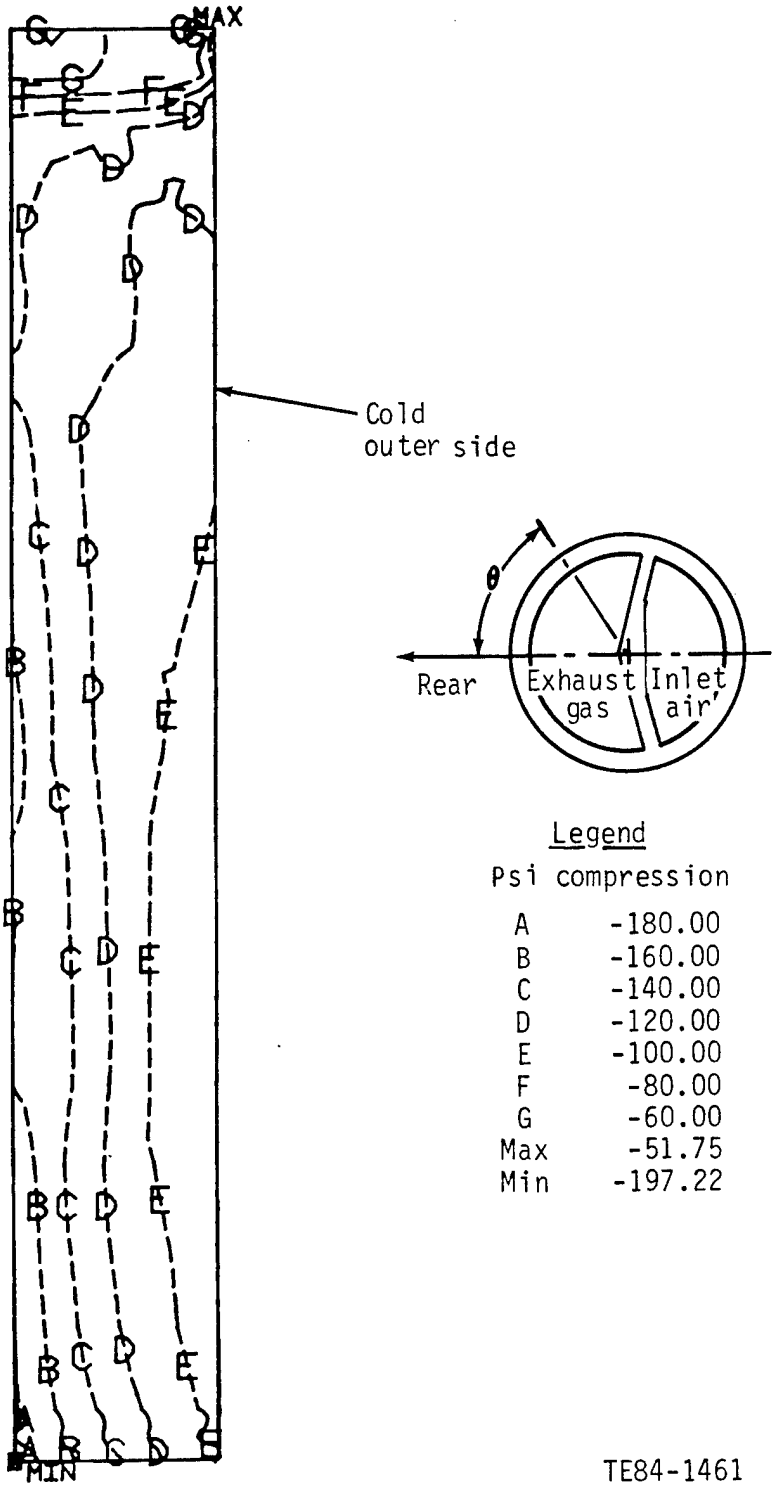

Figure 2-11. Radial Stress Due to all Loads at 100% Speed, Full Power: θ = 350 Deg (Plane of Maximum Stress)

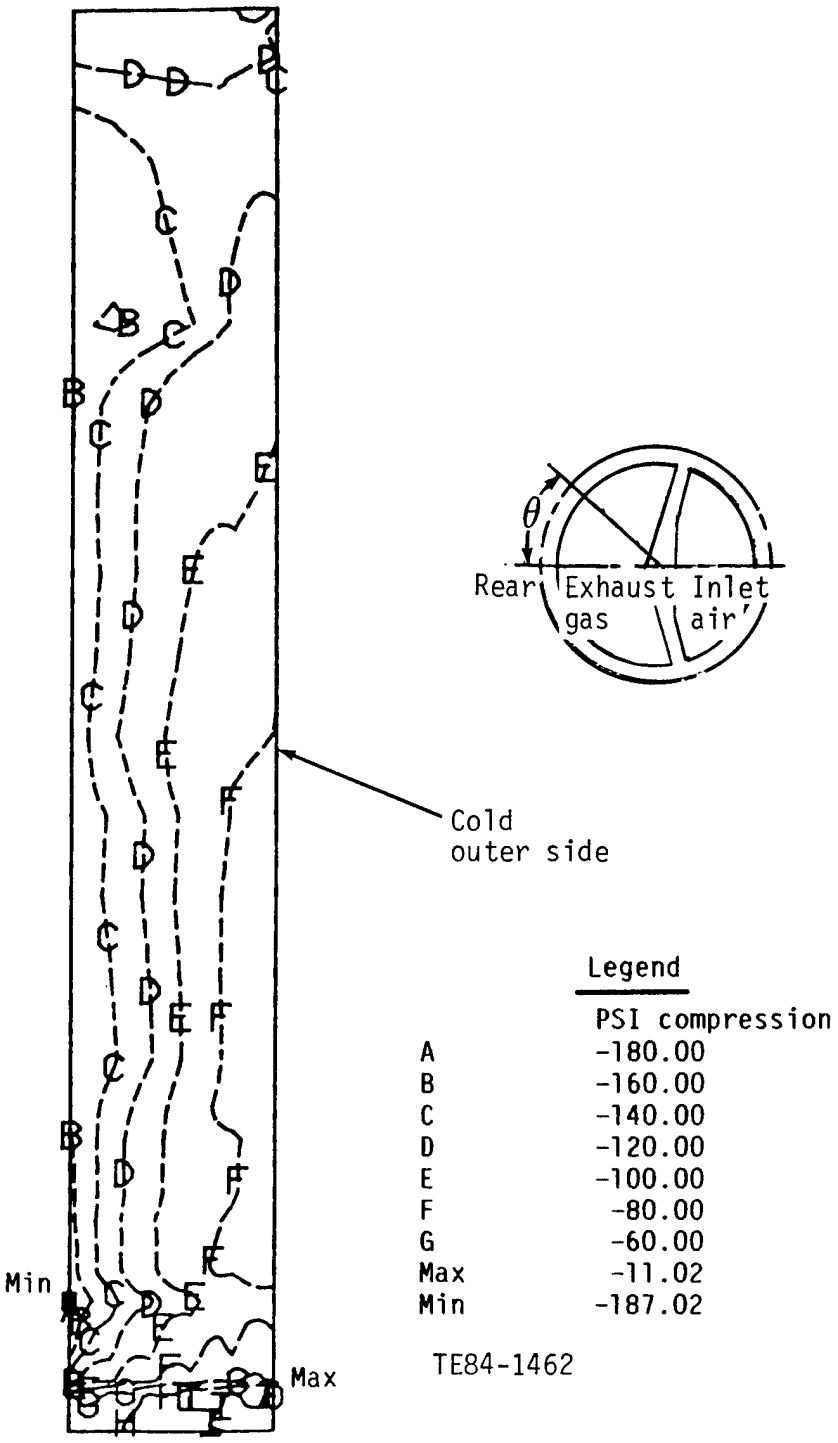

Figure 2-12. Tangential Stress Due to All Loads at 100% Speed, Full Power: θ = 60 Deg (Plane of Maximum Stress)

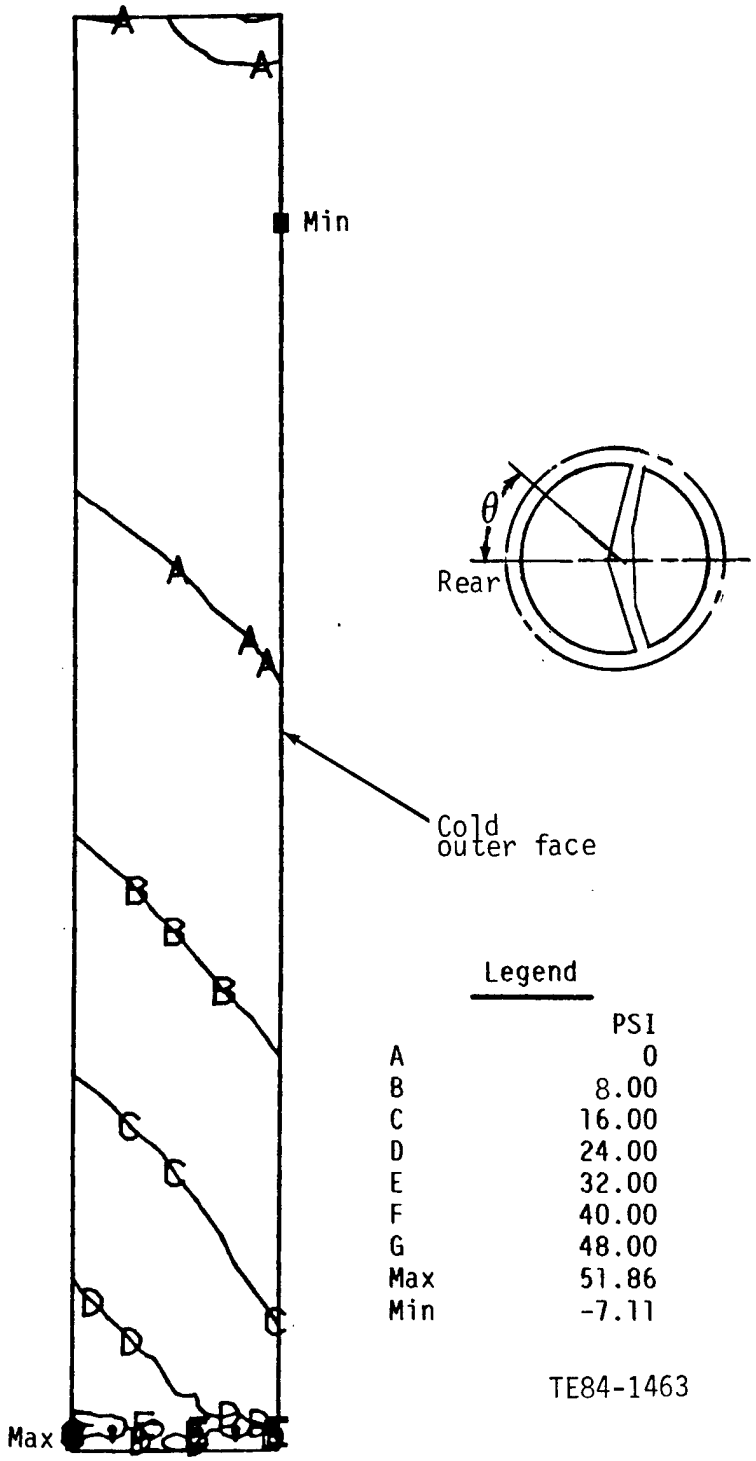

Figure 2-13. Shear Stress T_{rt} Due to All Loads at 100% Speed, Full Power: θ = 30 Deg (Plane of Maximum Stress)

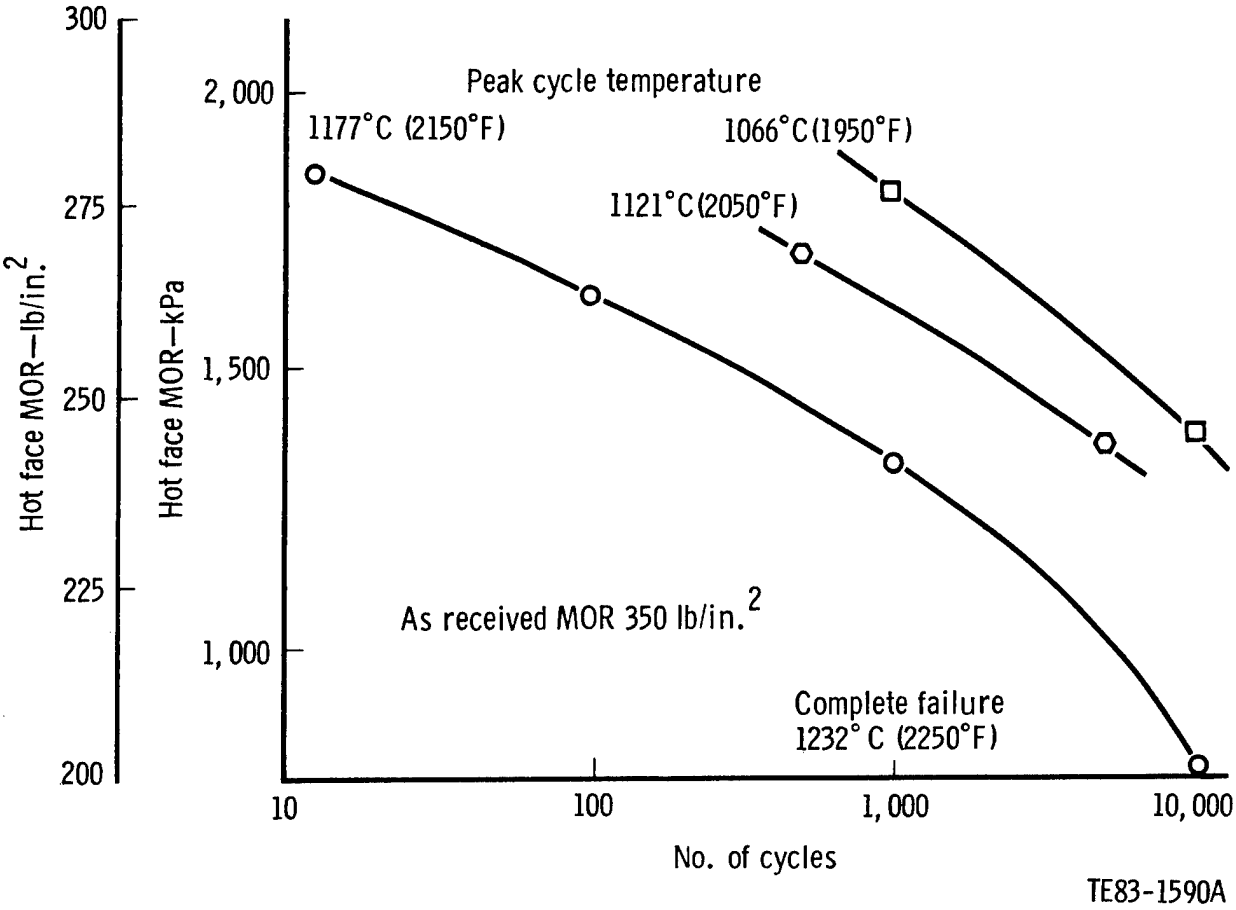

Figure 2-14. Loss of Strength in Corning AS with Cyclic Exposure

2.5. Disk Shock and Vibration

In response to concern raised at the oral review of Allison's AIPS Phase I work for the regenerator disk's ability to withstand the tank vibration and shock environment, Allison has successfully run tests at the specified conditions. Testing was not charged to this program but the results are pertinent.

The regenerator disk tested was Corning AS code 9460 spiral wrap with 4.3 mil wall thickness. The disk and drive gear assembly was supported at the hub with a graphite bearing on an Allison 404-4 regenerator cover bolted to the engine block with regenerator seals installed but without other engine components. The resulting total shaker weight was about 700 lb. The regenerator seals were not pressurized because this was believed to be a more severe case due to less seal restraint and damping. Seals would be unpressurized if the tank were towed. The engine block was mounted on its gear case attaching flange on the shaker for firm support. This resulted in the axis of turbine shafting (not installed) being vertical instead of horizontal. Excitation was also vertical. Specified vibration inputs were controlled at the regenerator mount location on the regenerator cover to ensure that the disk itself was driven at the specified input. Shocks and vibration imposed were according to AIPS Phase II Scope of Work Attachment I Item 2vv, "Shock and Vibration at Hull/Component Mounting Interface."

Disk response was monitored at four locations, one in line with excitation on the disk outer diameter (o.d.), one in line with excitation on the gear o.d., and two normal to excitation on the disk face. Several vibration sweeps were made at full specified level to record disk response and resonances. Dwells of 20 min each were made at the two lowest frequency and most prominent disk o.d. resonances and the two lowest and most prominent gear o.d. resonances. The disk and gear were highly responsive. Peak disk acceleration was 10 g at 65 Hz and peak gear acceleration was 19 g at 225 Hz with 5 g input. The 30, 55, and 50 g shocks were imposed, but not the 500 g due to shaker limitations. The disk showed no visual damage, no accumulation of released debris, nor any change in response indicative of failure. Since the first and second resonances of this disk are at 65 and 140 Hz, the response to the 500 g shock, which is equivalent to 1000 Hz, would be expected to be minimal and not to result in damage. Extruded disks intended for the AIPS application are expected to be appreciably stronger than this disk due to their precise truss-like structure.

Allison made extensive vibration measurements in the MBT-70 tank under all road conditions in connection with the automatic gun loader development. These measurements showed that only lighter brackets and components attached to the hull experienced a 5 g level. The hull itself is too massive to respond at that level. Further, the 5 g level is only achieved at full speed on a hard road due to track slap. Based on this experience, the specified 5 g is thought to be more severe than the regenerator disks in their rigid transmission-engine structure would actually experience. The proposed stronger extruded matrix should be even more resistant to shock damage.

2.6. Disk Drive Speed

Figures 2-15 and 2-16 show the effect of regenerator drive speed on engine SFC for the AIPS Phase I and Phase II engines. The effect at two battlefield day (BFD) points and maximum power is also shown. Triangular symbols show operating points when the regenerator is directly geared to the gasifier rotor with

maximum rpm set at 18. Allison proposed a hydraulic motor drive primarily to eliminate complex and precisely aligned bevel and worm gearing. The motors offer the additional advantage of speed control independent of engine speed. It is evident from the curves that a constant speed of 12 to 15 rpm would provide near minimum SFC without the need of speed scheduling. The lower constant speed of 12 rpm would be selected to minimize seal wear.

3.0. REGENERATOR SEALS

3.1. Hot Side Seal

We began this study with the assumption that our cooled metal hot seal, which was used for the NASA/DOE/CATE program and showed promising test results at 1800°F, could be improved to suffice at 2000°F. Improved cooling was to be obtained by employing finned surfaces. Not anticipated were the higher cooling flow pressure drops that were required and that resulted in intolerable seal wearface loads forcing us to select a less proven ceramic seal concept. During preparation of this report, a new cooled metal seal concept evolved that we believe could overcome these problems. Analysis would be required to prove that concept. The stress analysis performed in this study would pertain to such a new design. Although Allison feels more confident of metal seals based on past experience, it is nevertheless felt that the ceramic concept proposed in this study is viable. Success with a ceramic bulkhead, which supports cycle pressure ratio in the automotive gas turbine (AGT) 100 engine, lends support to the ceramic seal concept.

3.1.1. Cooled Metal Seal.

3.1.1.1. Seal stress and buckling. A scaled-up version of the three-piece cooled hot-side seal developed for the DOE/NASA Ceramic Applications in Turbine Engines (CATE) program, contract DEN 3-17, was used for stress analysis.

The geometry of the CATE seal model was modified so that the seal outside diameter (o.d.) is now 32 in., and the platform rim width is unchanged at 1.05 in. The crossarm has been scaled up by 1.298 in the x direction and 1.251 in the y direction.

The model temperatures for the CATE 70% power transfer were scaled up by 1.11 for the TACOM AIPS 120 hp conditions to reflect the increase to 2000°F gas inlet temperature. The platform ring temperatures for the 560 hp and 1500 hp conditions were calculated as a function of the 120 hp temperatures and the radius. The initial crossarm temperatures are a function of radius and were selected based on test data and stress analysis in the CATE program. These temperatures were also used as the initial goal for seal cooling studies. Plots of the initial temperature gradients are included in Figures 3-1 through 3-7.

The model-applied nodal pressure loads are based on the pressure differences specified by the performance group for the AIPS PD335-B1 engine.

The boundary conditions and substructure constraint equations in the CATE model were totally redefined to reflect the proposed TACOM three-piece seal structure.

The seal finite element model was also modified. Eight noded meanline shell quadralateral elements were used rather than the triangular plate elements.

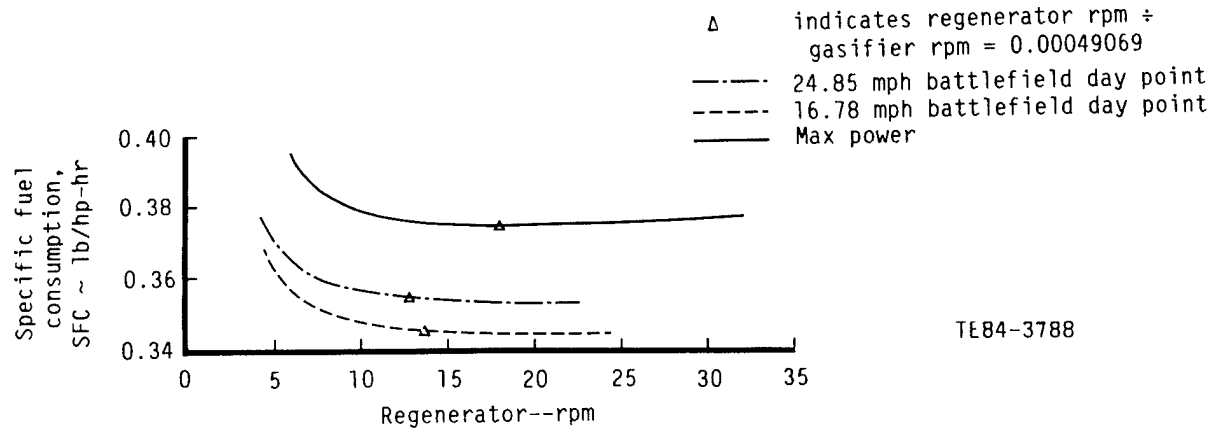

Figure 2-15. Regenerator Effectiveness Versus RPM--Phase I Engine

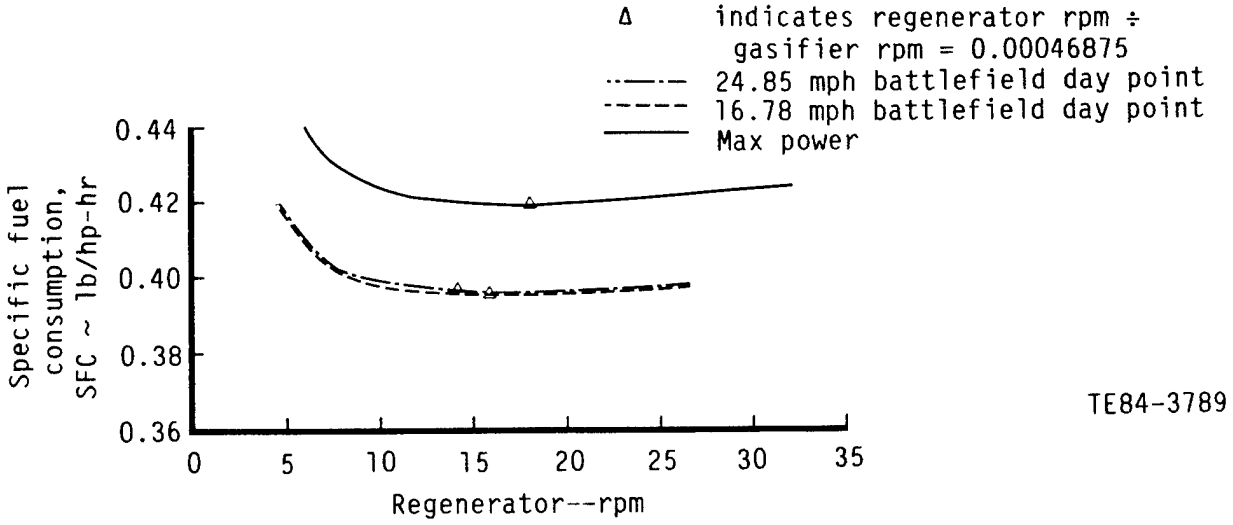

Figure 2-16. Regenerator Effectiveness Versus RPM--Phase II Engine

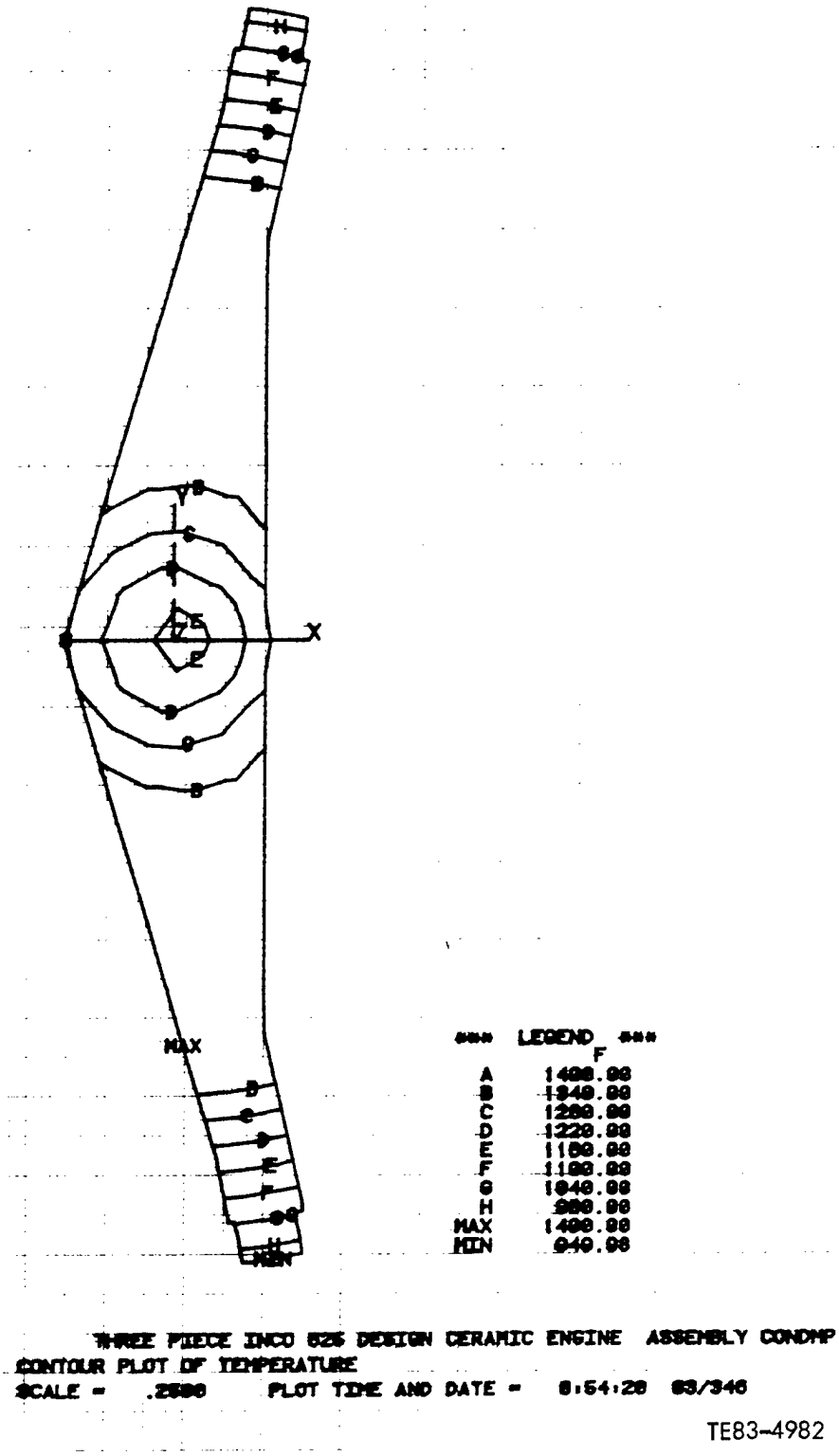

TE83-4982

Figure 3-1. Crossarm Temperature--120 HP Condition

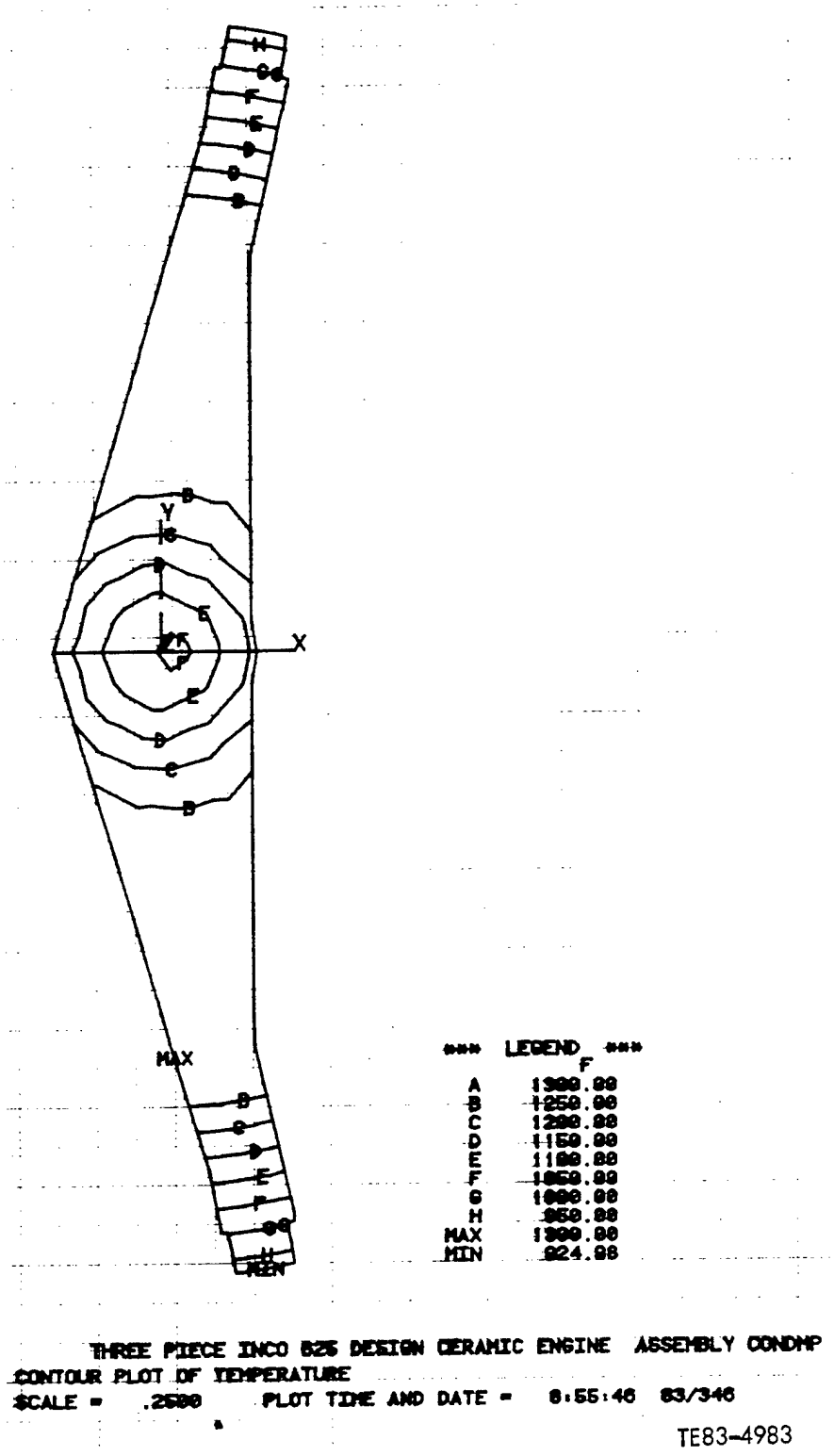

Figure 3-2. Crossarm Temperature--560 HP Condition

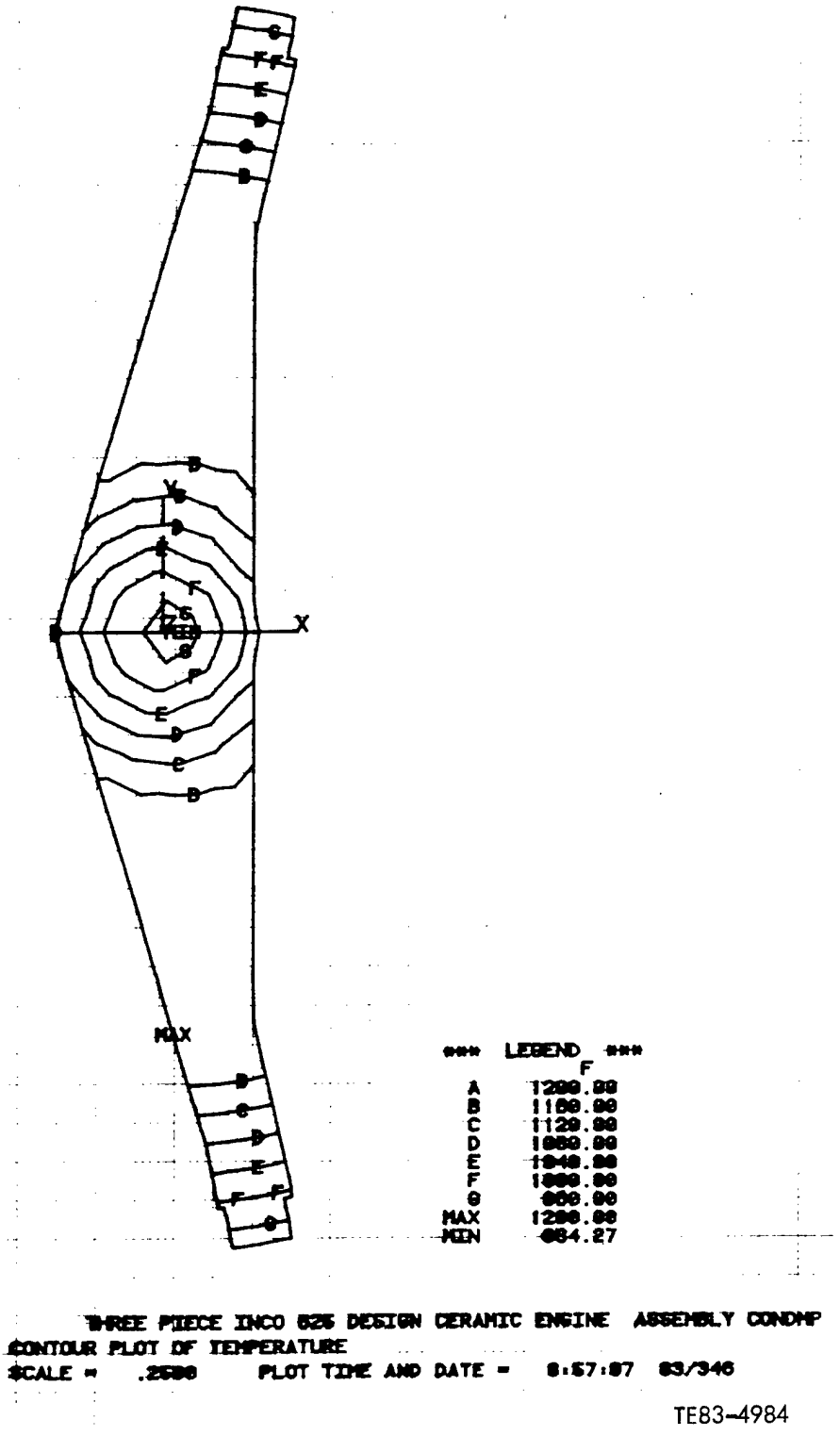

Figure 3-3. Crossarm Temperature--1500 HP Condition

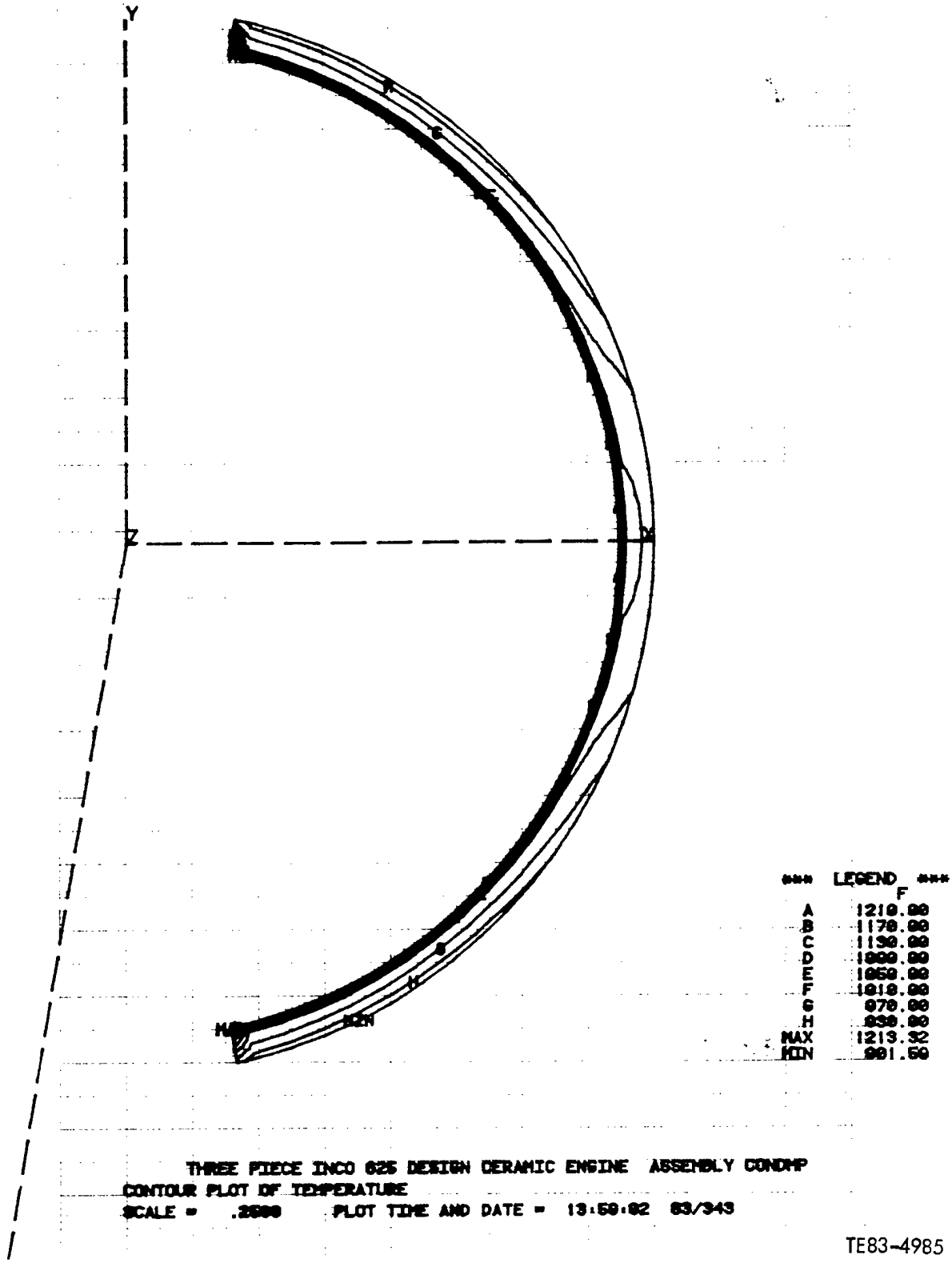

Figure 3-4. Inlet Ring Temperature--1500 HP Condition

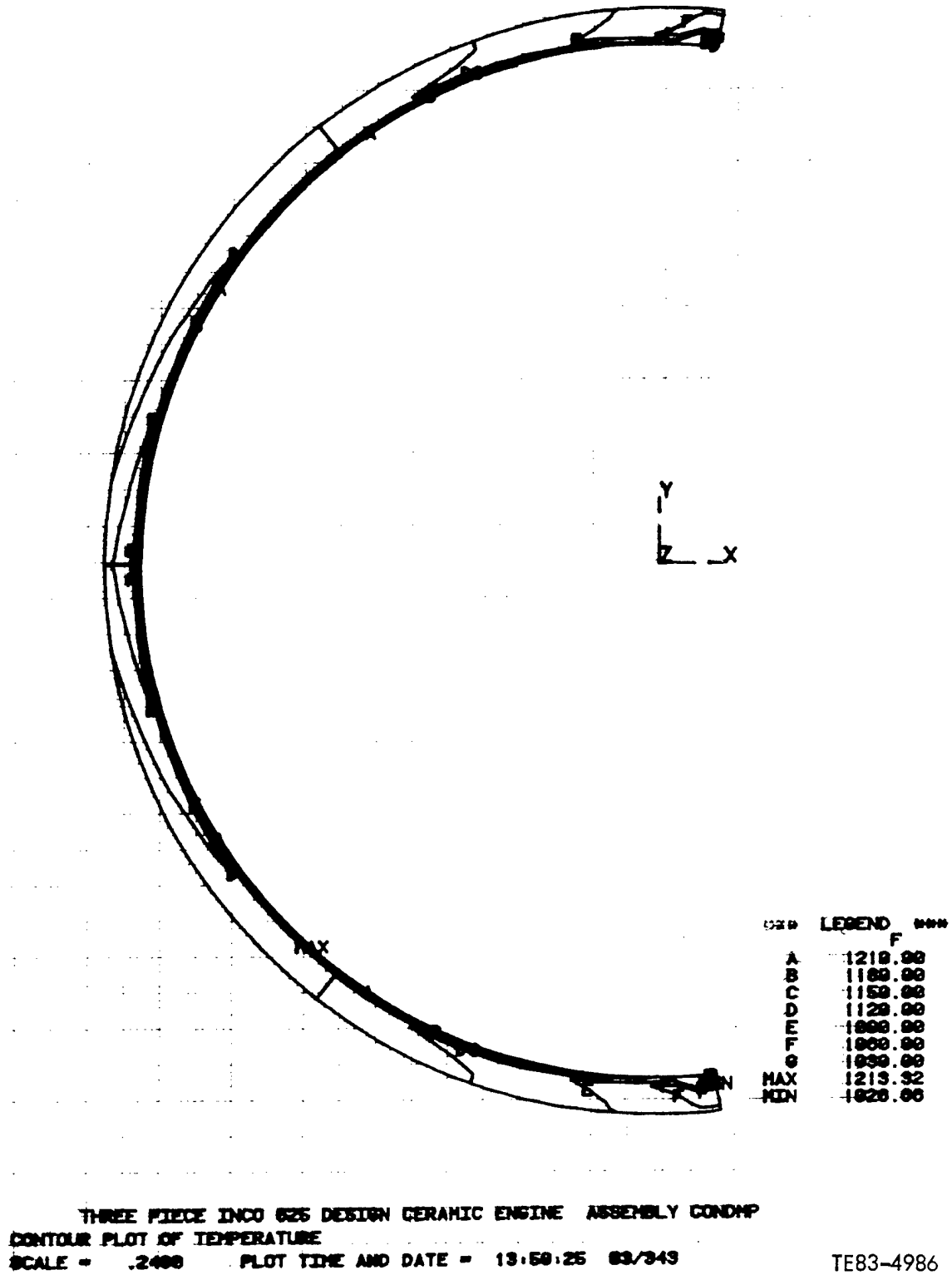

Figure 3-5. Exhaust Ring Temperature--1500 HP Condition

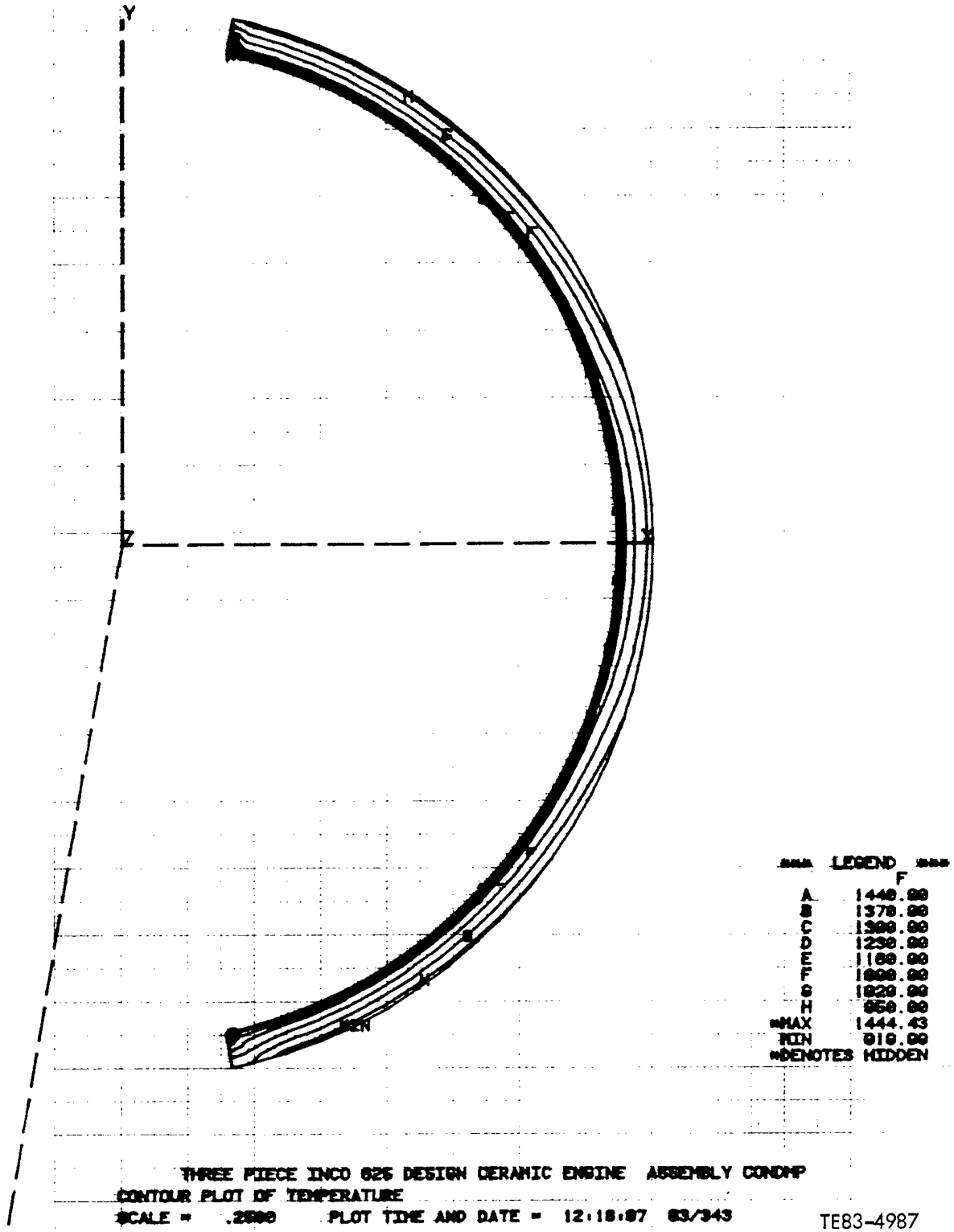

Figure 3-6. Inlet Ring Temperature--120 HP

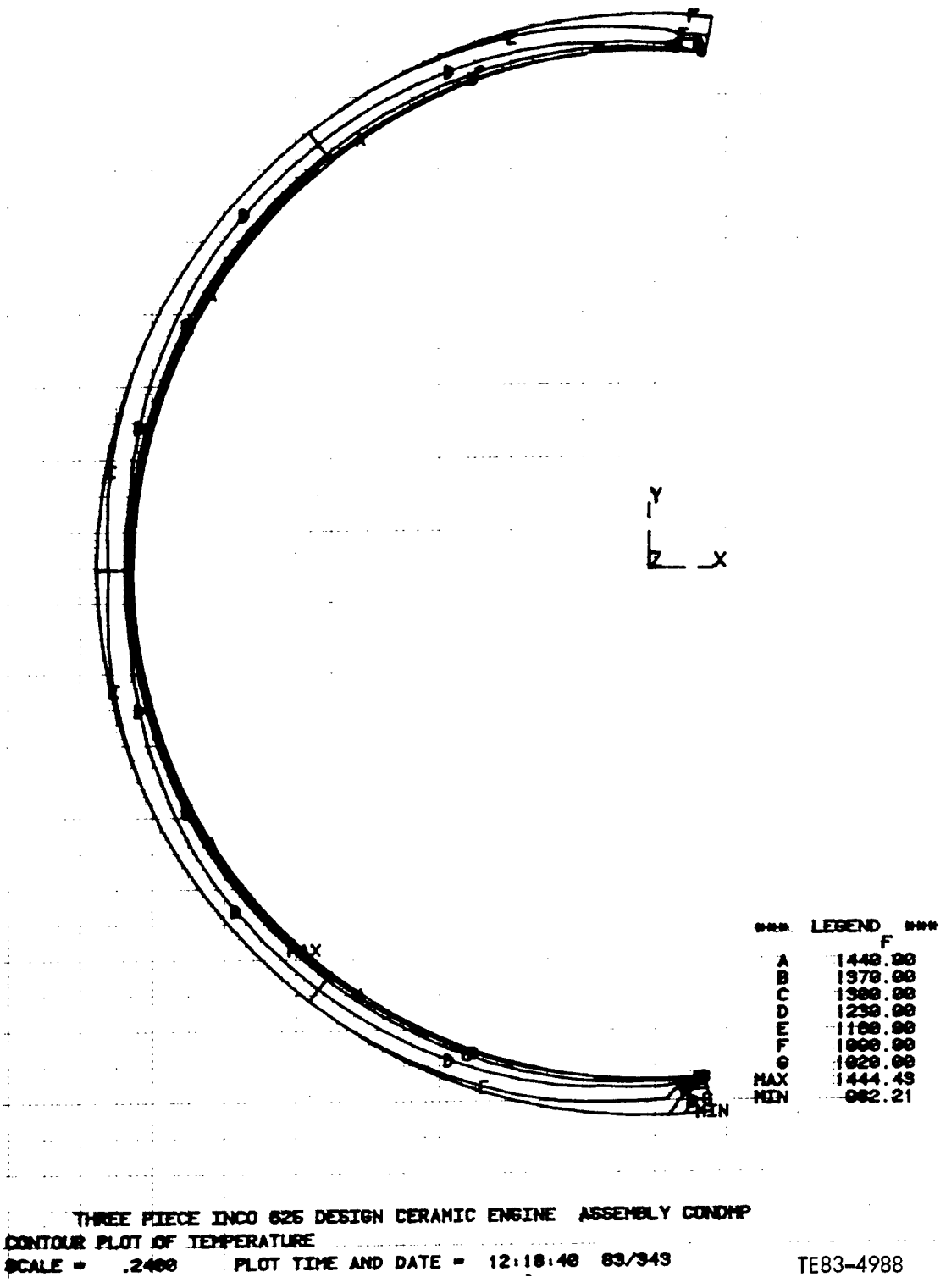

Figure 3-7. Exhaust Ring Temperature--120 HP

It was determined that the quadralateral element converges to the solution quicker than the triangular plate element, therefore allowing a coarser mesh density, with fewer degrees of freedom to be used.

In addition, a nonlinear buckling solution was used to go beyond the first order approximations given by the linear solution. Additional accuracy was obtained in the nonlinear solution since it accounts for the change of stiffness in the structure due to the applied loads.

Hot seal stress analysis was directed at the following concerns that resulted from higher pressure and temperature:

- o seal rim prestress required to prevent buckling and creep
- o crossarm stresses, due to pressure and thermal gradients, which might produce permanent distortion
- o seal leaf stresses due to pressure, which might produce distortion

Results of this stress analysis combined with cooling studies will determine whether a metal platform can be used or whether ceramic is required.

A thermal gradient across the seal rim from hot inside diameter (i.d.) to cooler outside diameter (o.d.) causes the rim segments to try to expand more than the crossarm. This produces high stress, creep, and buckling, which results in uneven seal wear and possible leakage. Allison uses a patented seal rim prestress concept (Patent 4357025) to counter this stress and buckling.

Interference fits between the rim segments and the crossarm to produce the prestress were established based on the following four criteria:

(1) a minimum of 5 lb of contact force between rim segments and crossarm at all operating conditions to minimize leakage

(2) creep strength not exceeding 0.2%-100 hr in the rim segments to prevent permanent distortion

(3) rim segments not buckling on cold assembly

(4) rim segments not buckling during engine operation

The following two engine operating conditions were analyzed:

(1) 120 horsepower (hp), which produces maximum 2000°F gas temperature and maximum rim temperature gradients with only 13 $lb/in.^2$ differential pressure across the rim and crossarm

(2) 1500 hp, which produces a maximum pressure differential across the rim and crossarm of 105 $lb/in.^2$ with only 1450°F gas temperature

Table 3-1 summarizes the amount of radial interference required at seal assembly to satisfy each of the preceding four criteria at three extreme conditions: 120 hp, 1500 hp, and cold assembly.

Examination of all limiting values of interference in Table 3-1 shows that the minimum value to prevent creep at 120 hp will satisfy all other criteria and conditions. The creep limit is critical only at the 120-hp condition where

Table 3-1. Radial Interference Required at Assembly Between Seal Rim Segments and Cross Arm in Inches

	Inlet air rim segment				Exhaust gas rim segment			
Condition	To maintain 5 lb contact force--min	To prevent 0.2%-100 hr creep--min	To prevent buckling Min	Max	To maintain 5 lb contact force--min	To prevent 0.2%-100 hr creep--min	To prevent buckling Min	Max
120 hp	0.50	0.55*	0.15	1.35	0.65	0.72*	0.25	1.85
1500 hp	0.22	Not critical	0	0.94	0.20	Not critical	0	1.07
Cold	---	Not critical	0	0.77**	---	Not critical	0	0.99**

All of the figures include 3.2 lb per lineal inch of lead preload with 35.7 lb/in. rate.
*Selected radial interference to satisfy all criteria and conditions
**Without lead load max would be 0.40

creep strength is lowered by high rim i.d. temperatures. Note that more interference is required to prevent creep than is required to maintain the 5-lb load or to prevent buckling. Also note that a maximum interference exists beyond which rim buckling is imposed rather than prevented. The buckling analysis includes the stabilizing normal loads exerted on the seal platform by the attached leaf seals. Figures 3-8 and 3-9 illustrate the buckling mode of the exhaust rim segment, which must be stabilized.

Allison testing of cooled seals in the NASA/CATE program showed that the introduction of seal crossarm cooling air at the hub and rim produced an increase in seal leakage thought to be due to stresses induced by crossarm temperature gradients. Figure 3-10 shows the temperature gradients and leakage that resulted from the introduction of cooling air at either the rim or the hub, as shown in Figure 3-11. The data show that the introduction of cooling air at the hub caused more increase in leakage than the introduction of cooling air at the rim. Stress analysis was directed at determining how much temperature gradient could be tolerated without exceeding material creep limits. This analysis was used in determining the feasibility of cooling the seal at the desired 2000°F operating temperature.

Two temperature profiles were examined. One was with circular isotherms as a linear function of radius, f(R), as measured from the crossarm hub center point, shown in Figure 3-12. This profile has been shown by testing to occur naturally when cooling air is introduced through a center hole. The second temperature profile examined was with straight isotherms as a linear function of distance y from the hub centerline, f(y), as shown in Figure 3-13. Shields have been shown to be effective in reducing overcooling, which could produce the straight isotherms. In both cases, the crossarm was assumed to be cooled to a constant 1400°F between the 4.5-in. and 11-in. radii. The figures show only half of the crossarm. The wide end is the centerline.

Stresses were calculated for two gradients between the hub and a 4.5-in. radius for each type of profile: 300°F and 570°F gradients for the f(R) profile and 300°F and 750°F for the f(y) profile. Calculations include the effect of differential pressure. Figures 3-14 and 3-15 show the stress distributions for 300°F gradients for each type profile. It is notable that no stress is generated for either profile in the narrow portion of the crossarm despite steep gradients there. It is concluded that only the wide portion, where greater differential expansion is possible, is susceptible.

Figures 3-16 and 3-17 show that stress at the hub increases with the thermal gradient for both profiles, demonstrating the importance of avoiding steep gradients in cooling. These plots are simply straight line approximations drawn through the two points actually run. Creep life is noted on each plot, but the locations chosen are not critical.

Figures 3-18 and 3-19 show stress and creep life for 300°F and 570°F gradients for temperature profiles established as a function of radius, f(R) (see Figure 3-12).

Highest stress and lowest creep life occur at a 2.5-in. radius. With 0.2% creep as a limit, the limiting gradient to provide a desired 2500-hr life would be only 200°F, established by semilog extrapolation. Figures 3-20 and 3-21 show stress and creep life for the f(y) type profile (see Figure 3-13). For this profile, lowest creep life occurs at the 4.5-in. radius, where stress is lowest but temperature is maximum. Extrapolation predicts that the limiting

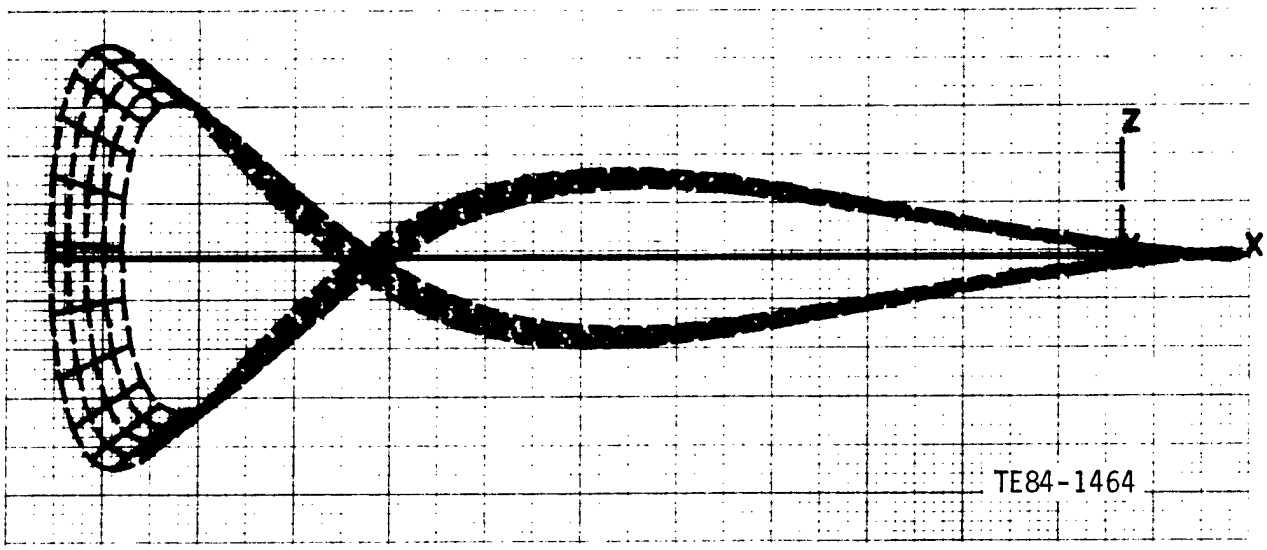

Figure 3-8. Exhaust Ring, Edge View, 1500 HP Condition

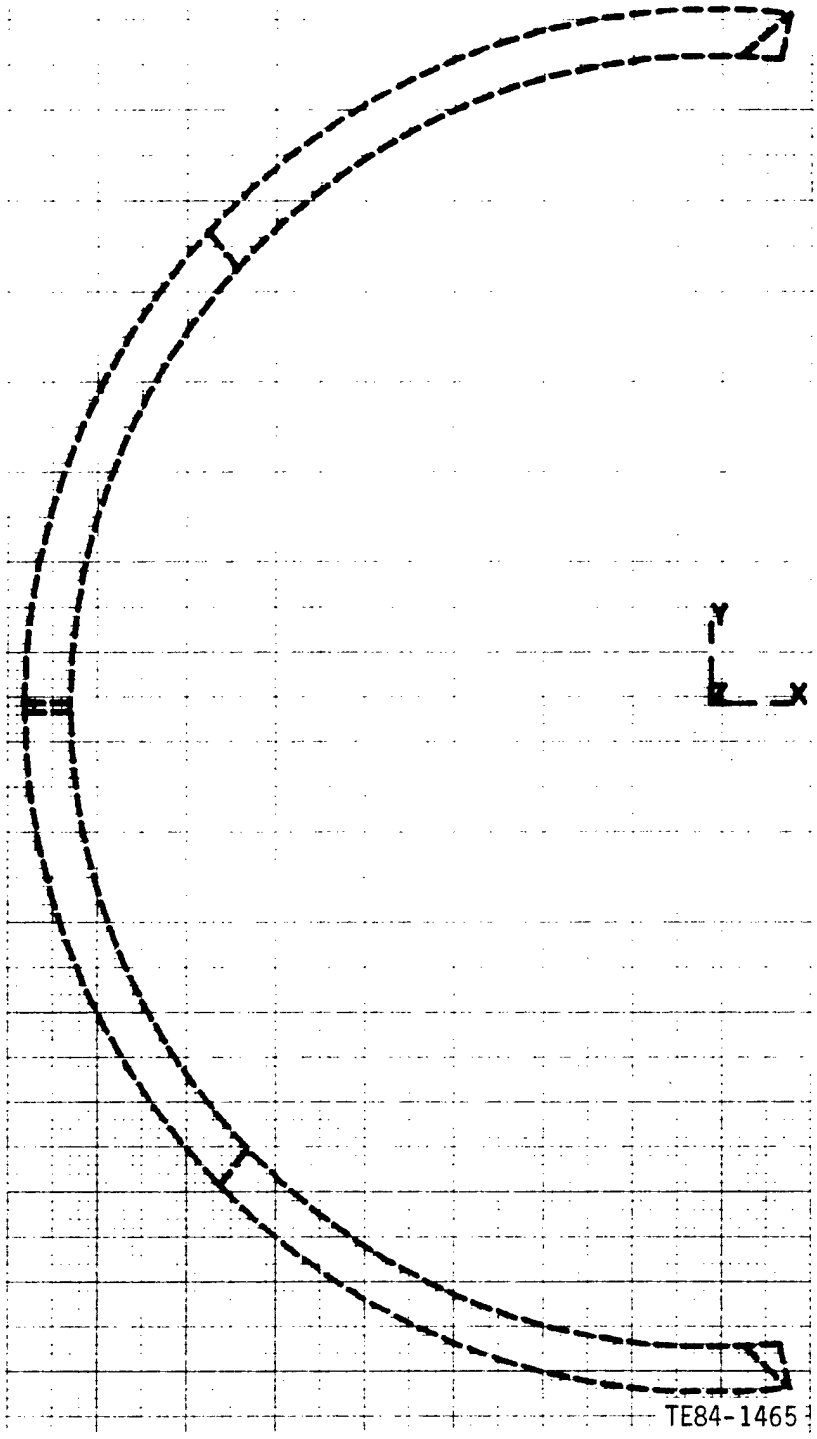

Figure 3-9. Exhaust Ring, Plane View, 1500 HP Condition

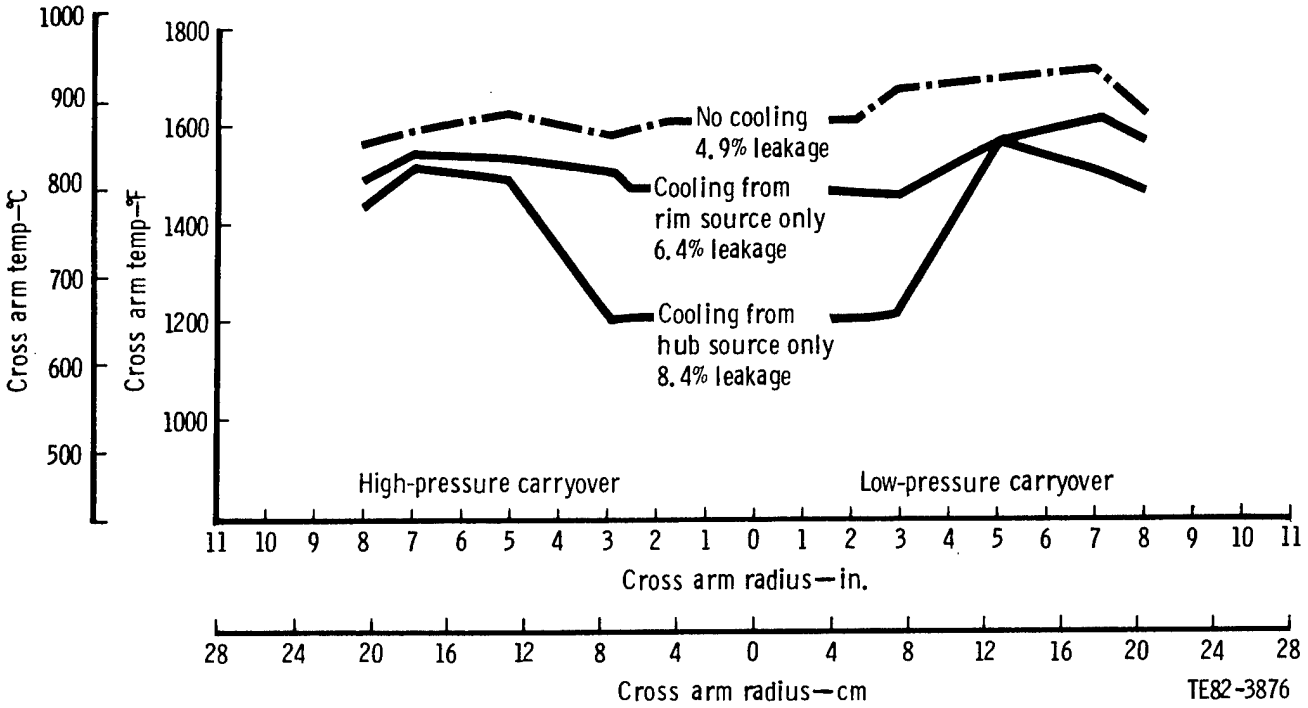

Figure 3-10. Three-Piece High-Temperature Regenerator Seal Crossarm Temperature With and Without Cooling for 60% Engine Speed Condition

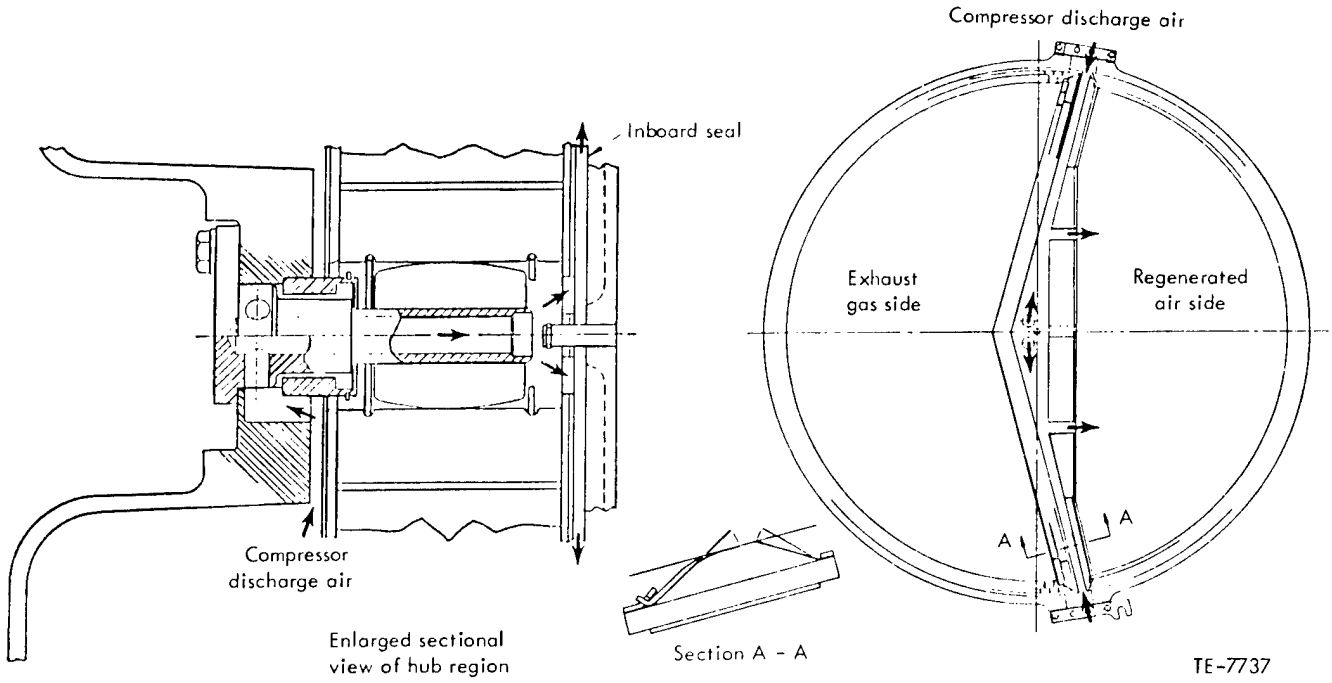

Figure 3-11. Regenerator Inboard Seal Cooling Air System

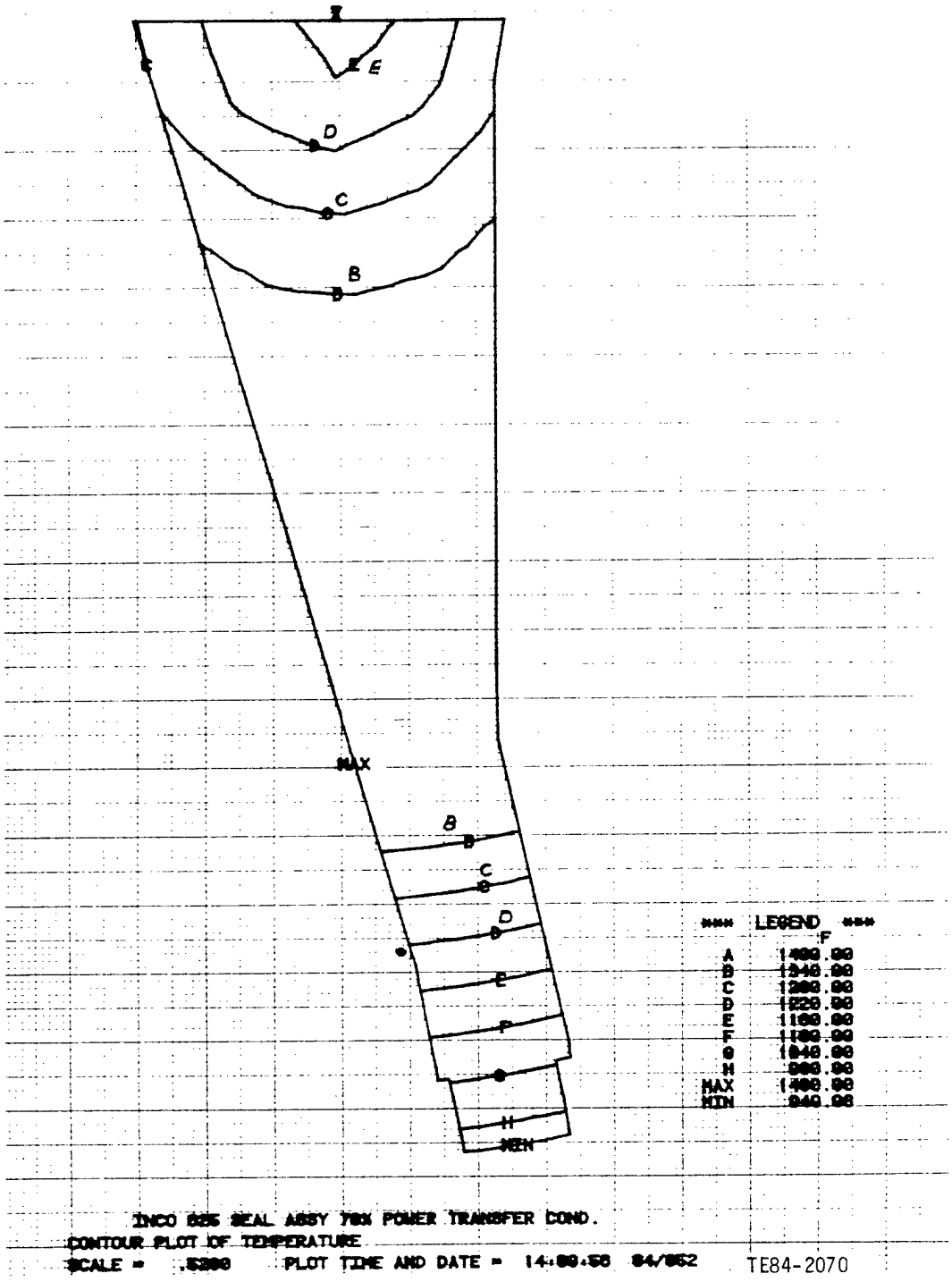

Figure 3-12. Seal Crossarm Temperature Profile, 120 HP Condition, $\Delta T = 300°F$, $T \sim f(R)$

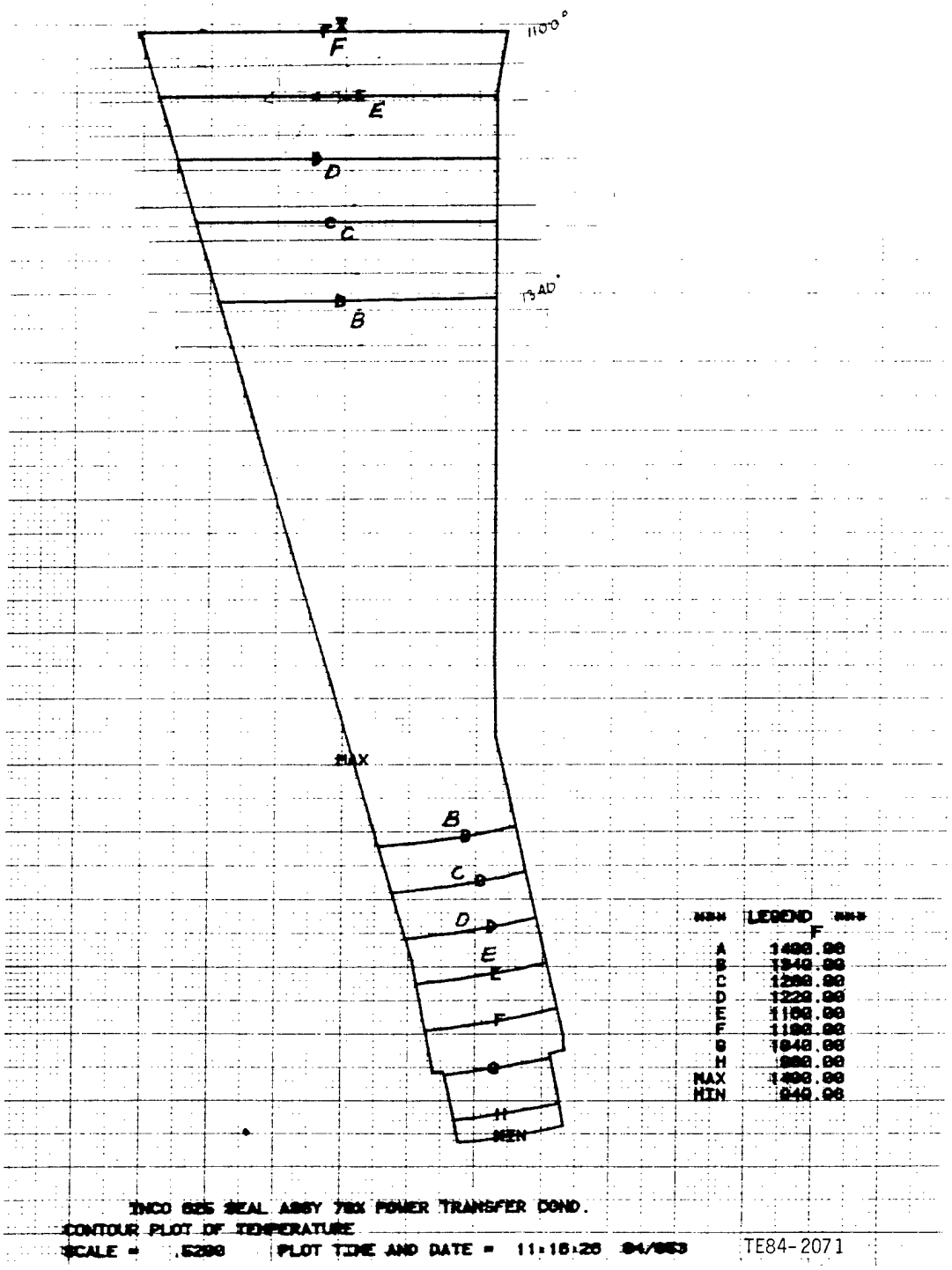

Figure 3-13. Seal Crossarm Temperature Profile, 120 HP Condition, $\Delta T = 300°F$, $T \sim f(y)$, Run 157

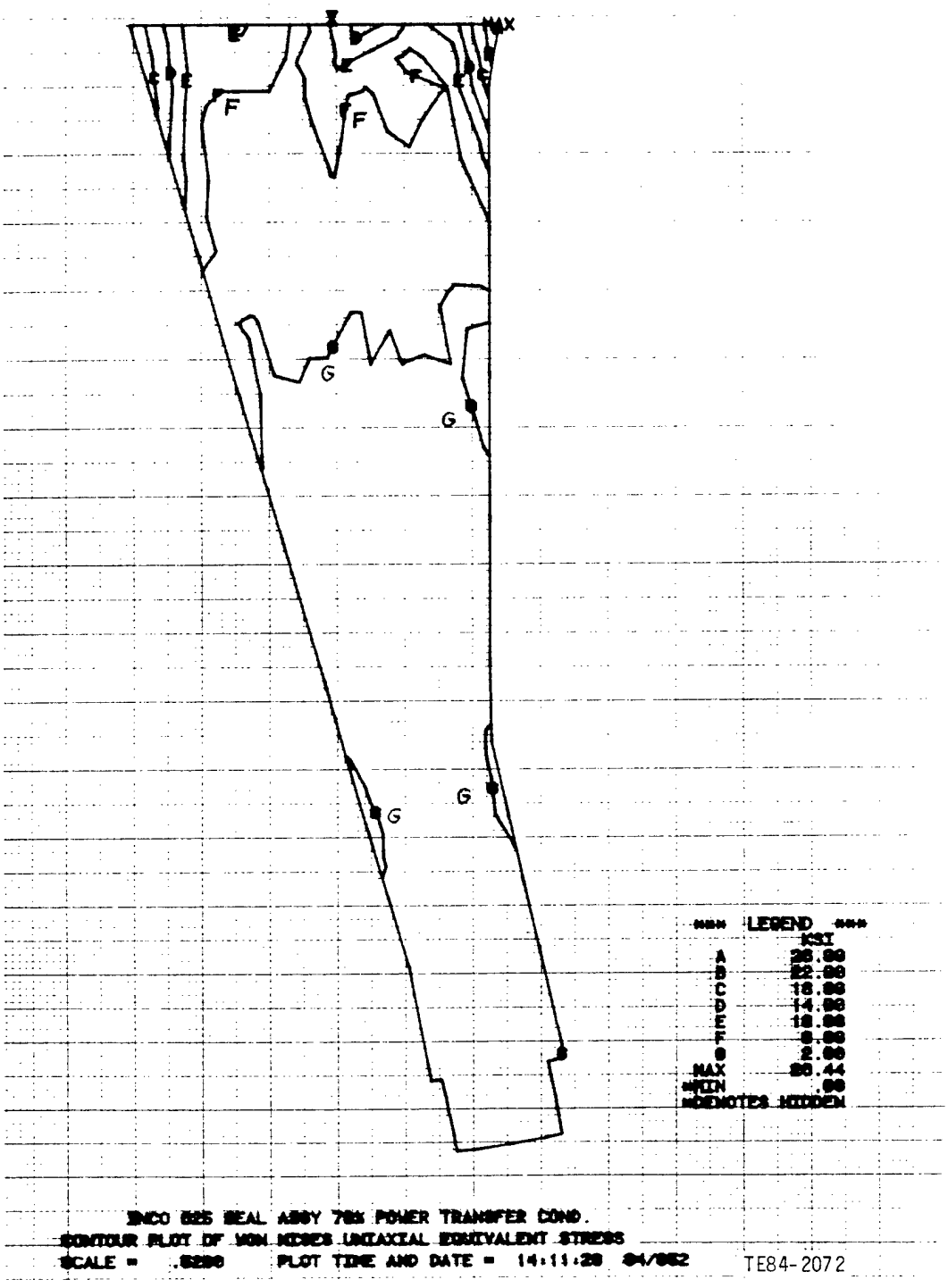

Figure 3-14. Seal Crossarm Stress, 120 HP Condition, $\Delta T = 300°F$, $T \sim f(R)$

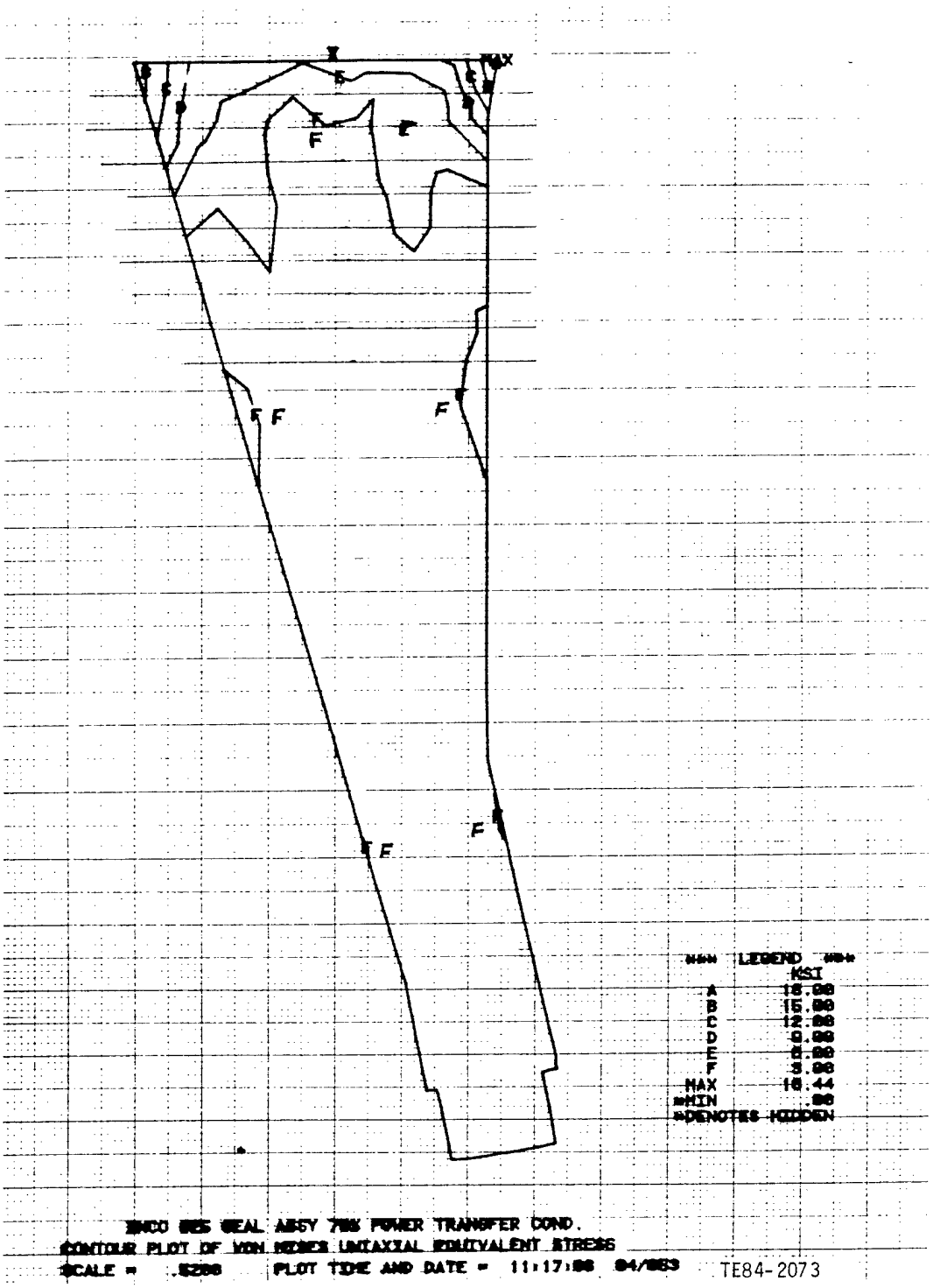

Figure 3-15. Seal Crossarm Stress, 120 HP Condition, $\Delta T = 300°F$, $T \sim f(y)$

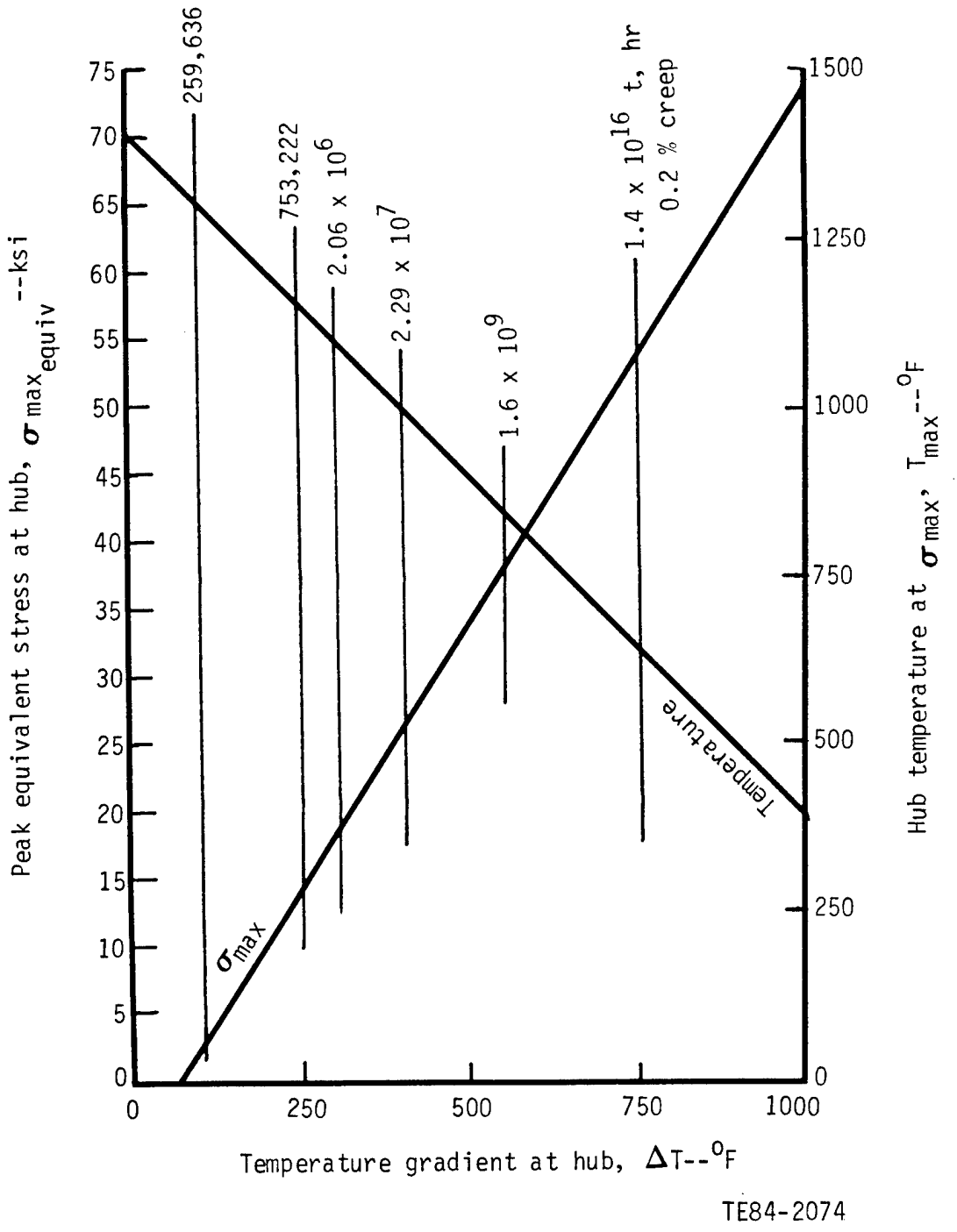

Figure 3-16. Effect of Crossarm Temperature Gradient at Hub, 120 HP Condition, $\Delta T \propto f(y)$ Linear, Runs 157 and 158

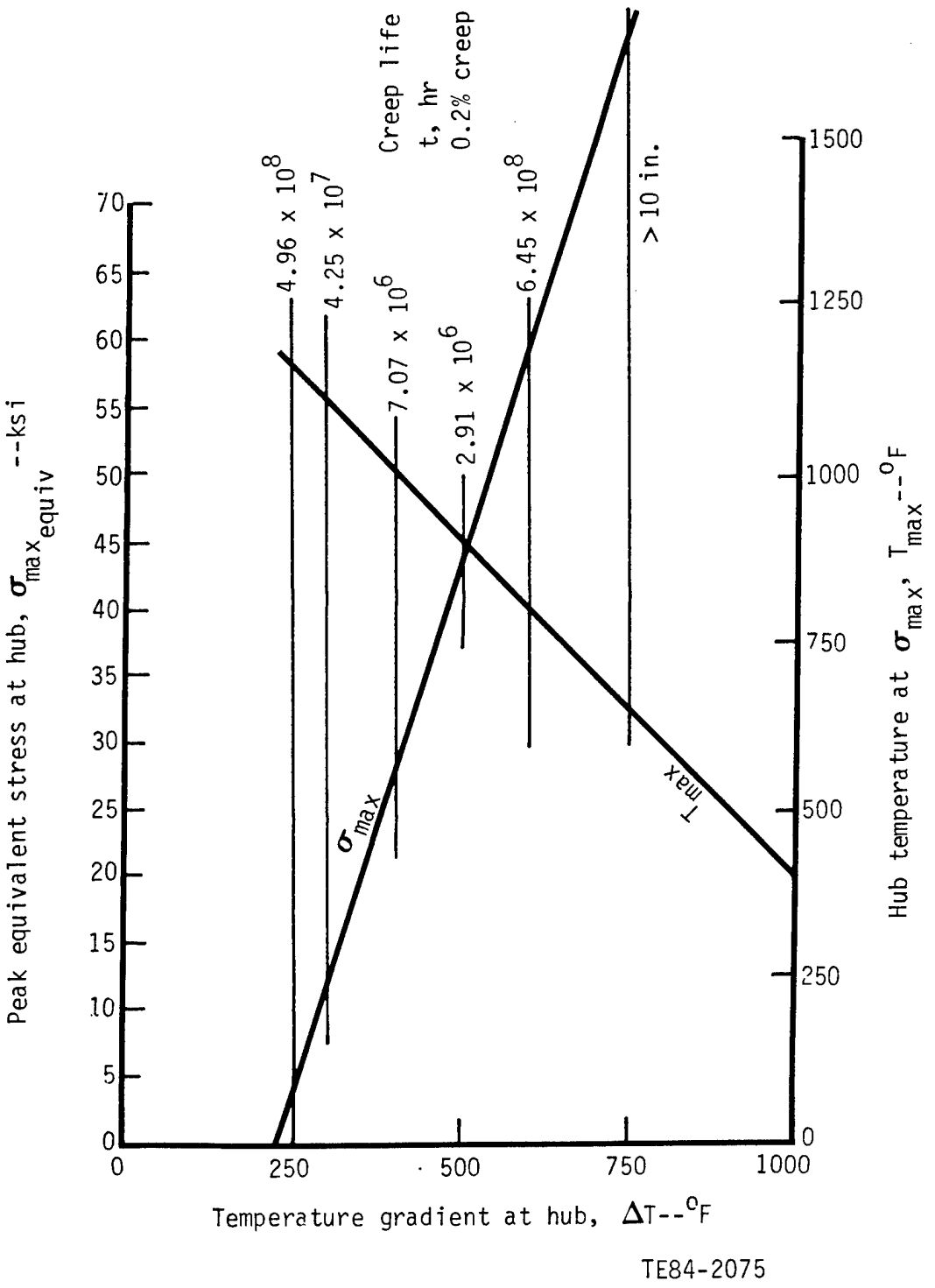

Figure 3-17. Effect of Crossarm Temperature Gradient at Hub, 120 HP Condition, $\Delta T \propto f(R)$ Linear, Runs 129 and 160

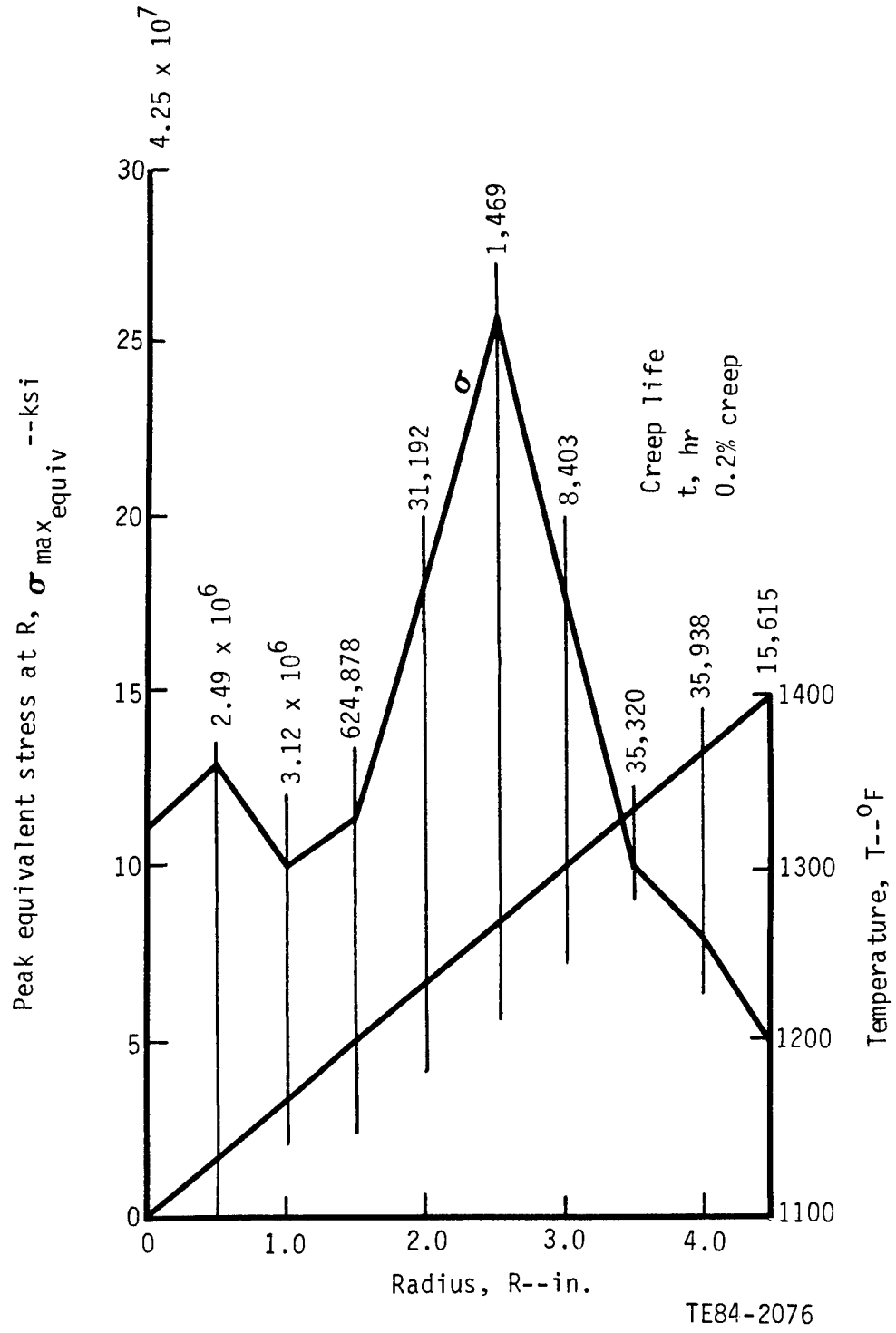

Figure 3-18. ΔT = 300°F Crossarm Gradient, 0.2% Creep Lives, 120 HP Condition, ΔT ∝ f(R) Linear

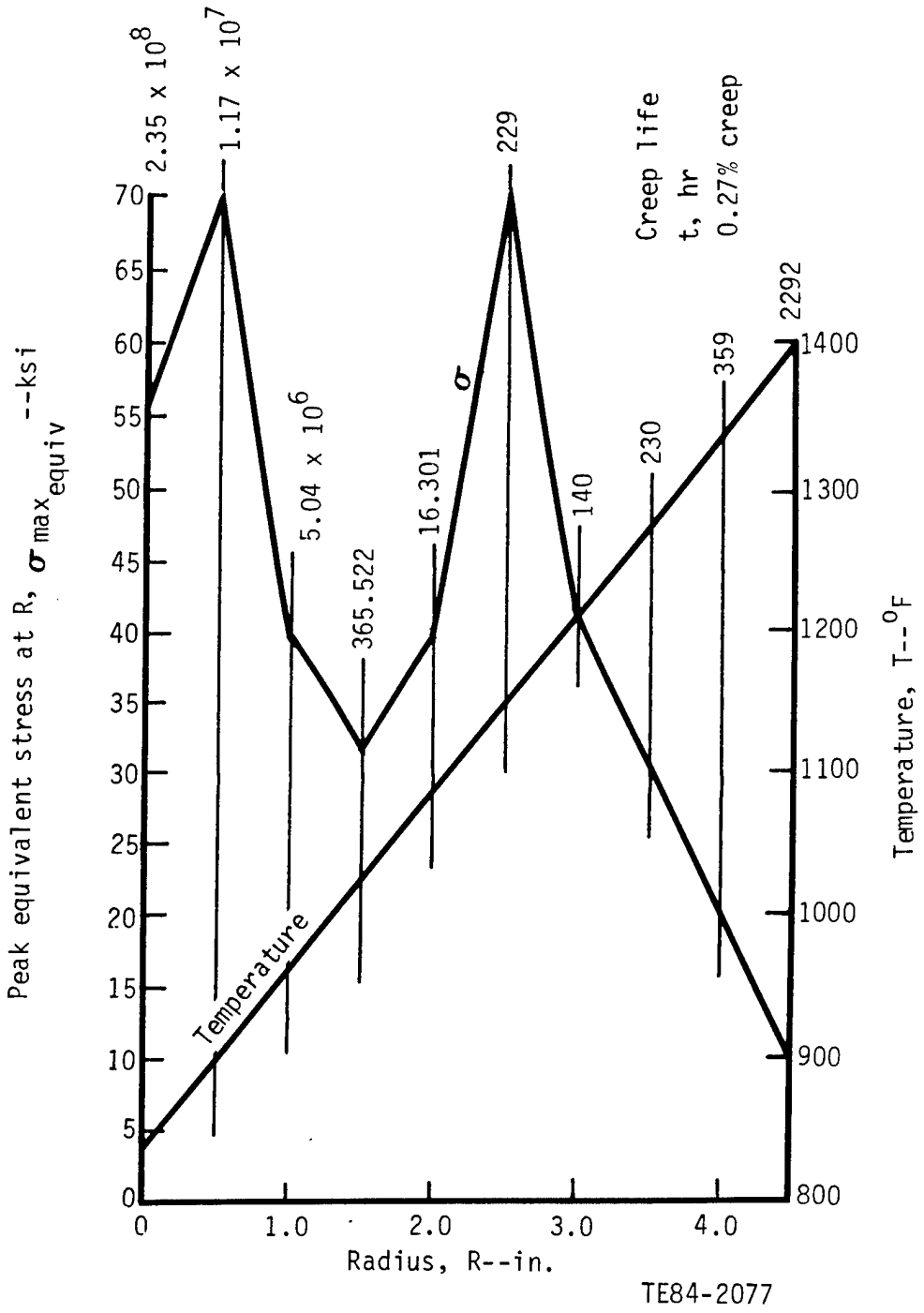

Figure 3-19. ΔT = 570°F Crossarm Gradient, 0.2% Creep Lives, 120 HP Condition, ΔT ∝ f(R) Linear

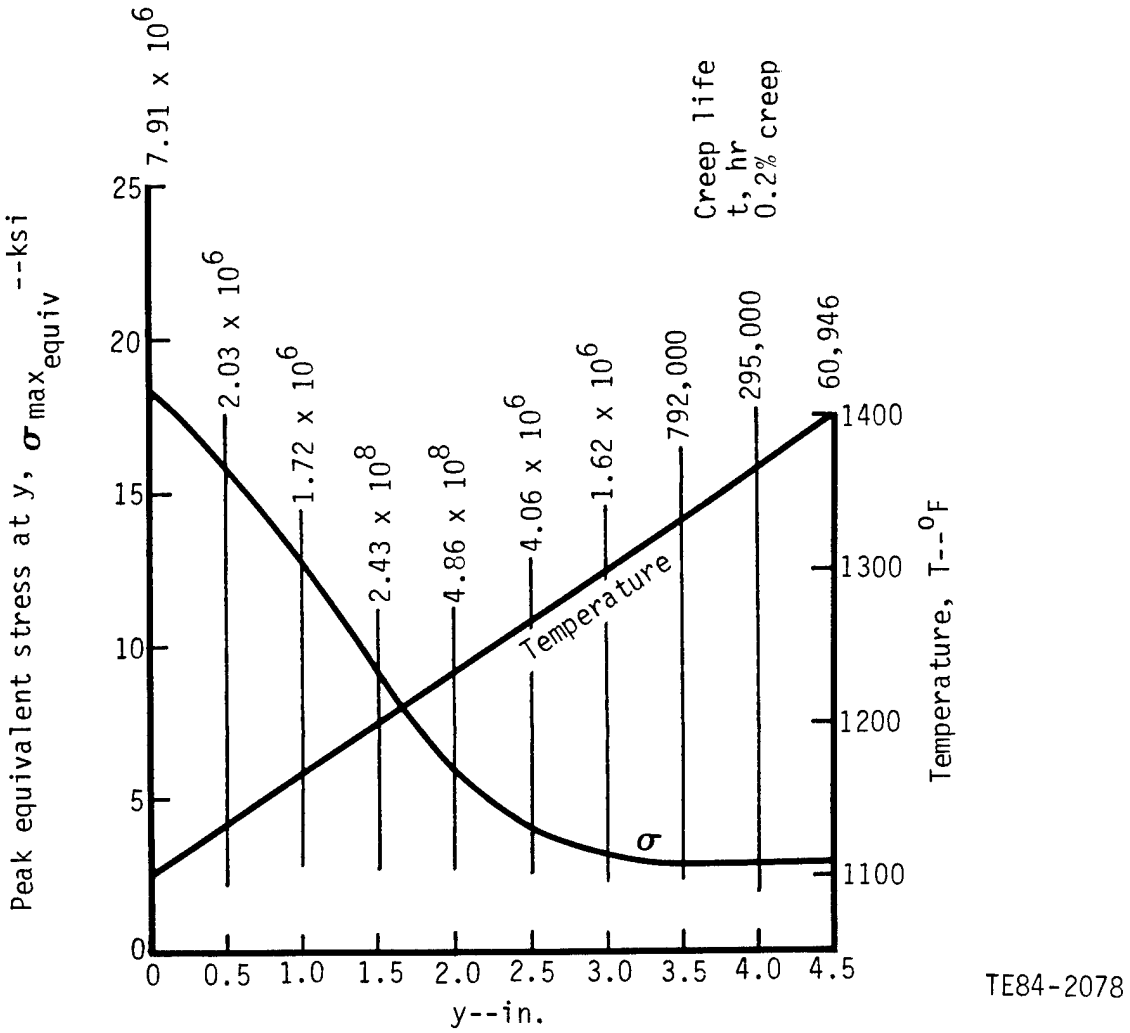

Figure 3-20. ΔT = 300°F Crossarm Gradient, 0.2% Creep Lives, 120 HP Condition, ΔT ∝ f(y) Linear

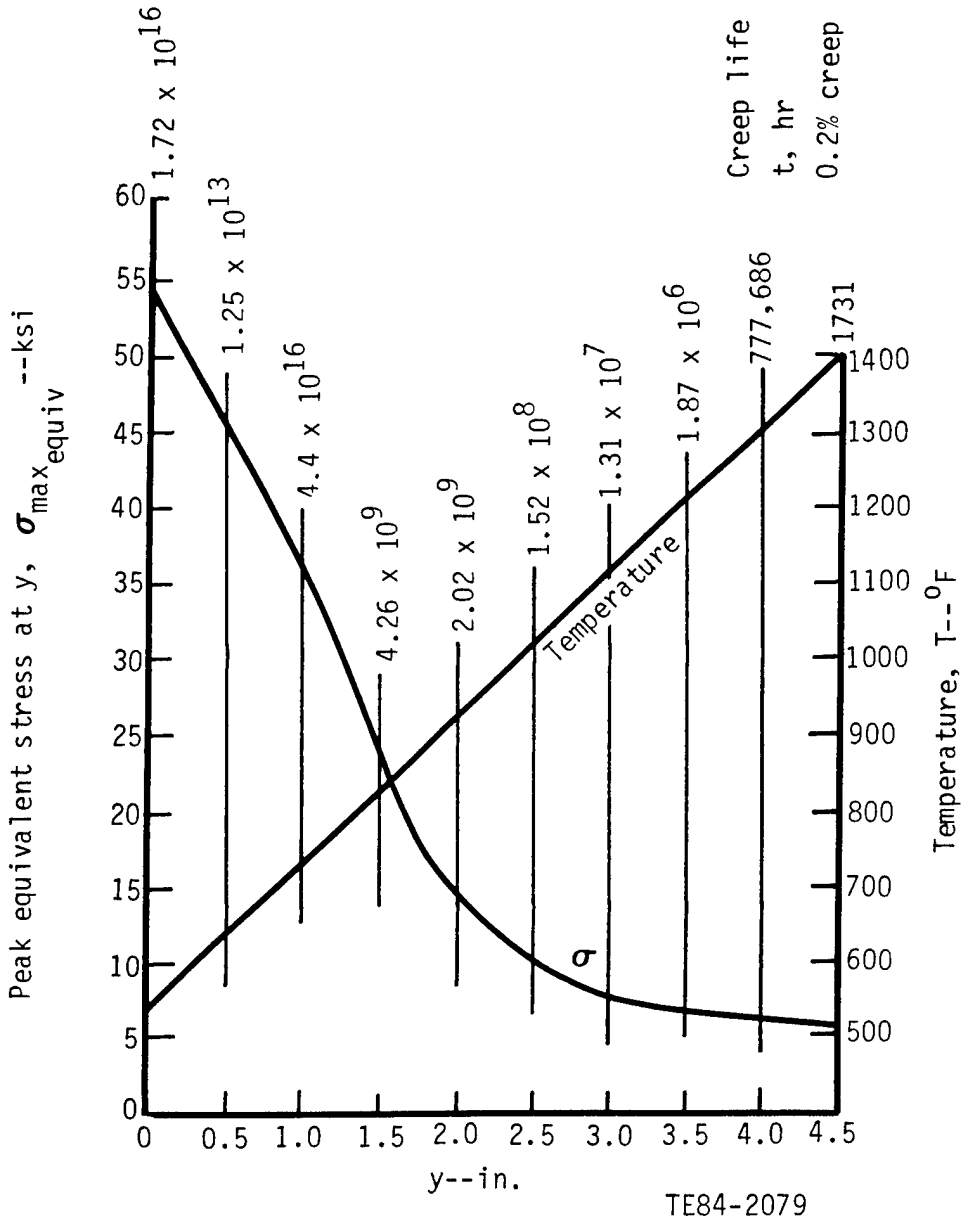

Figure 3-21. ΔT = 750°F Crossarm Gradient, 0.2% Creep Lives, 120 HP Condition, ΔT ∝ f(y) Linear

gradient for 2500-hr creep life for this profile would be 700°F. A 600°F gradient has been readily achieved, so it is concluded that tolerable crossarm stresses can be achieved.

Stresses were also checked in the static leaf seal and its support members, shown in cross section A-A of Figure 3-11. These parts must sustain the full 9:1 cycle pressure ratio while operating at a predicted 1300°F. A minimum margin of safety of 2.29 for the yield limit was calculated. Allison report TDR AX0000-769 covers details of the metal seal stress analysis.

3.1.1.2. Seal cooling. A preliminary heat transfer analysis of the CATE/IGT 404 crossarm was initiatedto identify and characterize the various heat transfer mechanisms governing seal temperature distribution at the 60% P.T., 1800°F turbine exhaust operating point. To predict steady-state seal temperatures for various cooling configurations, a two-dimensional (2-D) finite element model consisting of three layers of elements was built, which also allowed for the radially varying crossarm width (see Figures 3-22 and 3-23). Agreement between the CATE test data and the present predictions is quite good, as indicated in Figure 3-24. Increasing the cooling airflow through the hub by 50% caused a drop of 20-30°F in metal temepratures in the midportion of the crossarm, as shown in Figure 3-25. The finite element model was scaled up for the AIPS PD335-B1 Phase I engine conditions, and cooling air requirements, satisfying the allowable total pressure drop and temperature limits were then determined.

The regenerator crossarm seal is heated primarily by the hot burner inlet air leaking under the crossarm wearface as a result of the pressure difference between the burner inlet and turbine exhaust plenums. The wearface temperature runs close to the temperature of the exhaust gases due to the large conductance and high thermal conductivity of the hot gases. Heat transfer by radiation from the cavities of the regenerator matrix would be enhanced by the close proximity of the wear surface and the ceramic disk (see Figure 3-26), but the radiation flux incident on the wearface is reduced by the small temperature difference between the two surfaces.

The dominant resistance to heat flow through the crossarm is the relatively thick boundary layer formed by the low velocity cooling air. Flow velocities at the 60% speed condition are low because the governing pressure drop is only the small (0.1 psia) drop across the regenerator matrix.

Work continued on the heat transfer analysis of the 32-in. diameter TACOM PD 335-B1 hot side regenerator crossarm seal with the help of a 2-D finite element model that was scaled up from the CATE/IGT 404 crossarm dimensions.

The primary objective was to cool the nickel alloy (Inco 625) crossarm structure to 1400°F or less at the 120 hp, 60% power transfer design point with the cooling airflow governed by the 0.1 psia available pressure drop across the regenerator matrix.

In the first design investigated, the compressor discharge air enters the crossarm channel (formed by the engine block, crossarm plate, and leaf seals) from the rim and from the hub spindle. The cooling air picks up heat from the crossarm surface (see Figures 3-11 and 3-26) and is exhausted into the burner inlet cavity through exhaust ports located midway between the rim and the hub. In this design, two different configurations for the crossarm were investi-

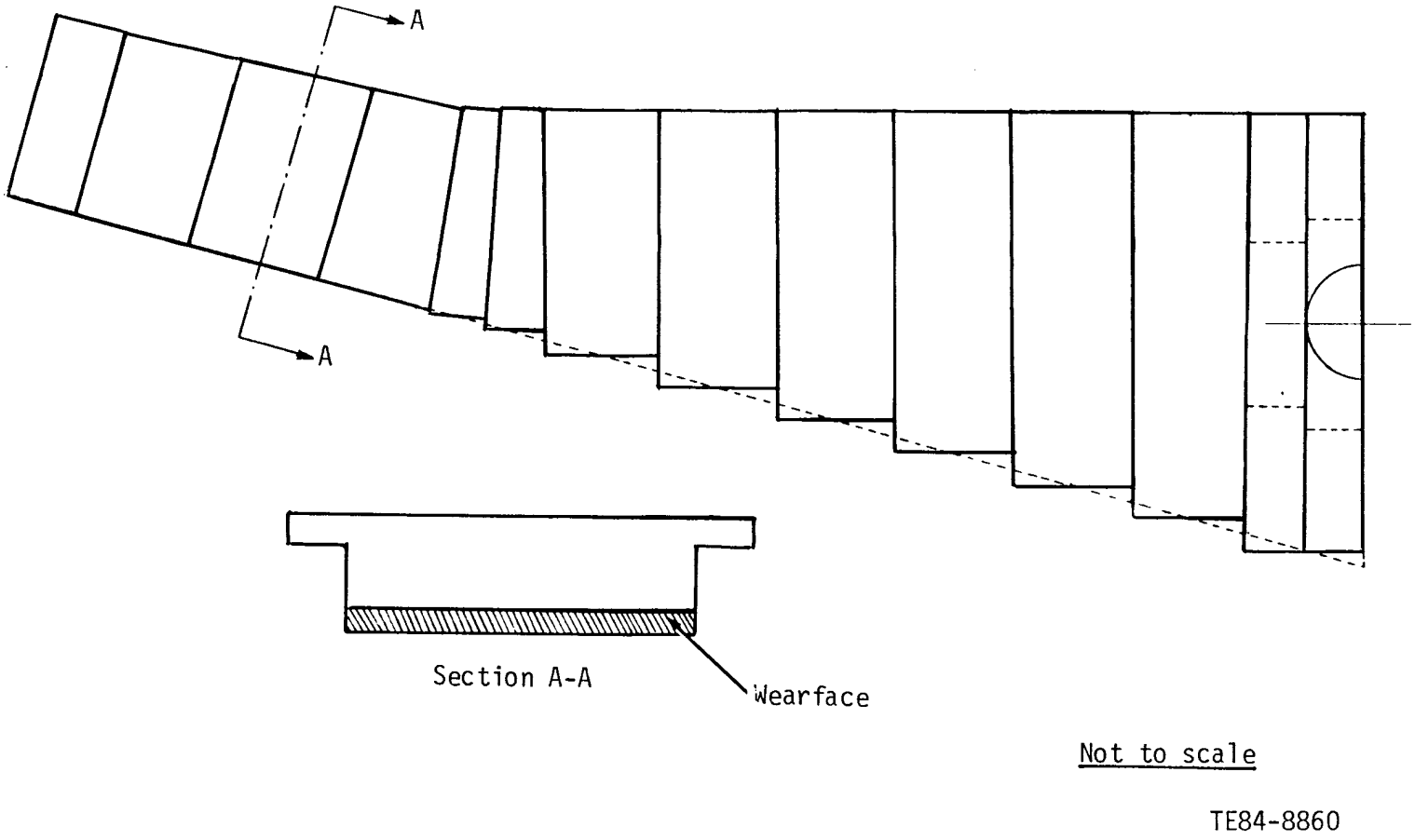

Figure 3-22. Finite Element Mold of CATE/IGT 404 Regenerator Crossarm

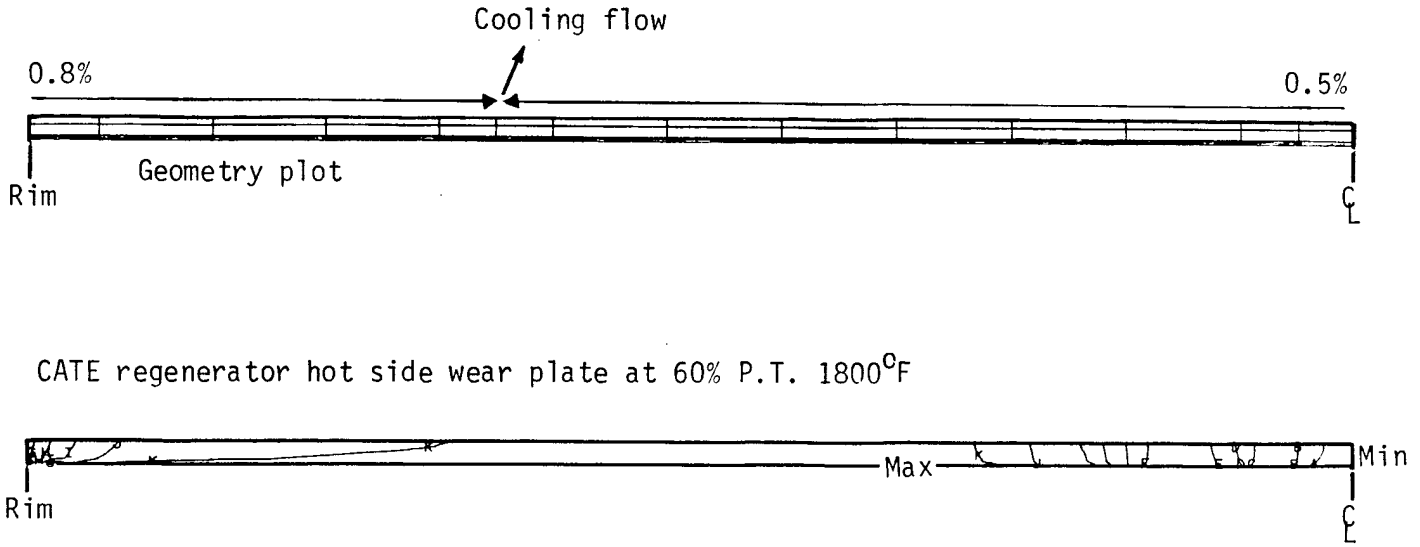

Figure 3-23. Details of 2-D Finite Element Model Showing Wearface Area (Shaded) and the Corresponding Temperature Isotherms Obtained at Steady-State for the Inboard Seal High Pressure Carryover Half

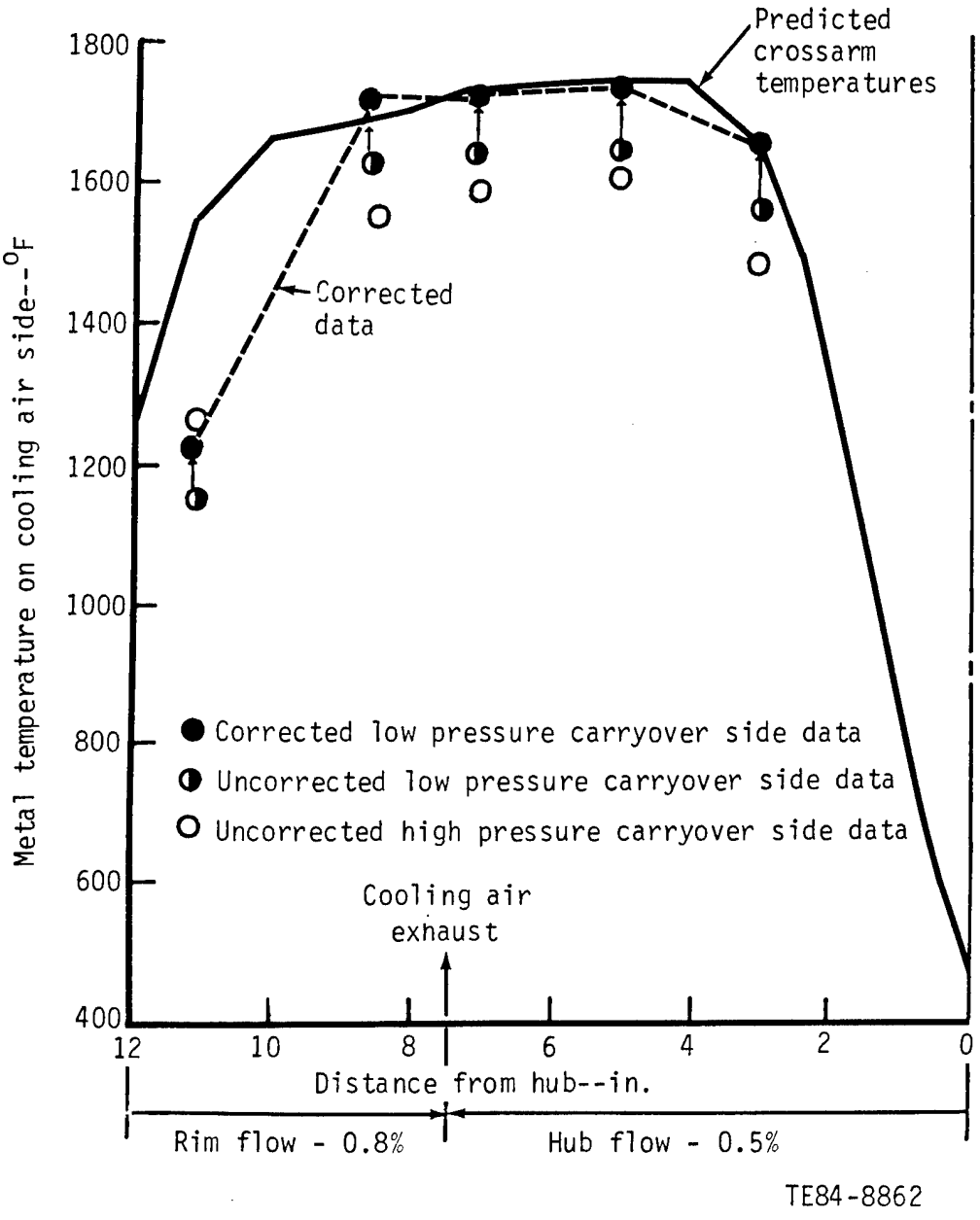

Figure 3-24. Comparison of Finite Element Model Predictions with CATE/IGT Crossarm Thermocouple Data at the 60% P.T. Condition (1800°F Exhaust)

Thermocouple conduction error correlation was estimated for 0.01 in. dia chromel-alumel Type K wires.

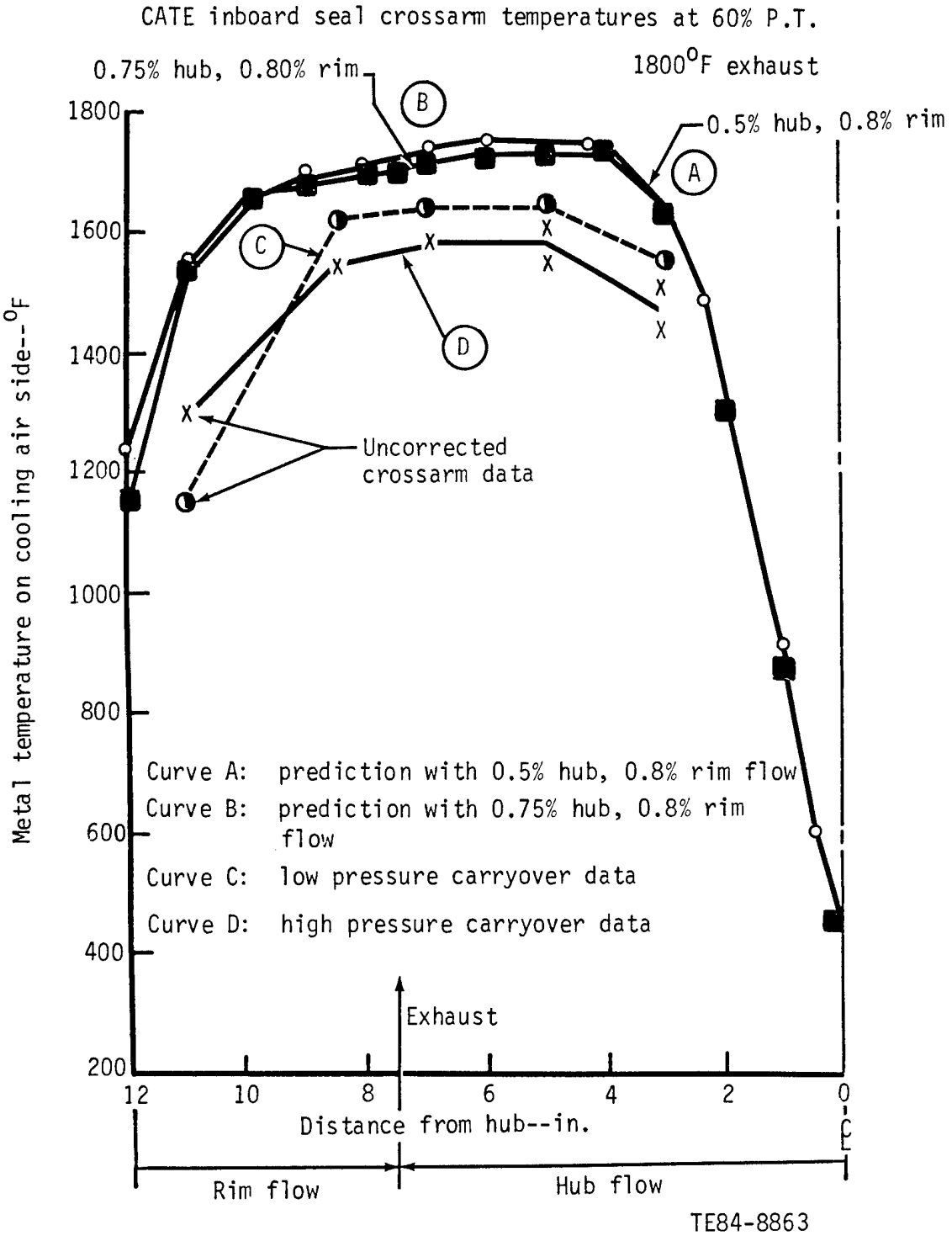

Figure 3-25. Effect of an Increase in Hub Cooling Airflow from 0.5% to 0.75% Predicted at the CATE/IGT 60% P.T. Condition

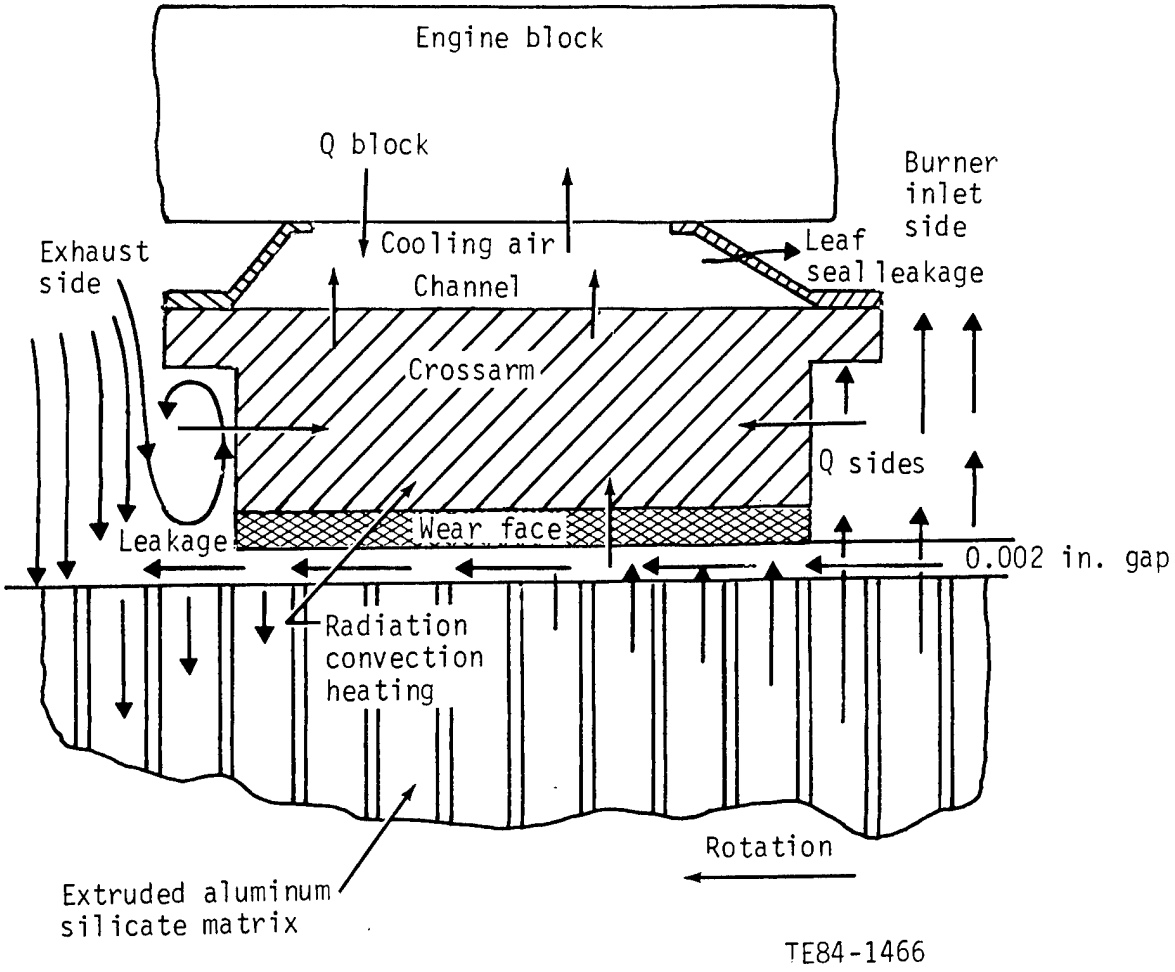

Figure 3-26. Schematic Representation of Heat Loads and Flow Around the Crossarm Showing the Layout of the Cooling Air Channel Relative to the Regenerator Disk and Engine Block

gated. In the first scheme (Scheme A), the NiO/CaF_2 wearface was applied directly to the Inco 625 substrate as in the CATE/IGT 404 design. In the second scheme (Scheme B), an insulating layer of 10% dense porous metal was placed between the nickel alloy and wearface layers (see Figure 3-27) to reduce the conduction of heat through the crossarm. The maximum total cooling airflows through the rim and the hub that satisfy the 0.1 psia pressure drop criterion are 2.72% and 4%, respectively, of the flow through each regenerator disk. In both these schemes the nickel alloy layer remained well above 1400°F (see Figure 3-27), and the thermal efficiency of the heat pickup by the cooling air remained low (~22%-24%). This was mainly because large cross-sectional areas were required for the cooling air channels to accommodate the low driving pressure drop. These large flow areas reduced the velocity and convective heat transfer capabilities of this design.

Providing the insulating porous layer in Scheme B reduced coolant side metal temperatures by approximately 80°F-90°F. Reducing the thermal conductivity of the porous layer by 50% (with K~1.0 Btu/hr-ft-°F) drops the metal temperatures by an additional 90°F-100°F to around 1600°F, as shown in Figure 3-27. Temperature distributions of the crossarm seal obtained with Scheme A and Scheme B crossarm models are shown in Figure 3-28. The effect of increasing the total rim flow from 2% (1% from each end) to 2.72% in Scheme B is shown in Figure 3-29. Channel side metal temperatures drop by approximately 70°F near the rim and by approximately 40°F near the midsection of the crossarm.

In order to further cool the nickel alloy substrate of the crossarm, it was necessary to design a more thermally efficient heat transfer augmentation scheme for the cooling air channels. This was expected to entail larger pressure drops in these channels and require a larger driving pressure differential available only by exhausting the cooling air into the turbine exhaust plenum.

In the second design for cooling the hot side regenerator crossarm seal, the cooling air was exhausted into the turbine exhaust side of the regenerator, and two different heat transfer enhancement schemes were investigated. In the first scheme (Scheme C), an impingement plate with 0.03-in. diameter holes was placed between the crossarm and engine block, as shown in Figure 3-30. Compressor discharge air entered from the rim and hub supply ports and, after discharging through the impingement holes and flowing along the crossarm face, was exhausted through gaps in the leaf seals at regular intervals. The close proximity of the impingement jets increased the heat transfer efficiency, but calculations indicated that this scheme would require more cooling flow than another viable scheme (Scheme D) with offset strip fins placed in the cooling air channels. The impingement scheme (Scheme C) required approximately 12.9% of the total regenerator flow for cooling the crossarm to 1400°F, with cooling air supplied from the rim and hub. A pressure ratio of 1.067 across the holes and a square array of 0.03-in. diameter holes, with hole-to-hole spacing of six diameters, provided adequate heat transfer coefficients on the impingement surface of the crossarm.

In the offset strip fin enhancement scheme (Scheme D), the cooling air flows between short strips of finned surfaces (see Figure 3-31) offset approximately 50% so that the leading edge of a fin is in the center of the passage formed by the two preceding fins. This scheme causes repeated growth and wake destruction of boundary layers on the short strip lengths. This promotes a very efficient transfer of heat from the fin surfaces to the cooling air, and for this scheme the total cooling flow required to hold the coolant side cross-

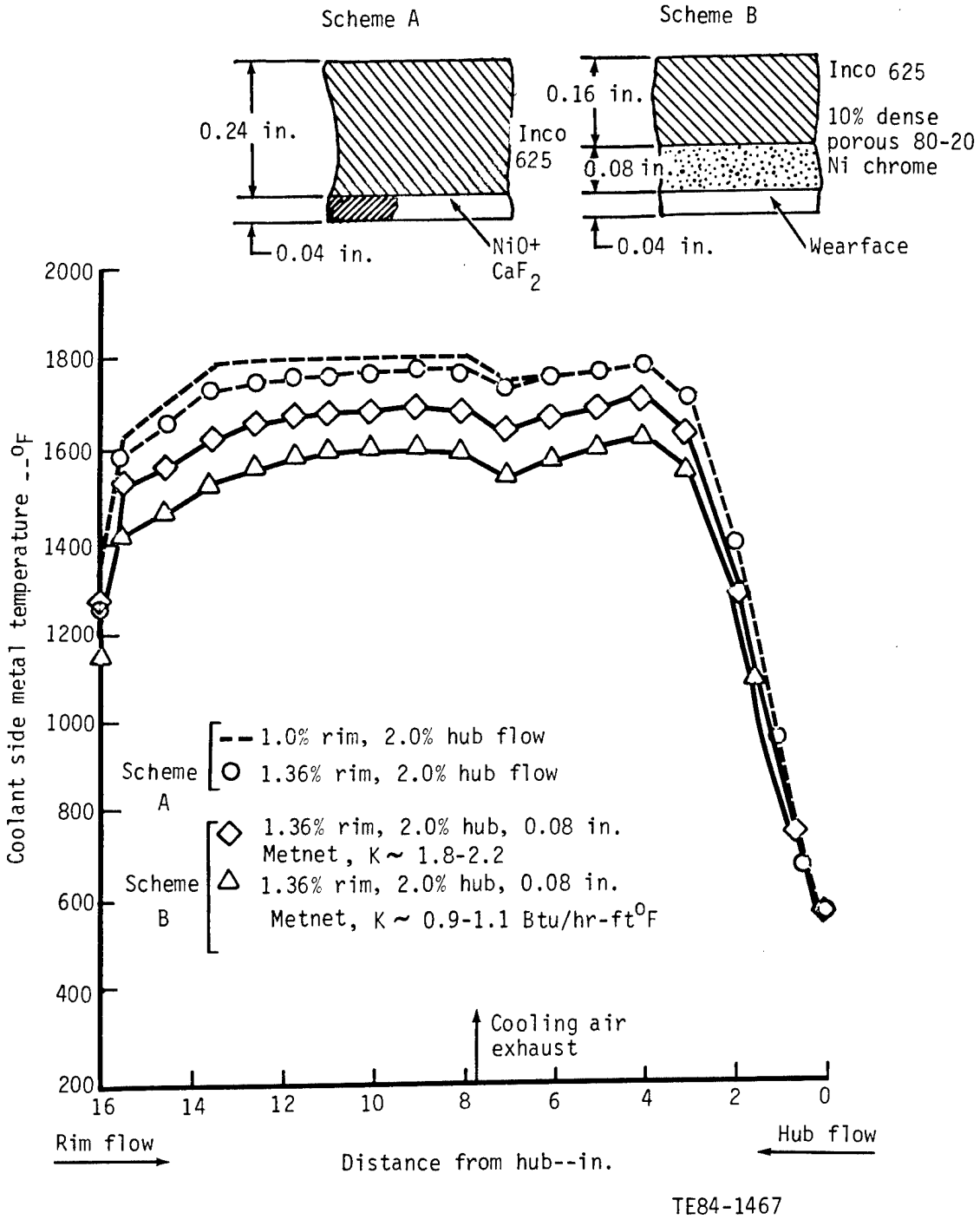

Figure 3-27. Regenerator Hot Side Crossarm Seal Temperatures with Cooling Air Vented to the Burner Inlet Cavity

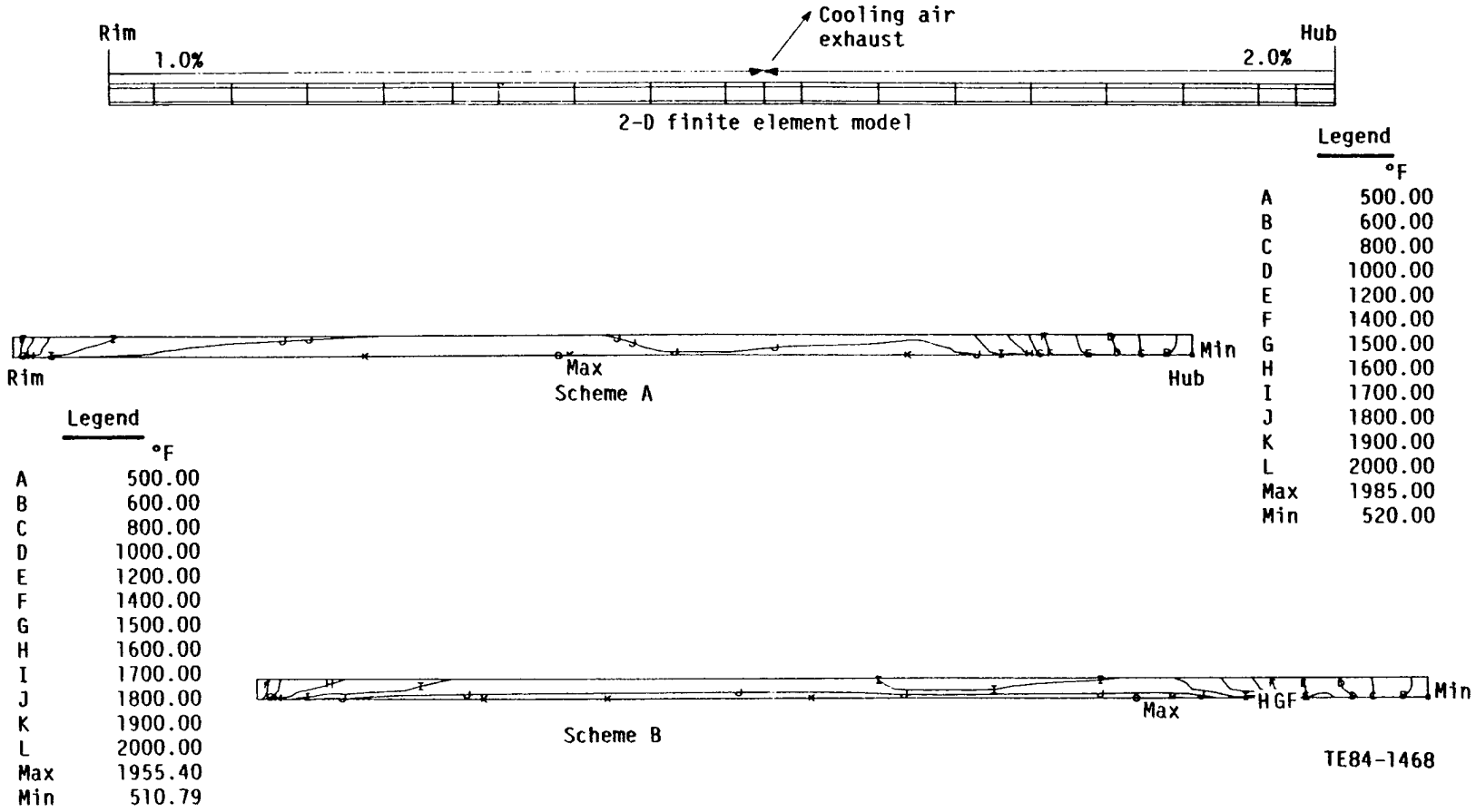

Figure 3-28. Predicted Steady-State Temperature Distributions on the Inboard (Hot) Side Regenerator Crossarm Seal for Scheme A and Scheme B with Cooling Flow Vented to the Burner Inlet Cavity

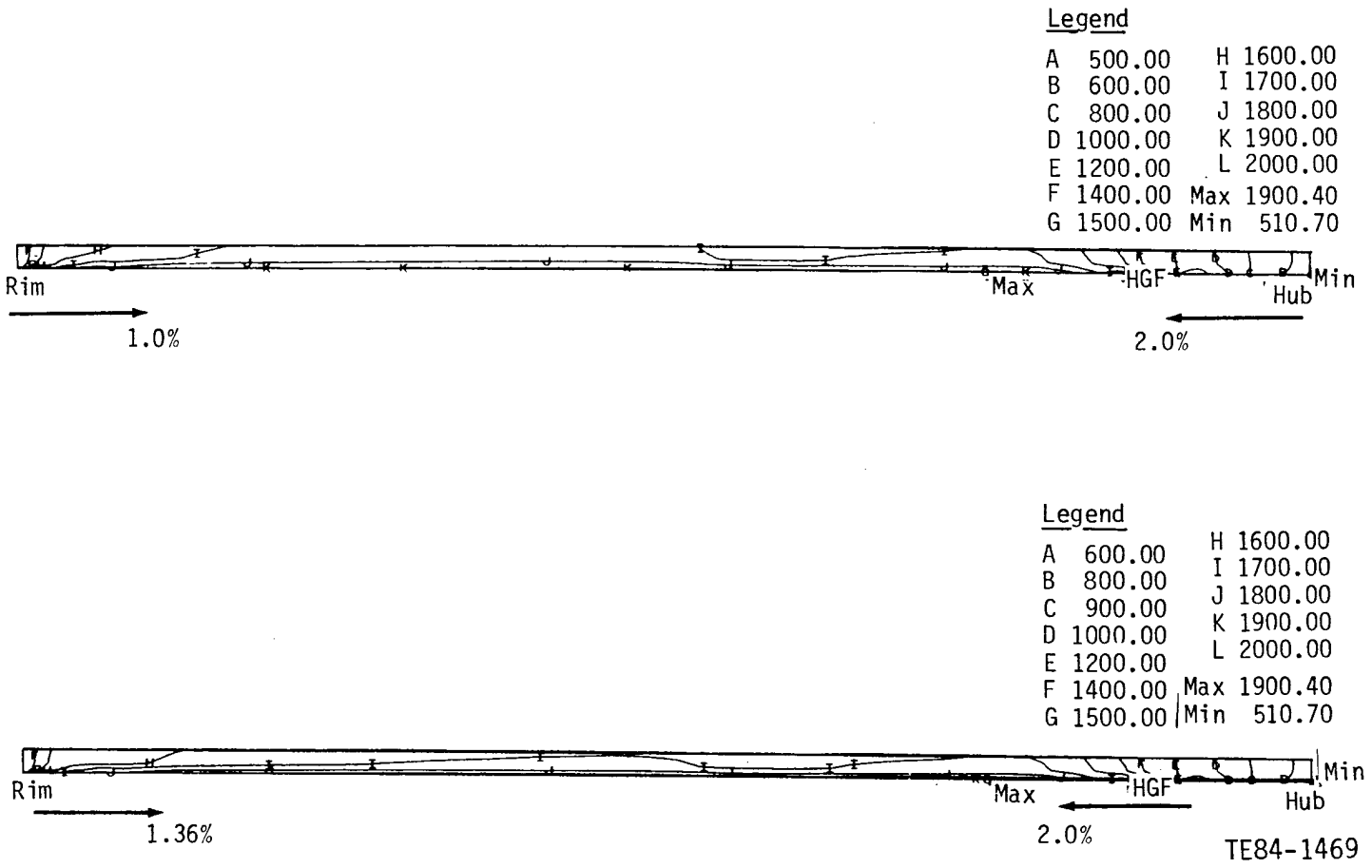

Figure 3-29. Effect of Increasing the Rim Cooling Flow from 1% to 1.36% on Inboard Side Regenerator Crossarm Temperatures for Scheme B with Cooling Air Vented to the Burner Inlet Cavity

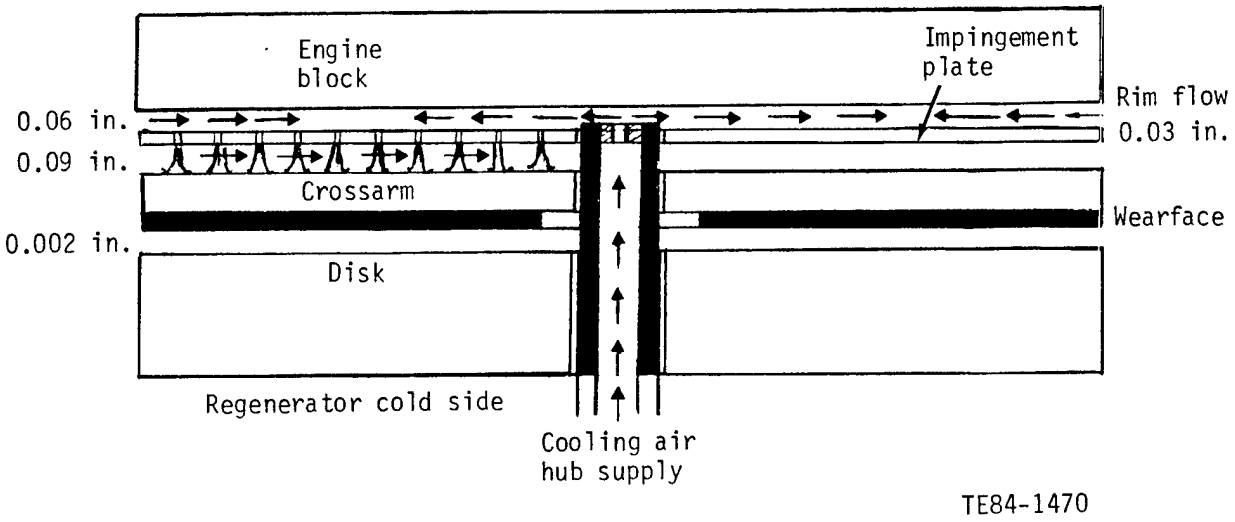

Figure 3-30. The Impingement Cooling Approach (Scheme C) for the Regenerator Inboard Side Crossarm Seal with Cooling Air Vented to the Turbine Exhaust Cavity

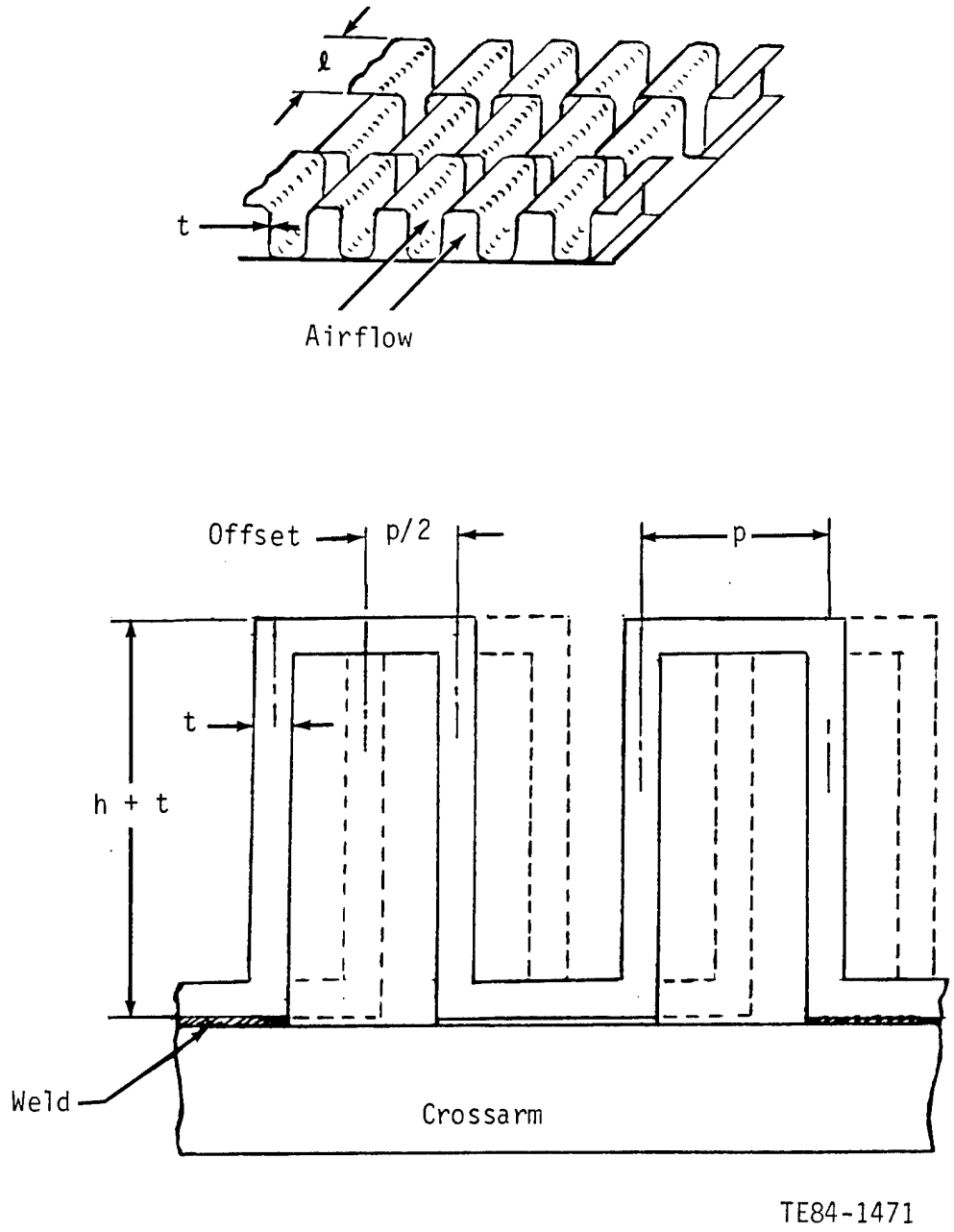

Figure 3-31. Features of the Offset Strip Fin Matrix

arm metal temperature to 1400°F is approximately 4% of the total regenerator disk flow. Preliminary analysis of the effect of this amount of seal cooling flow on total engine plus fuel volume shows that this scheme requires slightly less total engine plus fuel volume than an uncooled ceramic seal.

The main features of the strip fin design are shown in Figure 3-32, where the crossarm between the hub and the rim is divided into five regions with cooling air entering at the rim and discharging through an exhaust port at the hub.

The sections of the crossarm near the rim and the hub do not require the intense cooling provided by the strip fin assemblies but have ribs running parallel to the flow to improve the flow distribution through the smaller individual channels.

The length of the strip fin offsets is reduced as the width of the crossarm increases near the middle of the disk but is constant in each of the three different regions labeled A, B, and C in Figure 3-32. This design produces a frictional pressure drop of 3.9 psia, with cooling air supplied at 239°F. Since this is less than the 13.6 psia driving pressure difference between the compressor discharge and power turbine exhaust flow, a throttling orifice would be required to drop the cooling air pressure at the rim entrance to 18.8 psia.

The temperature contours obtained with this cooling scheme, in which the maximum metal temperature on the cooling air side is held below 1400°F, are shown in Figure 3-33. Figure 3-34 shows the rise in cooling air temperature as it flows over the crossarm plate. The predicted wearface temperature distribution and the gas side temperatures used as boundary conditions are also shown in this figure. The thermal effectiveness of this scheme is around 58% midway between the rim and the hub but increases to almost 90% near the hub as the cooling air bulk temperature increases.

The following is a summary of the cooling schemes that were investigated:

- Scheme A
  nickel alloy crossarm with NiO/CaF_2 wearface cooled by plain channel flow--2.72% rim flow, 4% hub flow exhausted to burner inlet cavity

- Scheme B
  same as Scheme A but with a porous metal insulating layer between wearface and nickel layer (10% dense, 0.08 in. thick)--2.72% rim flow, 4% hub flow

- Scheme C
  impingement cooling of crossarm with porous metal insulation present--12.9% hub and rim flow vented to turbine exhaust

- Scheme D
  cooling of crossarm using offset strip fins in cooling and channels--porous metal insulation present--4% rim flow vented to turbine exhaust

Schemes A and B satisfy the 0.1 psia pressure drop criterion but do not cool the nickel alloy crossarm to 1400°F. Scheme C requires much more cooling airflow than Scheme D, but both cool the crossarm to the required temperature

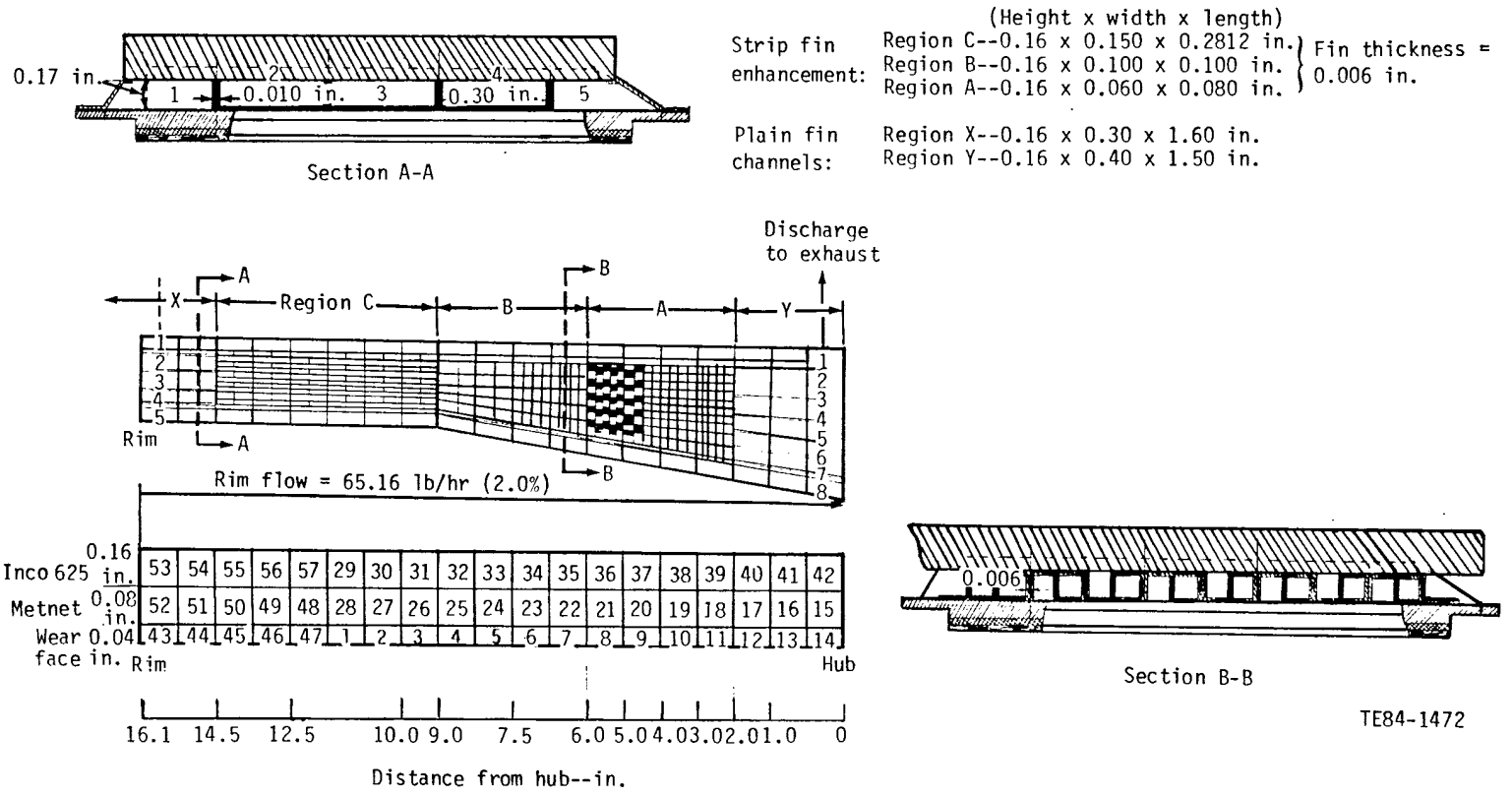

Figure 3-32. Details of the Offset Strip Fin Cooling Scheme (Scheme D) Showing the Cooling Air Channel Layout

Figure 3.33. Steady-State Isotherms for the Inboard Side Regenerator Crossarm Seal Using the Offset Strip Fin Enhancement (Scheme D) with Cooling Air Vented to the Turbine Exhaust Cavity

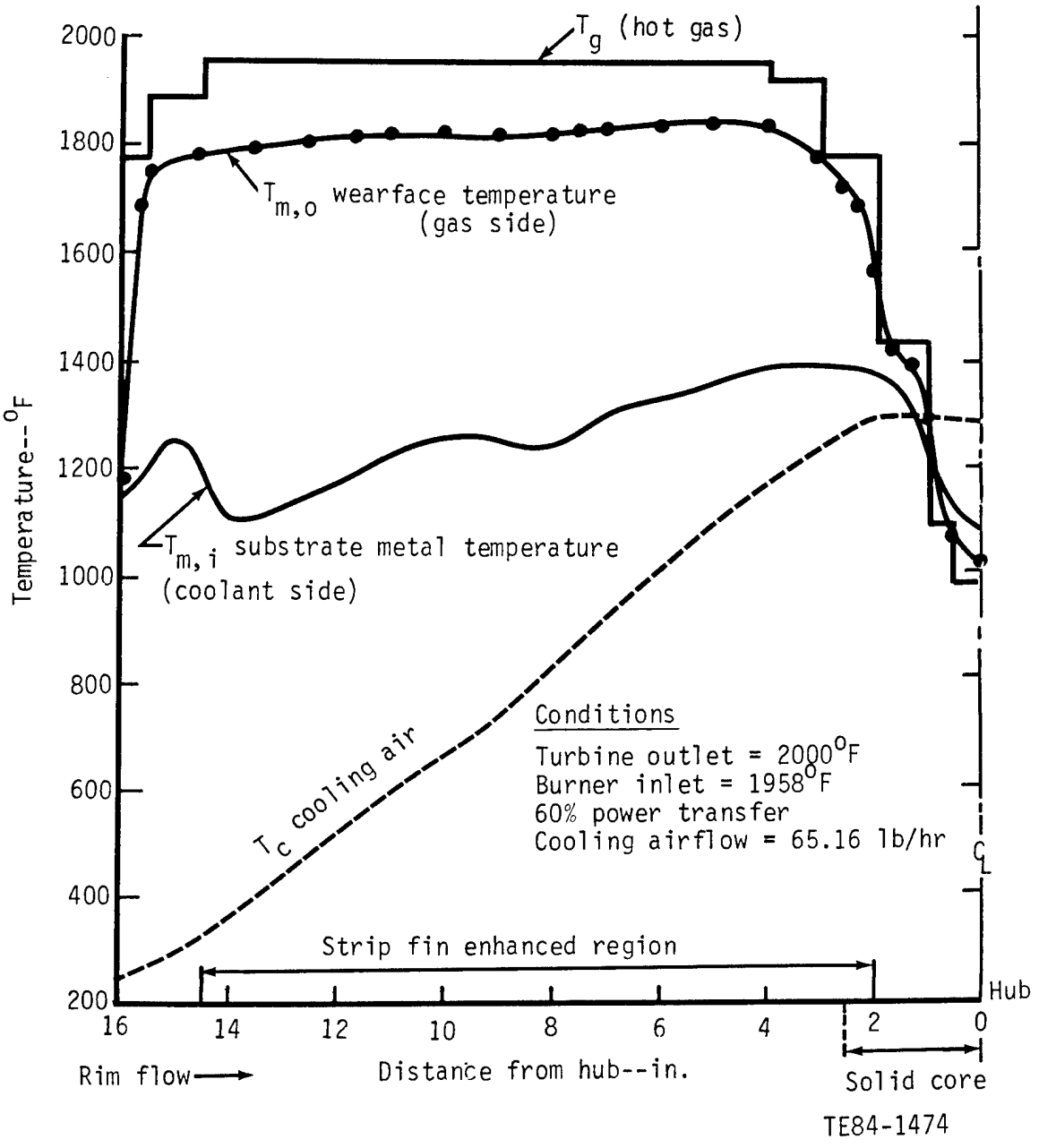

Figure 3-34. Performance of the TACOM Regenerator Crossarm Cooling Scheme Using Offset Strip Fins Predicted Using a 2-D Finite Element Model Scaled Up from the CATE/IGT

level at the cost of a loss in performance because of the bypassing of a portion of the regenerator flow past the turbine stages. Both Scheme C and Scheme D can accommodate changes in the heat loads on the crossarm; however, the impingement scheme cooling flow requirements are excessive.

The 2-D finite element model of the 32-in. diameter TACOM PD335-B1 hot-side regenerator seal crossarm was modified to study the effect of the presence of the engine block (see Figure 3-26) on the crossarm metal temperatures. A heat transfer analysis was also done to determine a cooling channel design and a corresponding maximum exhaust gas temperature that would permit cooling air to be exhausted to the burner inlet and, at the same time, allow the nickel alloy crossarm to be cooled to around 1400°F-1450°F. The gas temperature was reduced in steps from 2000°F (corresponding to the 60% speed, 120-hp condition) until the limited cooling potential of this design was fully utilized by maximizing the heat pickup by the cooling air while keeping the coolant side metal temperatures below 1450°F.

Since the engine block forms the upper face of the cooling air channel, it is important to investigate the influence of engine block heating on coolant side crossarm temperatures. In this study, a 2-D finite element substructure of the engine block was added to the existing model of the crossarm high pressure carryover half (see Figure 3-35a). The cooling air flowing between the two substructures picked up heat as it flowed toward the exhaust port at the regenerator hub.

Since the hot gases in the burner inlet and turbine exhaust cavities also transfer heat to the ceramic block insert (see Figure 3-36), an appropriate cooling scheme for the block is required to limit temperatures and prevent block distortion. Ambient air is forced past the cavity on the side of the block away from the crossarm and flows from one end of the regenerator case to the opposite side (see Figure 3-36). In the present analysis, a linearly increasing block temperature profile was imposed on the finite element model. Steady-state solutions were obtained for average ceramic block insert temperatures between 1090°F and 1390°F. The results indicate that with the inclusion of the block, cooling air temperatures were higher near the rim but were lower near the hub for block temperatures below the cooling air exhaust temperatures. The overall influence of this on coolant side crossarm temperatures was small. The low thermal conductivity of the air and the absence of direct contact and conduction from the strip fin surfaces on the seal reduced the transfer of heat from the block. The temperature plots for average block temperatures of 1190°F and 1390°F with cooling air discharged to the turbine exhaust plenum are shown in Figures 3-35b and 3-35c. Typically, metal temperatures near the rim were approximately 20°F-25°F higher with the inclusion of the ceramic block insert. A cooled bare metal block would not cause this increase.

Since the cooling air discharged to the turbine exhaust plenum for 2000°F capability bypasses the turbine stages with a potential loss in engine efficiency, an attempt was made to investigate the maximum cooling capacity available with the more advantageous design with cooling air vented to the burner inlet cavity.

Earlier studies with this design using plain coolant channels had revealed that the low thermal effectiveness generated for the design was inadequate, and metal temperatures around 1700°F for the 120-hp condition had been obtained. Enhancing the heat transfer from the cooling air channels was investigated by

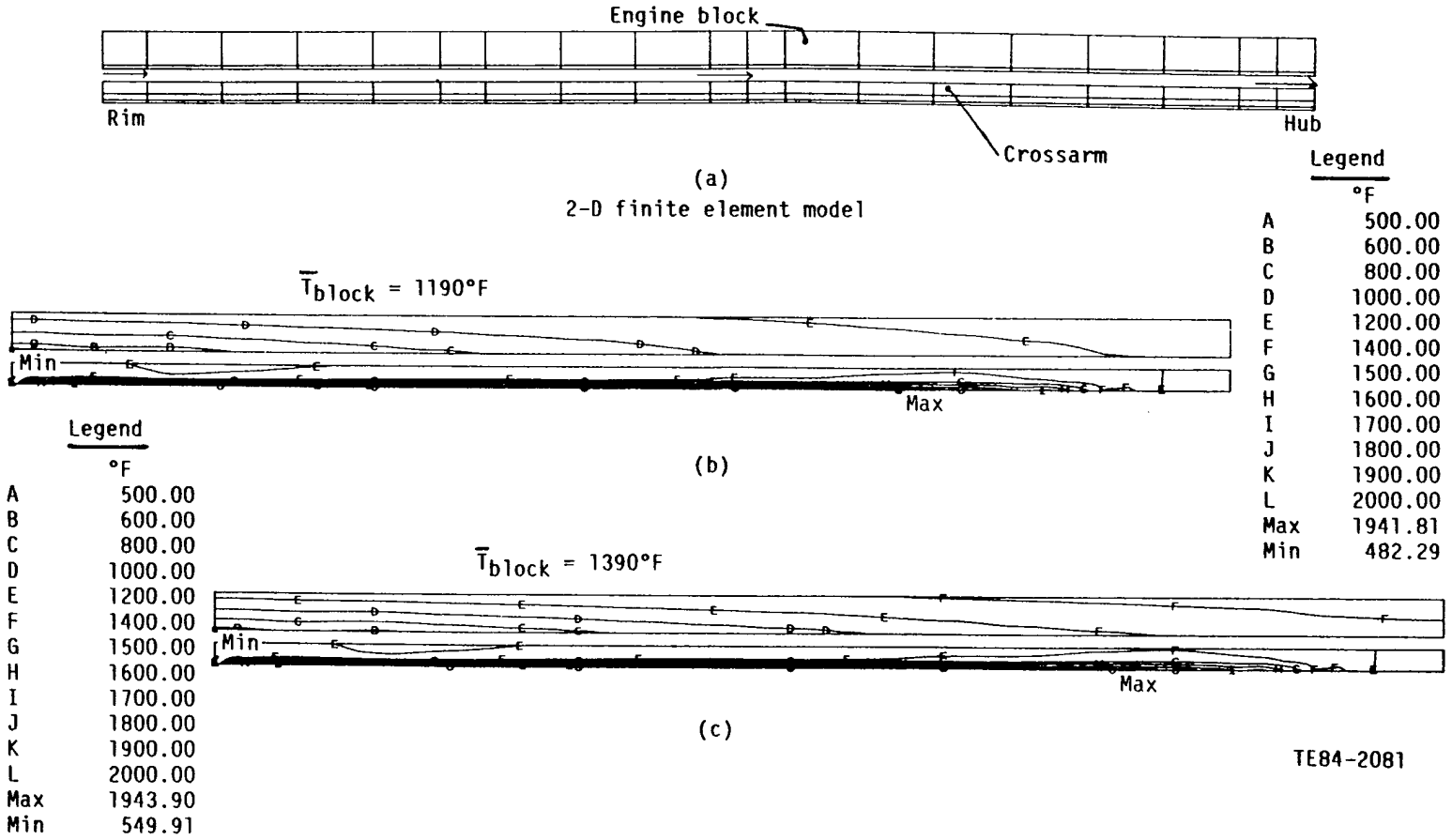

Figure 3-35. Influence of the Engine Block on Crossarm Temperatures for the Strip Fin Enhanced Cooling Scheme

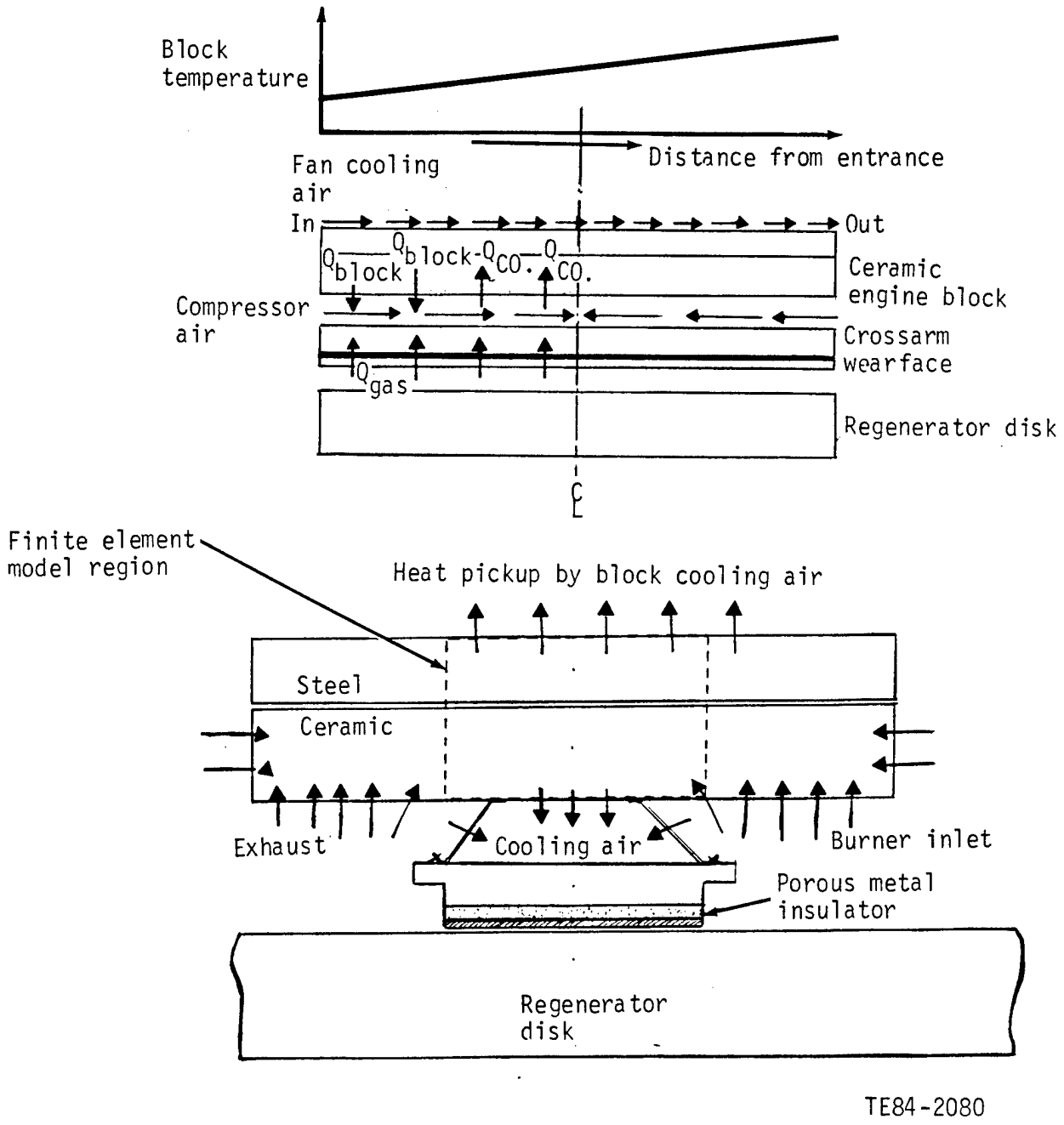

Figure 3-36. Sketch Showing Heat Balance on Engine Block and Block Temperature Distribution Assumed for Analyzing Block/Crossarm Interaction

comparing the performance of several different plain fin configurations. The triangular finned surfaces chosen have a pitch of 0.16 in. and a height of 0.22 in. and are 0.006 in. thick. The layout of these fins in the crossarm channel is shown in Figure 3-37. Good contact (brazed/welded) between the fin base and the crossarm metal is essential to this design since heat conduction through the fin is primarily responsible for the enhancement.

The performance of this scheme is shown in Figure 3-38 where the gas temperature profile used (at 1700°F exhaust) has been scaled down from the profile assumed at the 120-hp, 2000°F exhaust condition. The maximum metal temperature on the coolant side was 1443°F and occurred at the discharge port/midsection location. Increasing the exhaust temperature to 1800°F produced a maximum temperature of 1528°F at the same location for the same flow distribution of 1.6% through the rim and 2% through the hub for both crossarm halves.

To compare the cooling performance of the finned channel design with plain channels for the same total flow of 3.6%, the steady-state coolant side metal temperatures across the crossarm are plotted in Figure 3-39. It should be noted that these temperatures were averaged over the width of the crossarm and were calculated for an exhaust gas temperature of 1700°F. The maximum metal temperature of 1440°F with fins was 123°F lower than the maximum without them, which illustrates the superiority of the finned cooling scheme. In both designs, introducing cooling air through the hub spindle caused appreciable thermal gradients near the hub. These gradients are illustrated in Figures 3-39 and 3-40. The effect of such gradients on seal stress was considered in section 3.1.1.1.

The solid hub of the regenerator disk near the hub also contributes to the reduced wearface heating and lower metal temperatures by blocking the throughflow of hot gases underneath and around the crossarm. Coating the crossarm coolant side face near the hub with a ceramic insulator double wall should reduce excessive cooling by the compressor discharge air in this region.

The following summarizes the conclusions from this preliminary study of the 32-in. inboard crossarm seal at the 120-hp condition:

- In order to hold the coolant side of the Inco 625 crossarm seal to 1400°F at the 120-hp point with 2000°F exhaust, the compressor discharge cooling air had to be vented into the turbine exhaust plenum, with a resulting efficiency loss. A strip fin enhancement scheme for the cooling air channel with coolant supplied from the rim and discharged at the hub required 4% of the regenerator mass flow.

- Cooling the nickel alloy crossarm to 1400°F using compressor air discharged to the burner inlet cavity, while satisfying the 0.1 psia maximum imposed pressure drop limit, requires a reduction in the exhaust gas temperature from 2000°F to 1700°F. A comparison of two candidate schemes, one using plain triangular fins and the other with bare/plain channels, indicated that the scheme with fins was more effective, cooling the inner side of the crossarm seal below 1450°F for an exhaust temperature of 1700°F. For the same total cooling flow of 3.6% (117.3 lbm/hr), the coolant side metal temperatures with the plain channel scheme were over 120°F higher than the corresponding temperatures with the finned channel design. Both schemes satisfy the 0.1 psi channel pressure drop

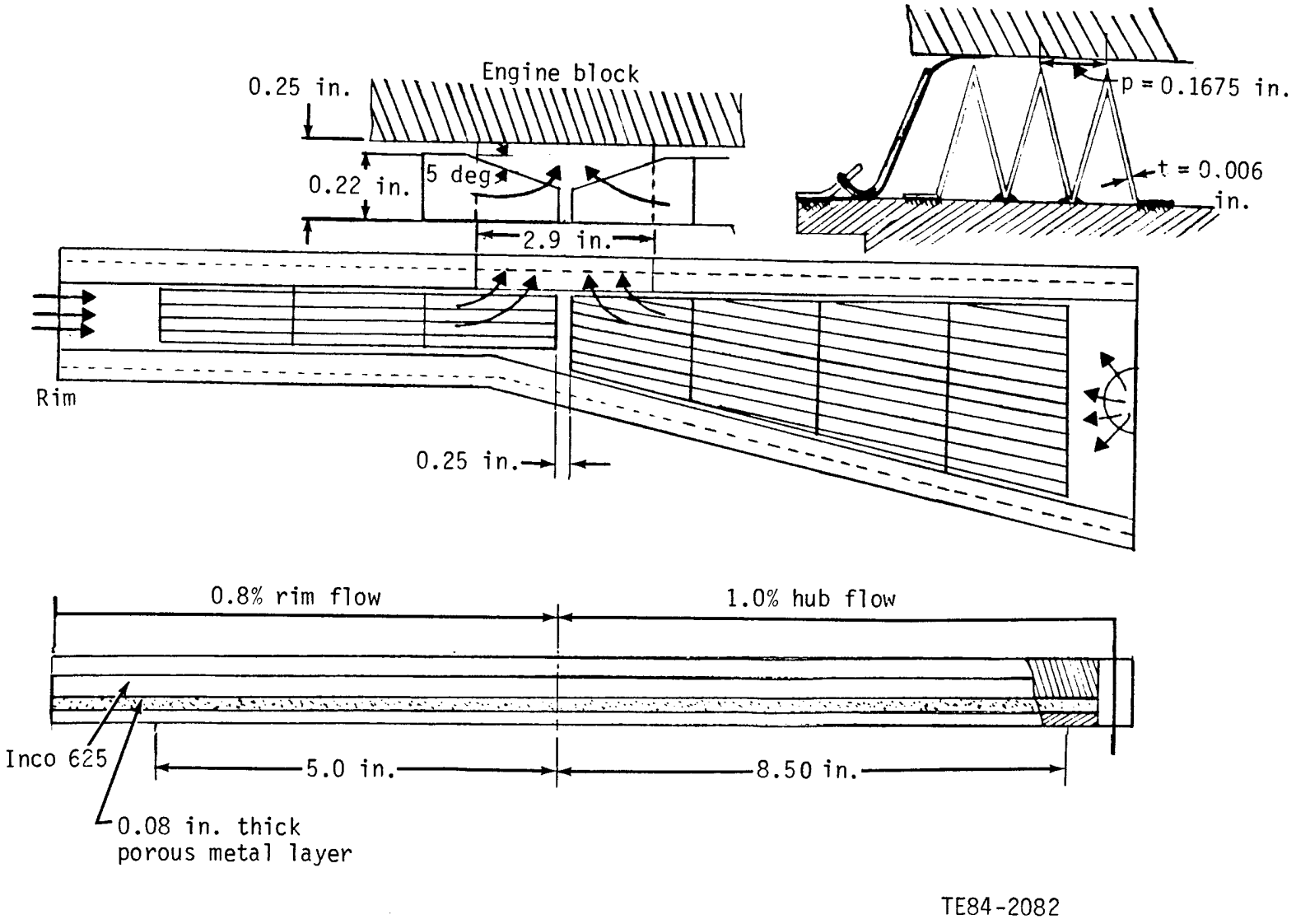

Figure 3-37. Layout of the Plain Triangular Fins in the Cooling Air Channels with Details of the Exhaust Port Design

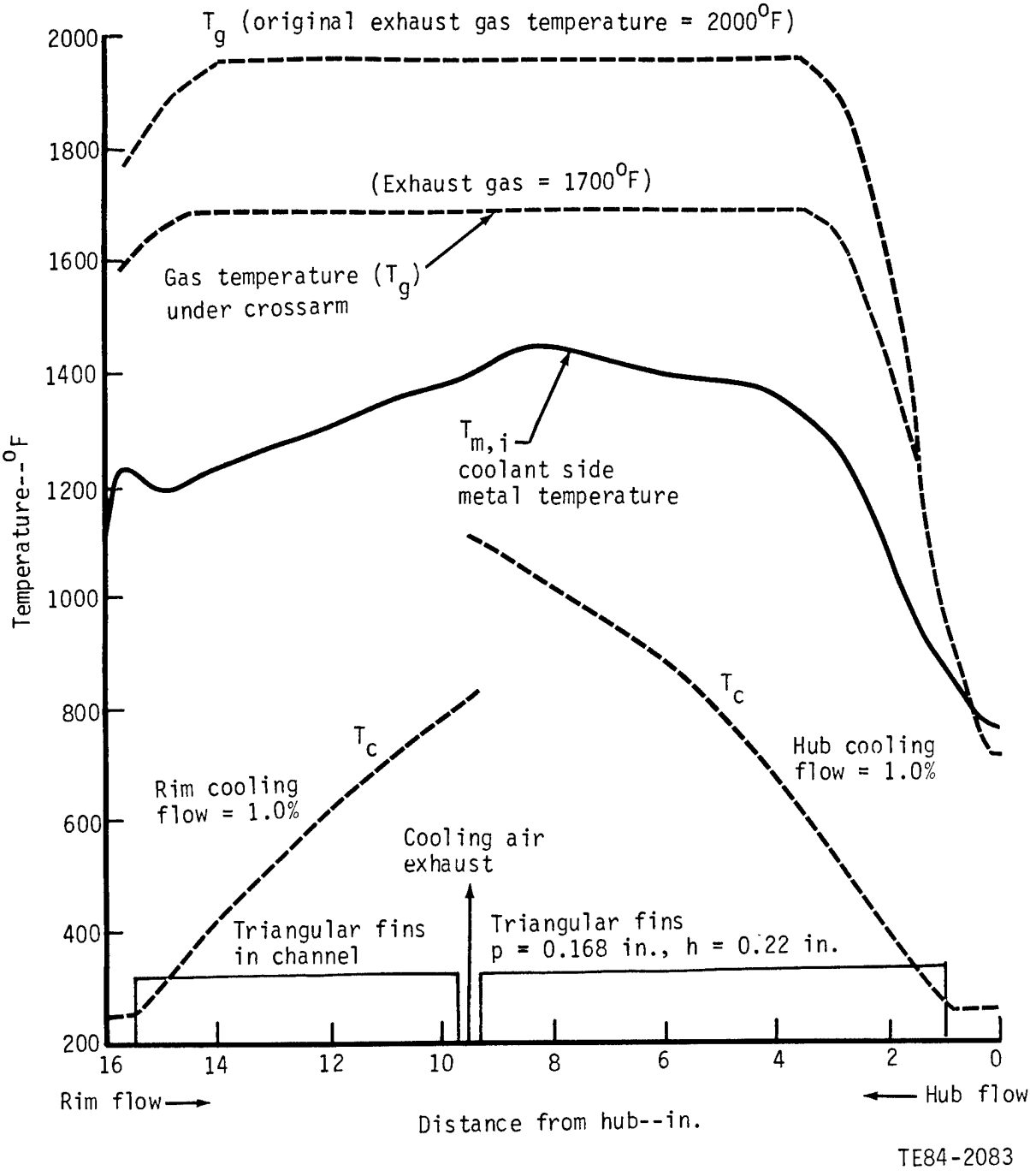

Figure 3-38. Performance of the Triangular Fin-Enhanced Cooling Channels with an Exhaust Temperature of 1700°F Showing Metal and Cooling Air Temperature Distributions

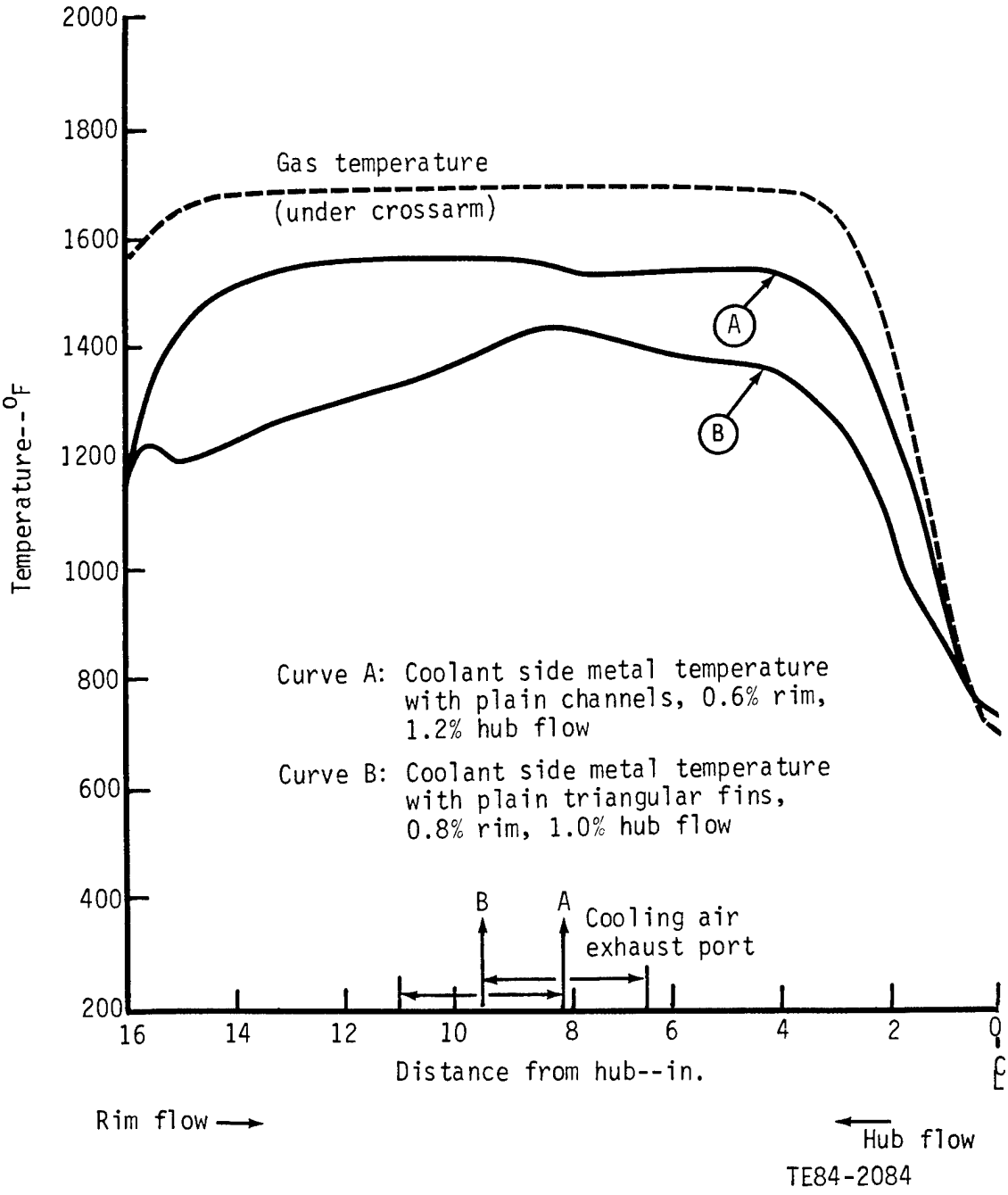

Figure 3-39. Comparison of the Plain Channel and the Finned Channel Cooling Schemes for an Exhaust Temperature of 1700°F with Cooling Air Vented to the Burner Inlet Plenum

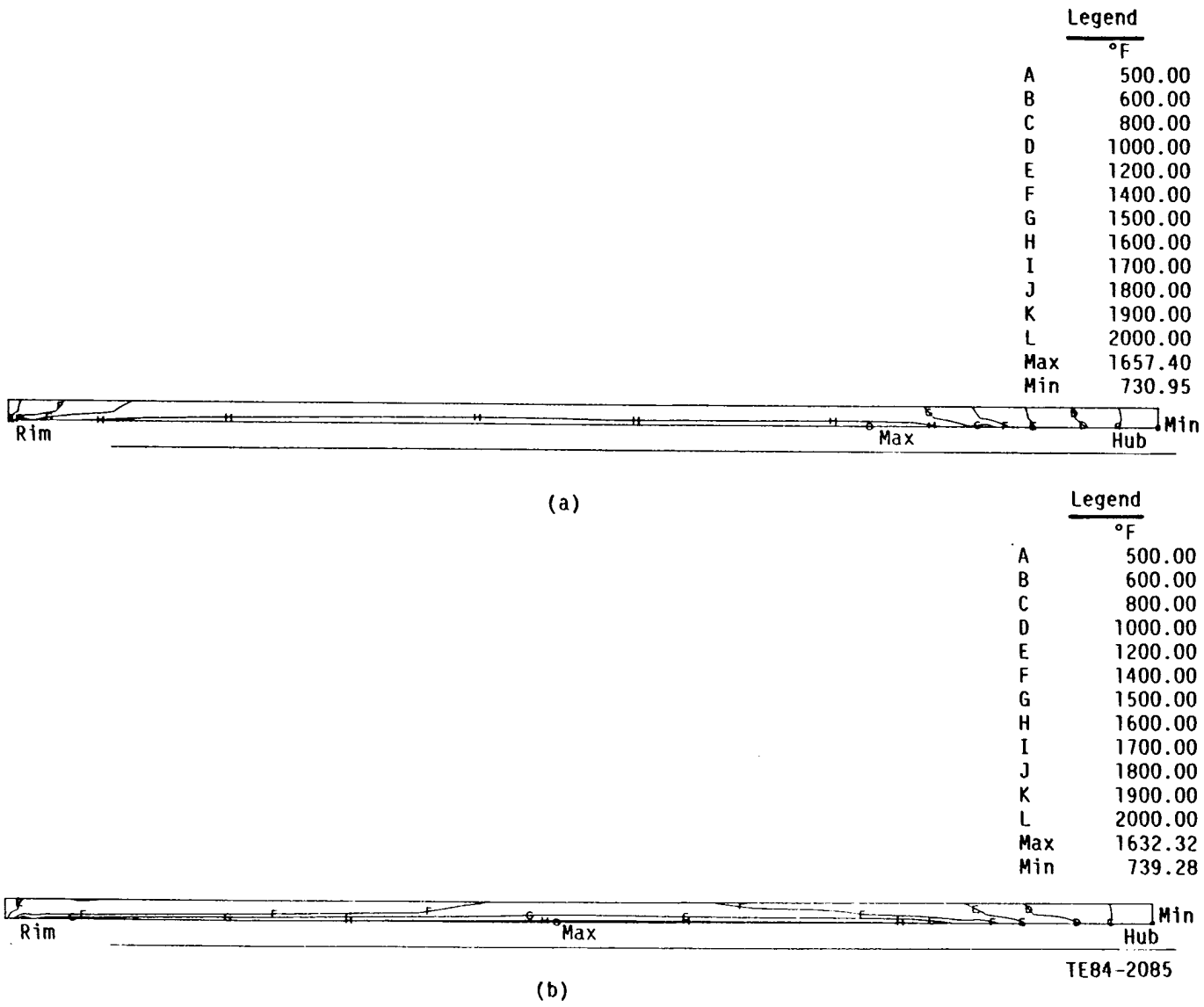

Figure 3-40. Temperature Isotherms on the Regenerator Crossarm Seal for the Plain Channel (a) and the Triangular Finned Channel (b) Designs with the Exhaust Gas Temperature Reduced to 1700°F

limit, and both use a 10% porous metal insulating layer between the wear-face material and the nickel alloy structure, which is 0.08 in. thick.

- o Secondary factors that influence the performance of a given scheme have been identified as the following:
  - o leakage through the leaf seals on either side of the cooling air channels, which increases seal temperature about 40°F
  - o engine block temperatures, block cooling schemes, and block material and thickness above the coolant channel, which appear to have minor effects
  - o quality of fin/crossarm surface brazing or welding and fin material selection
  - o varying crossarm/regenerator disk gap

To get a better understanding of the crossarm cooling problem, a more refined, 3-D finite element model based on the present 2-D model incorporating some of these factors could be developed. Allison report TDR AD0440-035 covers details of the metal seal cooling.

3.1.1.3 Cooled seal loading. Preliminary load calculations for the cooled seal crossarm show that if a groove pattern is established to provide Allison's typical loading at low speed, a much higher than normal, untolerable loading results at high speed. This is caused by secondary effects of lower pressures required to produce the cooling flow on the cooled side of the crossarm. The high load at high speed will require valves that vent separate portions of the groove pattern to exhaust or to compressor discharge at appropriate speeds for load control. In addition, a cooling flow cutoff valve is required to prevent high load on the cold seal crossarm at high speed. Cold seal load at low speed would still be higher than desired but would be tolerable. The high load occurs because the low pressure associated with cooling flow is not present on the uncooled cold seal. Pressure pattern on the cold seal and hot seal wear-faces cannot be set independently because whatever is set for one is communicated through the disk to the other. Load control valving has not been demonstrated and represents a development risk for the cooled seal. An uncooled ceramic seal would have high but tolerable loads at high speed and would not require load control valving. A comparision of cooled metal and uncooled ceramic seal concepts is made in the following paragraphs.

Because of the seal loading problems introduced by the pressure drop required to cool the metal seal, the decision was made to shift to the uncooled ceramic design. During preparation of this final report, a new concept evolved that we believe would provide efficient cooling for a metal seal without incurring the loading problem. Time did not permit supporting analysis. Figure 3-41 shows the concept. Cooling air is again introduced to the crossarm at the center hub and both ends and is contained between sealing leaves on either side. It is then admitted to a row of holes spaced according to cooling needs along the high pressure edge. These holes feed a finned space sandwiched between seal halves that exhausts to the low pressure edge. The holes throttle the flow and maintain virtually full pressure on the outer loading surface thus eliminating the loading problem previously described. Although it seems evident that this scheme would solve loading and cooling problems, crosswise thermal gradients could produce a leakage problem by thermal distortion just as lengthwise gradients were shown to do near the end of section 3.1.1.1.

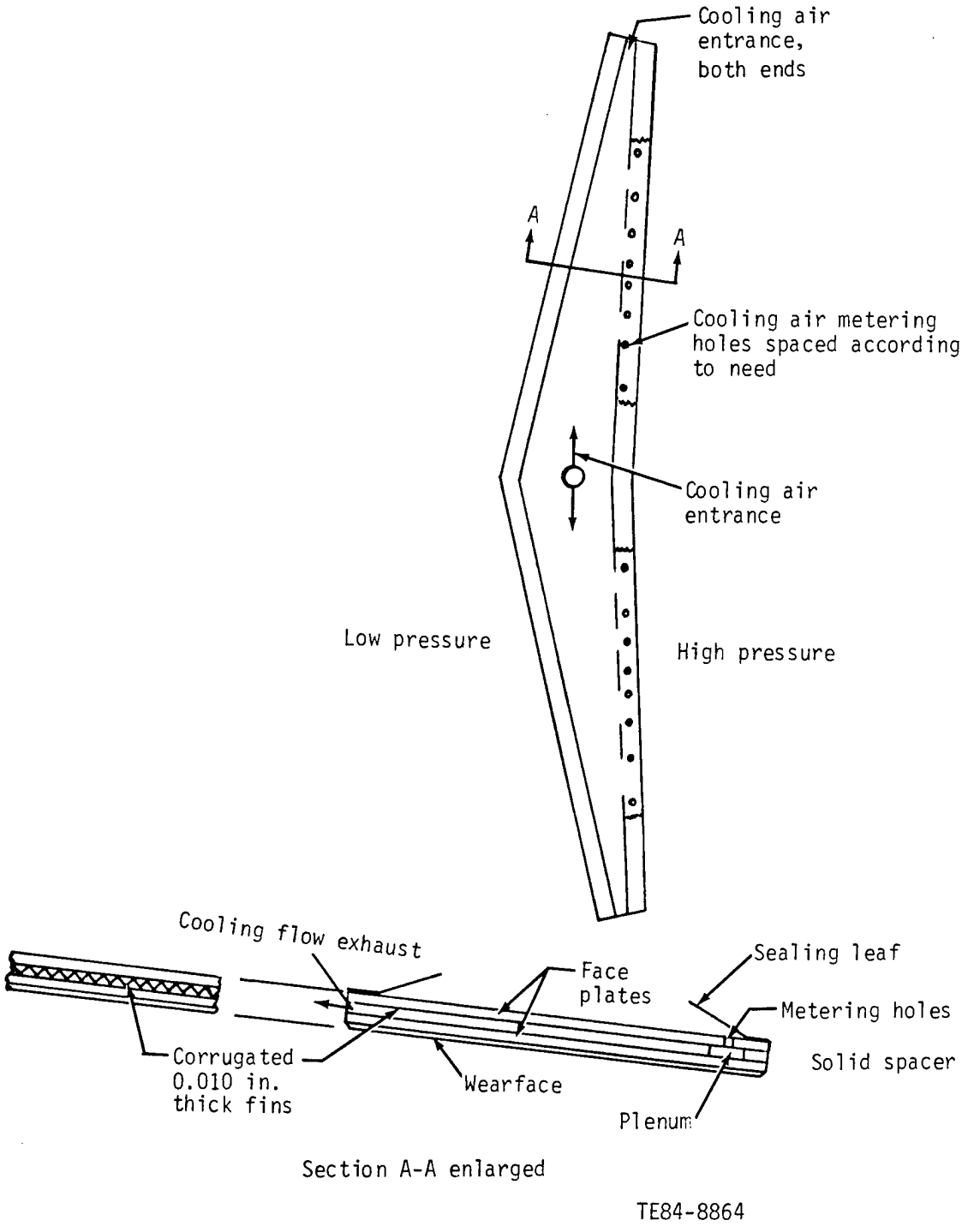

Figure 3-41. Cooled Regenerator Seal Crossarm

3.1.2. Ceramic Seal

3.1.2.1. Seal Stress. Stress analyses of a lithium aluminum silicate (LAS) ceramic regenerator seal indicate a reasonable 0.979 probability of survival with current material and 0.999 with material improved by 20% in strength and Weibull slope.

Table 3-2 summarizes the stress results for maximum horsepower. Stresses were calculated with pressure alone and with combined pressure and temperature since pressure is the main source of stress and the greatest unknown. Maximum stresses are shown for the various portions of the seal. The fillet area, which joins the rim and crossarm, has the highest stress. Further refinement of the finite element mesh and the fillet shape probably would reduce those stresses. Both tensile (+) and compressive (-) principal stresses are shown although only tensile stresses are used in calculating probability of survival. This is conventional practice because the compressive strength of ceramics is commonly 5 to 10 times the tensile strength.

The crossarm has the lowest probability of survival partly because a large volume of the crossarm is highly stressed while only a small volume of the fillet area is highly stressed.

The highest tensile stress of 6400 lb/in.^{2} occurs with pressure only and is in the air side fillet. It is relieved by inclusion of temperature. With combined pressure and temperature, the highest tensile stress of 5000 lb/in.^{2} is on the exhaust side of the crossarm and is primarily caused by bending due to the pressure load. Rim stresses are mostly compressive (-).

Weibull material properties for the LAS ceramic used to calculate the probabilities of survival are as follows:

	Surface	Volume
Characteristic strength	11,853 lb/in.^{2}	8,826 lb/in.^{2}
Weibull slope	12.48	14.37

Figures 3-42 through 3-45 show the distribution of the two principal stresses for the combined pressure and temperature. Figures 3-42 and 3-43 show the tensile principal stress and Figures 3-44 and 3-45 the compressive principal stress. Figures 3-42 and 3-44 are for half of the complete seal, while Figures 3-43 and 3-45 show details of the rim to crossarm joint and fillets. Figures 3-46 through 3-49 show the same features for the pressure only case.

The leaf carrier is shown as item 12 in part 3 of Figure 3-50. Although the metal cross-arm portion (item 12C) seals 1960°F burner inlet air from 2000°F exhaust gas, it is totally surrounded by 240°F compressor discharge air introduced through the hub shaft and at both ends. Heat shields (item 16) on both edges duct the 240°F leakage air around the edges and are themselves cooled by it. This leakage air is finally discharged to burner inlet and exhaust by a series of holes in the shields. Although the leaf carrier for the ceramic seal serves a somewhat similar function as the cooled metal seal, it does not suffer the high rate of heat input through a wearface as does the cooled metal seal (see Subsection 3.1.1).

Table 3-2. Maximum Ceramic Seal Stresses and Probability of Survival at Maximum Power

	Maximum stress		Probability of survival		
Location	With pressure and temperature	With pressure only	With pressure and temperature	With pressure only	With pressure and temperature plus 120% strength*
Exhaust side					
Fillet	-8750 +2600	-7170	0.99948	0.99999	0.99995
Rim	-7000	-5000 +1800			
Crossarm	+5000	+4500	0.97995	0.98901	0.99922
Air side					
Fillet	+4200	+6400	0.99981	0.98925	0.99999
Rim	-6000 +1800	-5000 +4500			
Crossarm	-5000	-5000			
		Overall	0.97925	0.97837	0.99916

*assumes 20% increased material strength and Weibull slope
+ denotes tensile stress
- denotes compressive stress
only tensile stresses were considered for probability of survival

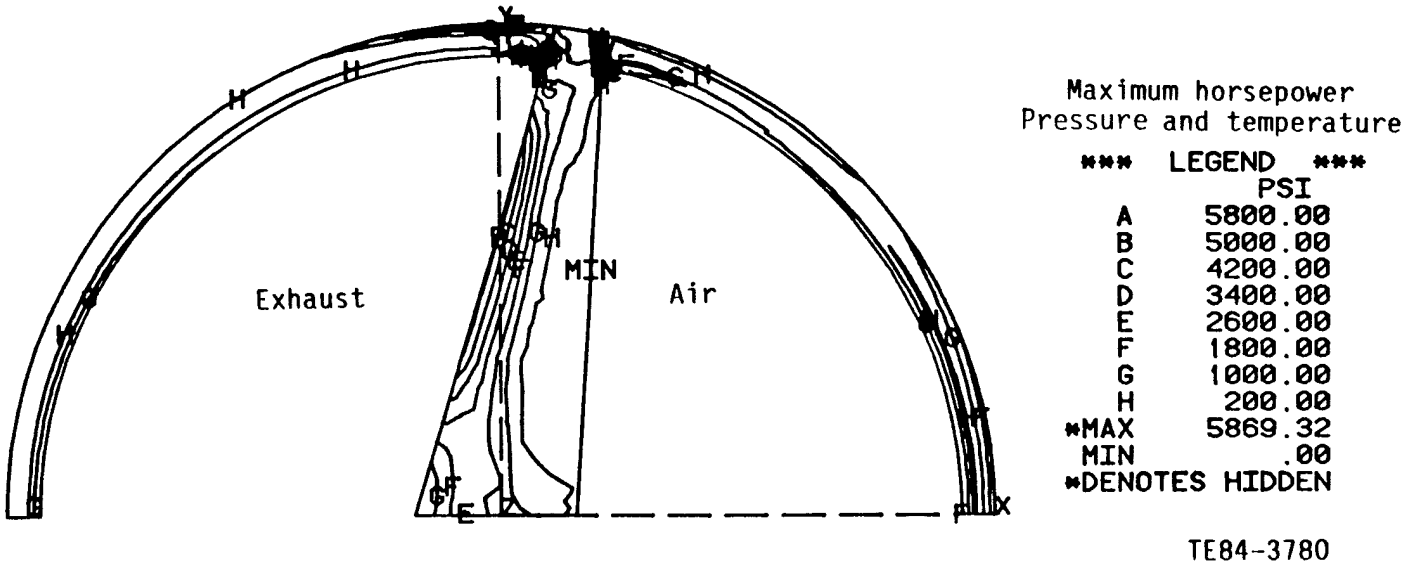

Figure 3-42. TACOM Ceramic Regenerator Seal Contour Plot of Maximum Principal Stress (Tensile)

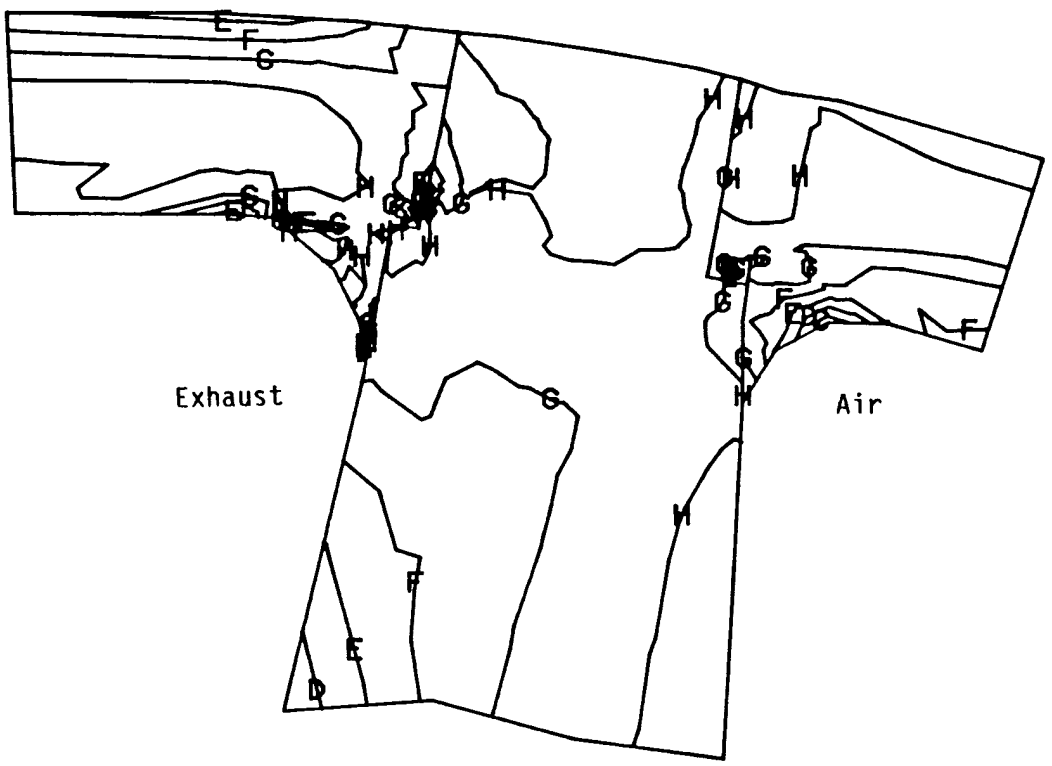

Maximum horsepower
Pressure and temperature

*** LEGEND ***	PSI
A	5800.00
B	5000.00
C	4200.00
D	3400.00
E	2600.00
F	1800.00
G	1000.00
H	200.00
*MAX	5869.32
*MIN	2.16

*DENOTES HIDDEN

TE84-3781

Figure 3-43. TACOM Ceramic Regenerator Seal Contour Plot of Maximum Principal Stress (Tensile)

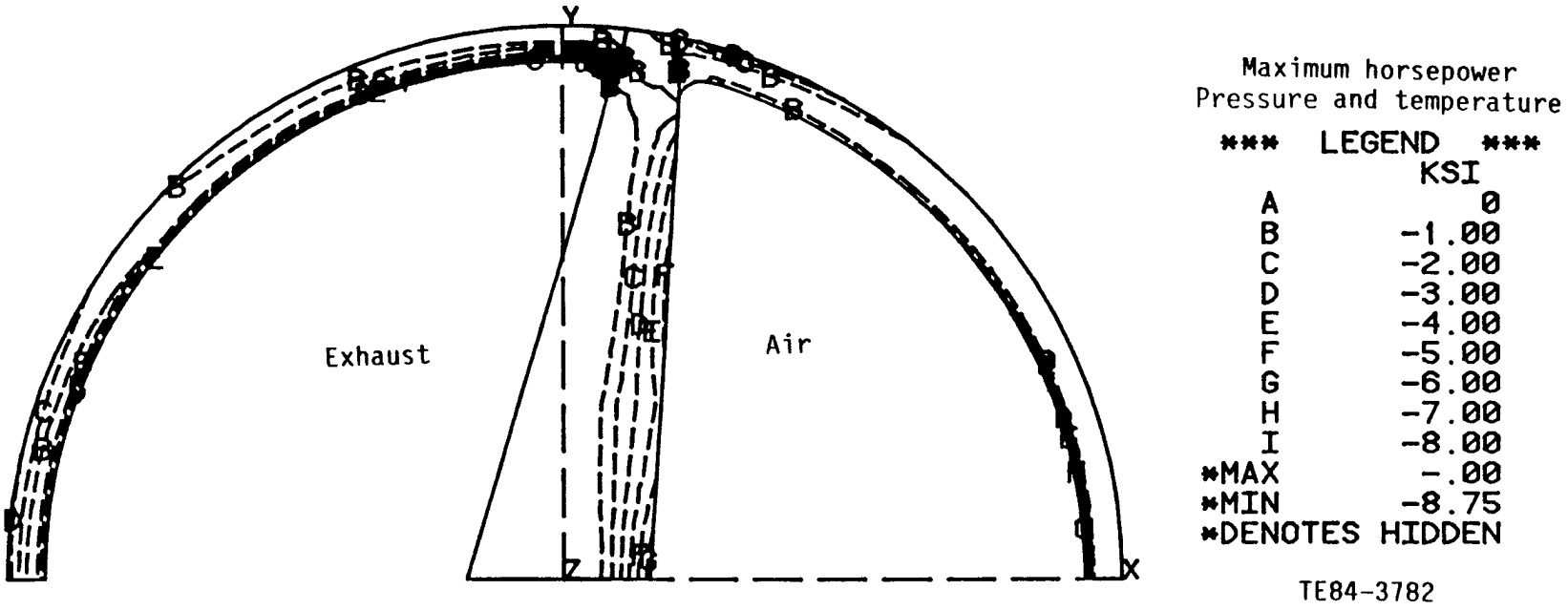

Figure 3-44. TACOM Ceramic Regenerator Seal Contour Plot of Minimum Principal Stress (Compressive)

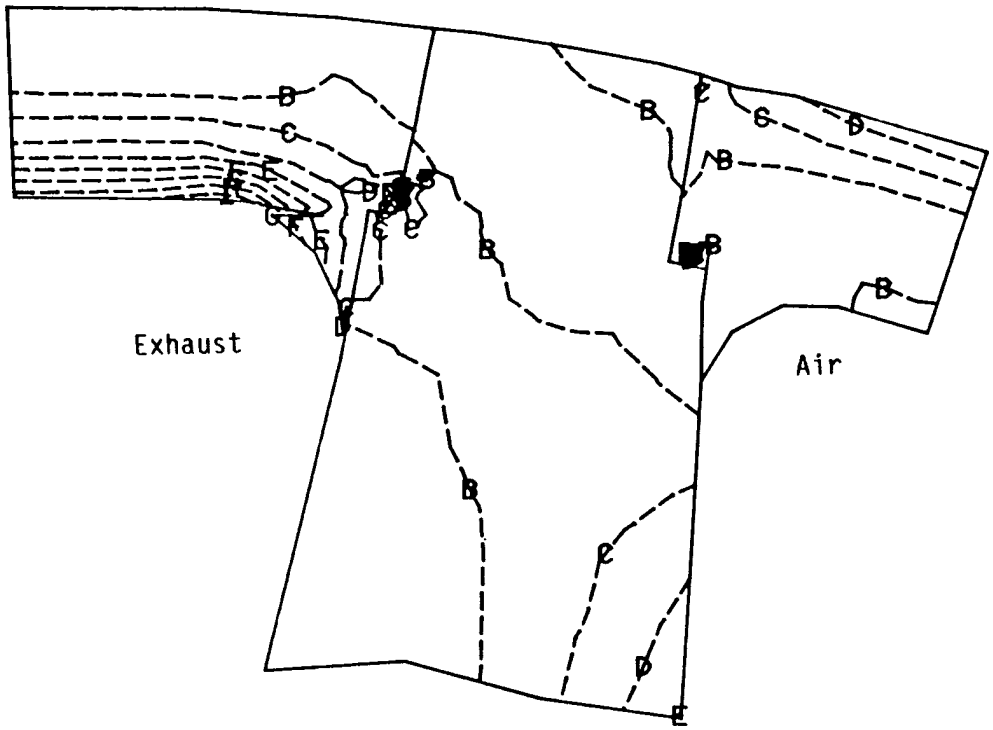

Figure 3-45. TACOM Ceramic Regenerator Seal Contour Plot of Minimum Principal Stress (Compressive)

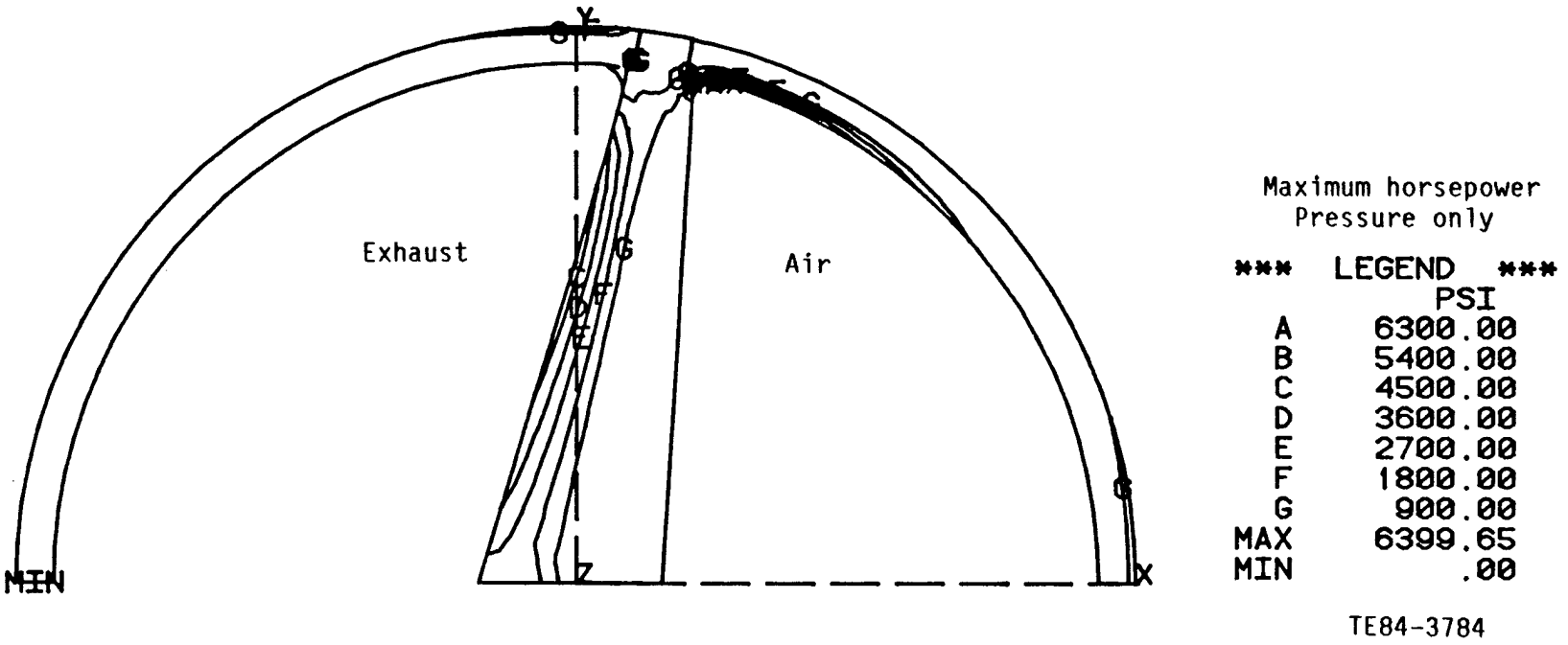

Figure 3-46. TACOM Ceramic Regenerator Seal Contour Plot of Maximum Principal Stress (Tensile)

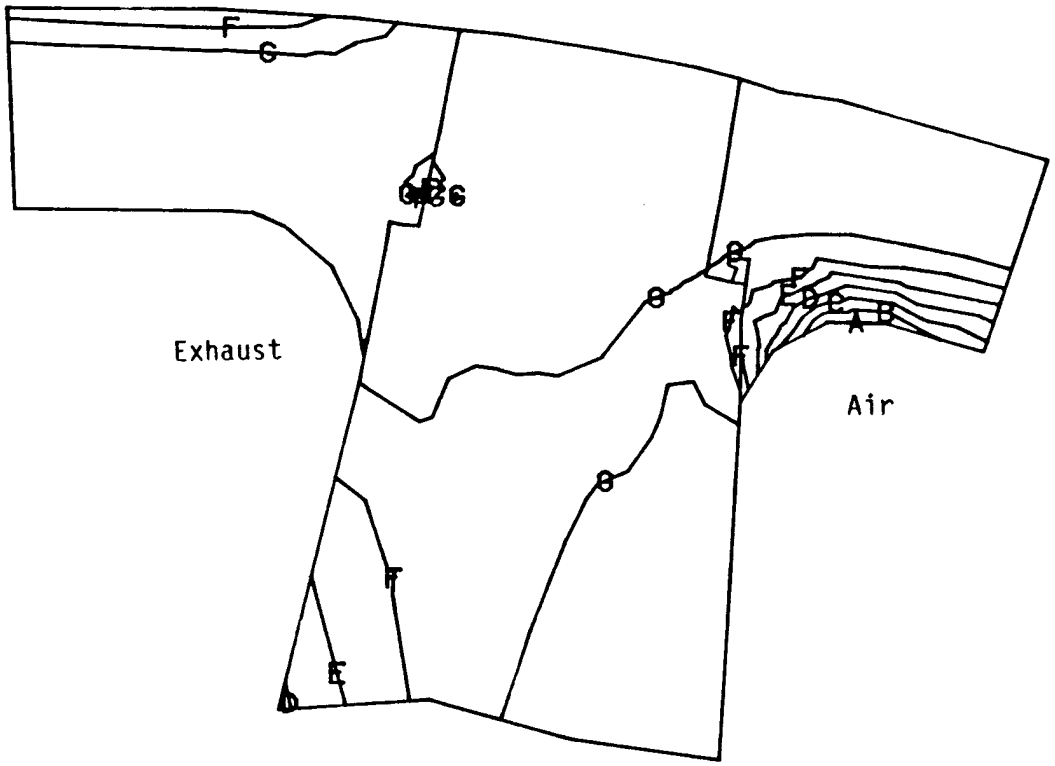

Maximum horsepower
Pressure only

***	LEGEND ***
	PSI
A	6300.00
B	5400.00
C	4500.00
D	3600.00
E	2700.00
F	1800.00
G	900.00
*MAX	6399.65
*MIN	.00

*DENOTES HIDDEN

TE84-3785

Figure 3-47. TACOM Ceramic Regenerator Seal Contour Plot of Maximum Principal Stress (Tensile)

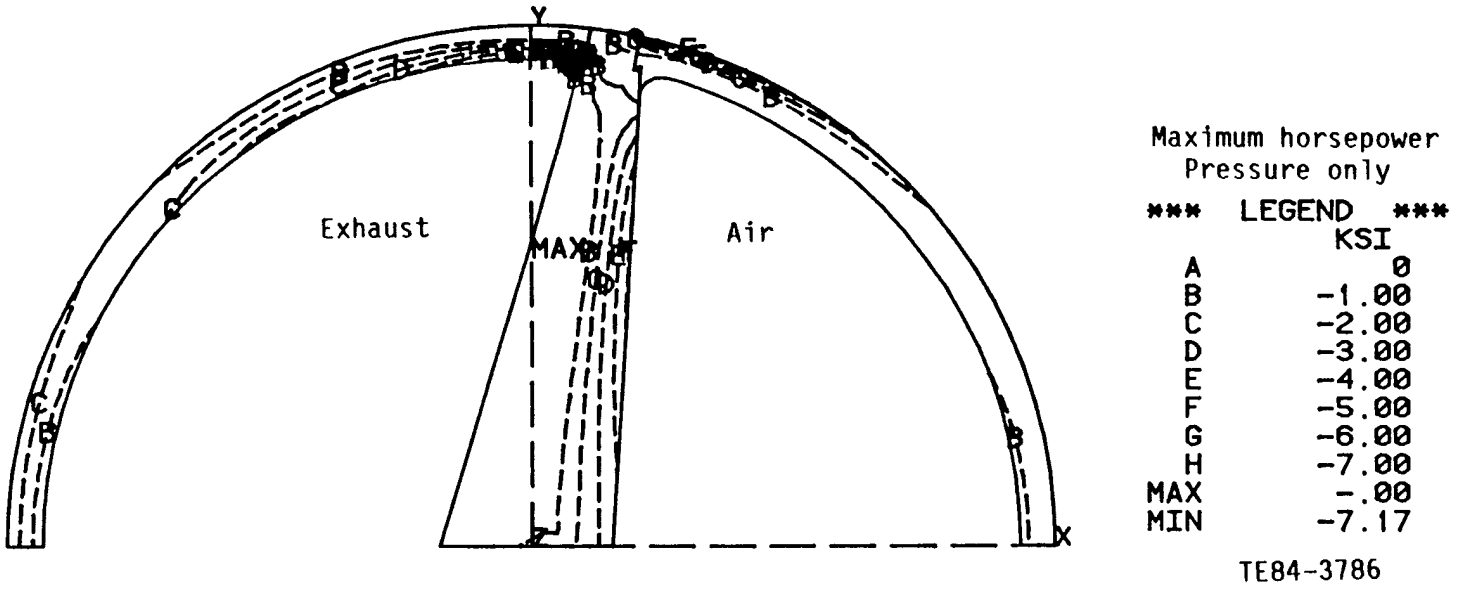

Figure 3-48. TACOM Ceramic Regenerator Seal Contour Plot of Minimum Principal Stress (Compressive)

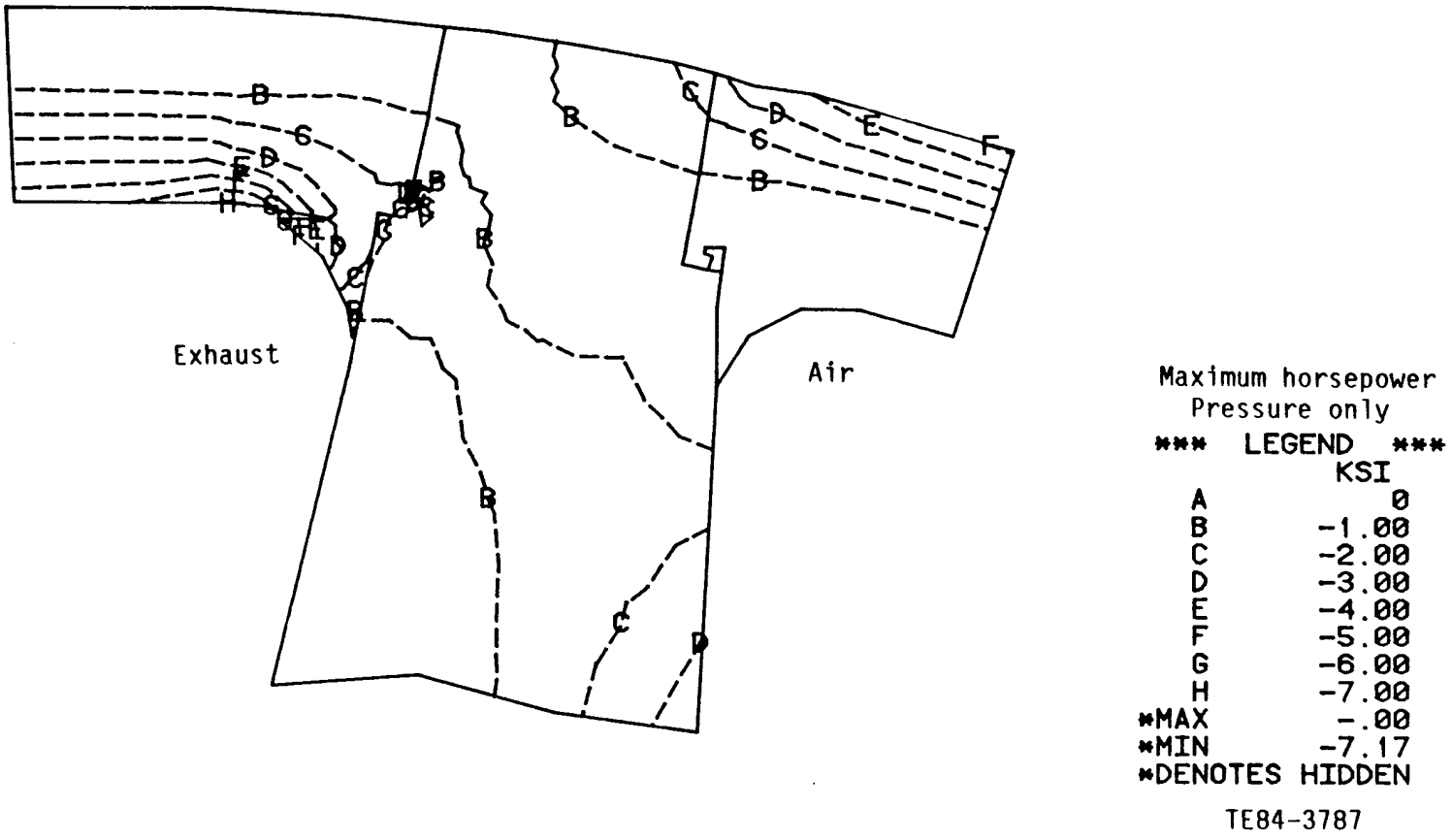

Figure 3-49. TACOM Ceramic Regenerator Seal Contour Plot of Minimum Principal Stress (Compressive)

3.1.2.3. Seal wearface. Allison has not yet performed the laboratory friction and wear testing required to select a seal wearface material for 2000°F operation. Some candidate materials have been selected and purchased in powder form for evaluation in the DOE/NASA AGT 100 automotive turbine program. AGT 100 priorities do not permit wearface testing at this time.

A ceramic seal substrate or carrier with near zero thermal expansion to minimize thermal stress is now favored. Wearface attachment problems would be minimized if the wearface also had low expansion even though it was not bonded to the substrate. The wearface is currently envisioned to be hot pressed and sintered with beveled edges and retained by ceramic cement, as shown in Figure 3-51. The wearface would not be bonded to its substrate. It would be divided into segments with thermal expansion joints and clearance (also shown in Figure 3-51). A similar attachment scheme with expansion joints has been used successfully by Allison for years to attach graphite seal wearfaces to metal substrates. For a low expansion ceramic substrate, differential expansion would be reversed from that of the metal substrate. With a metal substrate, the wearface is installed with a tight fit and becomes loose at high temperature, while the reverse would be required with a ceramic substrate.

Fortunately, ZnO provides the lowest friction, lowest wear, and lowest expansion of the many wearface materials that have been evaluated. Therefore, ZnO would be selected as the primary or possibly the sole constituent of candidate wearfaces.

In the past, ZnO wearfaces have incorporated large quantities of CaF_2. A small quantity is desirable as a solid lubricant. Larger amounts are used to produce a thermal expansion match with metal substrates by combining the high expansion of CaF_2 with the low expansion of ZnO. When 25% or more CaF_2 is added to ZnO the wearface becomes too soft to resist abrasive damage. SnO_2 or MnO_2 is added to increase hardness.

Allison has shown that CaF_2 reacts with the aluminum silicate (AS) disk material at temperatures of 1800°F and above, producing calcium fluorosilicate and aggravating wear. Therefore, CaF_2 content should be kept to a minimum. For a ceramic substrate, CaF_2 content also should be kept to a minimum to achieve less differential expansion. SrF_2 has also demonstrated good friction properties and should be tested to determine whether reaction with the disk would be reduced.

With the foregoing concerns in mind, the following wearface candidates are recommended for use with a ceramic substrate at 2000°F:

- o 100% ZnO
- o 95% ZnO/5% SrF_2--if friction of 100% ZnO is too high
- o 90% ZnO/10% SnO_2--if more abrasion resistance is required
- o 85% ZnO/10% SnO_2/5% SrF_2--if lower friction and more abrasion resistance are required

Development testing is required.

3.2. Cold Side Seal

No new technology is required for the cold side seal. The cold side seal shown in Figure 3-50, items 18 through 23, is typical of Allison seals in use. It features a stainless steel substrate with weld attached leaf seal and plasma spray attached graphite wearface. The graphite has demonstrated capability for operation at 1100°F on hot seal rims and would not be expected to operate above 950°F in this cold seal application. As mentioned in the hot seal discussion, stress analysis of the leaf structure at 9:1 pressure ratio showed a minimum margin of 2.29.

3.3. General Seal Concerns

3.3.1. Seal Leakage. The analytical approach to seal leakage depends on an assumption of a leakage gap between the seal wearface and the regenerator disk surface. Allison employs the method defined by D. B. Harper in the February 1957 ASME Transaction wherein the successive disk matrix walls are treated as orifices in series with consideration of disk rotation. An average seal clearance of about 0.002 in. is required for calculated leakage to equal actual measured leakage. Since the full sealing area of a seal wearface normally shows a rubbed surface, the implied clearance must be due to unevenness in the disk surface. A disk shows rub spots only at junction points of the matrix walls, which are strong points tending to carry all the seal load, while walls between junctions are more readily worn away. Disk wear, however, is minimal, only amounting to about 0.004 in. wear in the 2,500 hr seal life required of this application.

If the seals are in contact at present operating pressure, as evidence shows, then increased pressure will not decrease the leakage gap, and leakage will become a direct function of pressure. This is the case that has been assumed in Allison's leakage projection for the AIPS where leakage was only projected to increase from the present well-established IGT 404-4 engine level of 4.0% to 4.8%. The increase was solely due to an allowance of 0.8% for uncertainties; scaling predicted no change with a reduction in disk thickness from 3 in. to 2.5 in. The following scaling equation was used:

$$L_2 = 0.3L_1 \frac{R_{c_2}}{R_{c_1}} \frac{D_2}{D_1} + 0.3L_1 \frac{R_{c_2}}{R_{c_1}} + 0.1 \frac{R_{c_2}}{R_{c_1}} \frac{D_2}{D_1} + 0.3\, L_1 \frac{R_{c_2}}{R_{c_1}} \left(\frac{D_2}{D_1}\right)^2 \frac{N_2}{N_1} \frac{\omega_2}{\omega_1}$$

wearface leaf joints leaves carryover

where

- L = absolute leakage
- D = disk diameter
- R_c = engine compression ratio
- W = engine airflow
- N = disk speed
- ω = disk thickness
- 1 = baseline
- 2 = new design

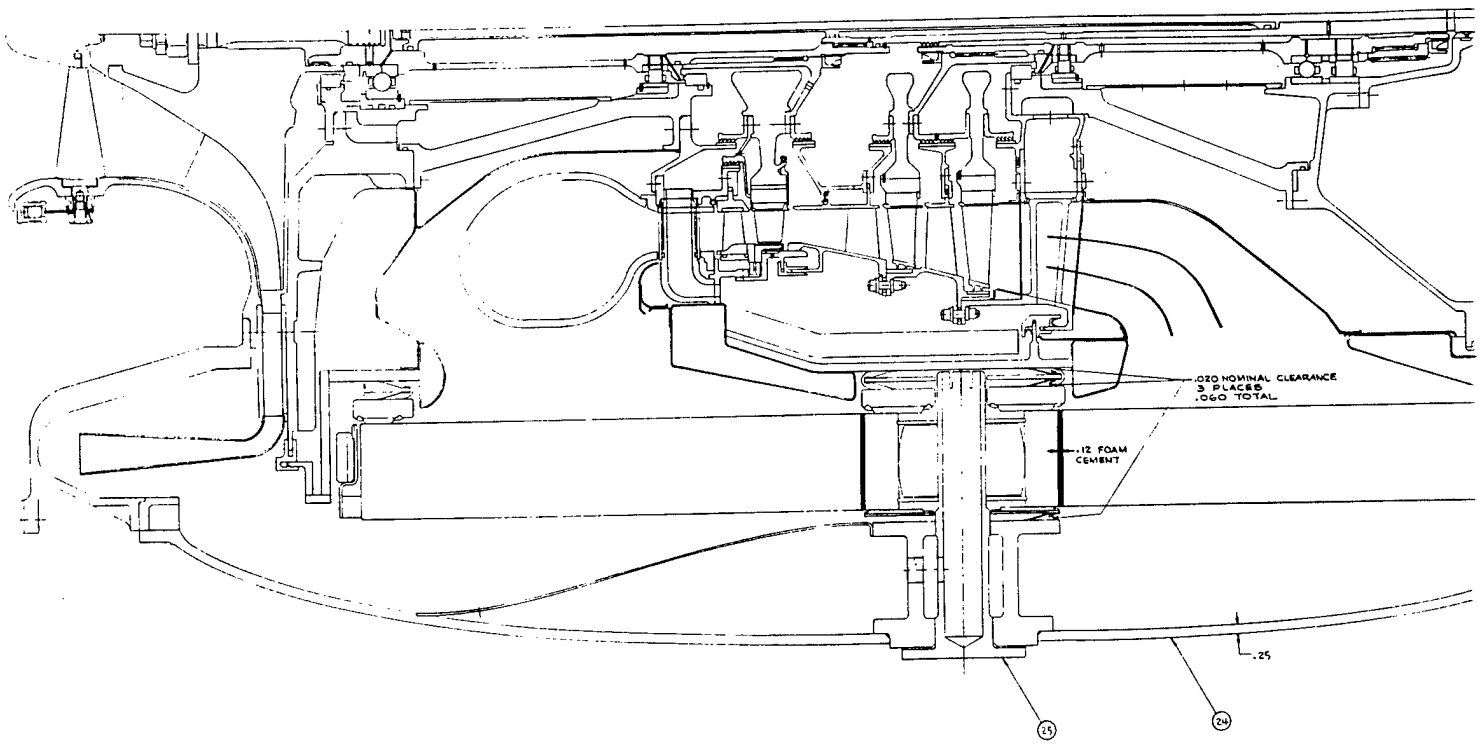

NO.	PART NAME	MATERIAL	QTY
27	STRAPS	INCO 625	2
26	FLAPPER	L605 (COLD REDUCED) 17-25% OR RENE 41	2
25	SPINDLE	4140	1
24	COVER	4130	1
23	LEAF	L605 (COLD REDUCED) 17-25% OR RENE 41	2
22	LEAF SUPPORT	430 SS	2
21	LEAF HINGE	430 SS	2
20	OUTBOARD SUBSTRATE	430 SS	2
19	WEARFACE PLASMA SPRAY	75 NICKEL 25 GRAPHITE PLASMA SPRAY	2
18	OUTBOARD WEARFACE	STACKPOLE GRAPHITE GRADE 2174	2
17	LEAF	L605 (COLD REDUCED) 17-25% OR RENE 41	2
16	HEAT SHIELD	L605 (COLD REDUCED) 17-25% OR RENE 41	2
15	LEAF HINGE	INCO 625	2

NO.	PART NAME	MATERIAL	QTY
14	LEAF SUPPORT	INCO 625	2
13	LEAF SUPPORT BUMPERS	INCO 625	2
12A&C	LEAF SUBSTRATE	INCO 625	2
11	WEARFACE SUBSTRATE	CORNING LITHIUM ALUMINUM SILICATE 9458	2
10	WEARFACE CEMENT	CORNING FOAMING CEMENT	2
9	INBOARD WEARFACE	HOT PRESSED ZINC OXIDE	2
8	GEAR	RING ROLLED SAE 1050 (TUNGSTEN CARBIDE COATED)	1
7	GEAR RUBBER	GENERAL ELECTRIC RTV106	1
6	GEAR ADAPTER	430 SS	1
5	BEARING SNAP RINGS	INCO 718 RC 36-46	2
4	HUB BEARING	PURE CARBON GRADE P5N-33	2
3	DISC HUB	CORNING LITHIUM ALUMINUM SILICATE 9458	2
2	HUB CEMENT	CORNING FOAMING CEMENT	2
1	DISC MATRIX	CORNING ALUMINUM SILICATE 9461	1

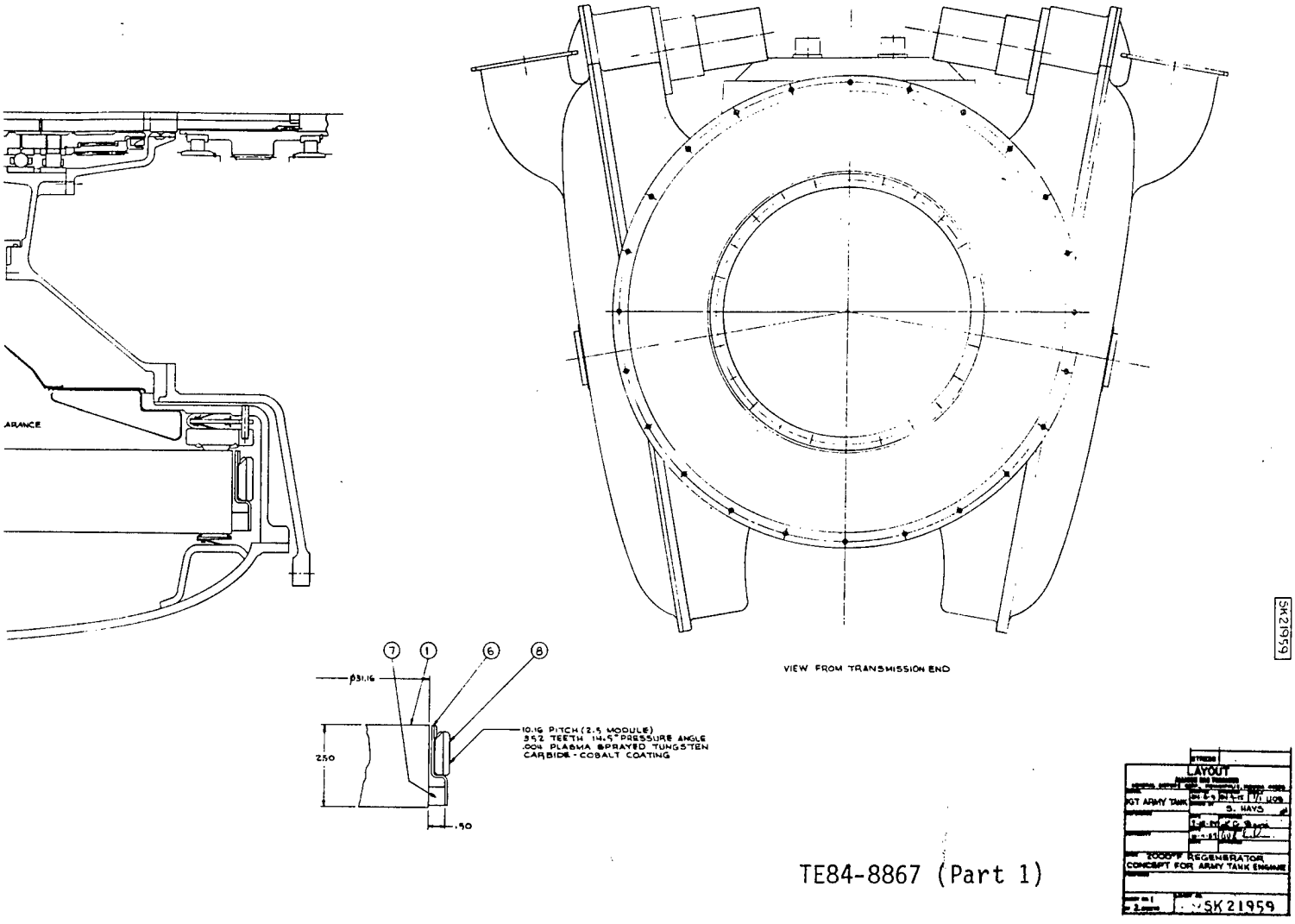

TE84-8867 (Part 1)

Figure 3-50. Conceptual Layout Drawing of Selected Regenerator Design (Part 1 of 3)

2 of 2

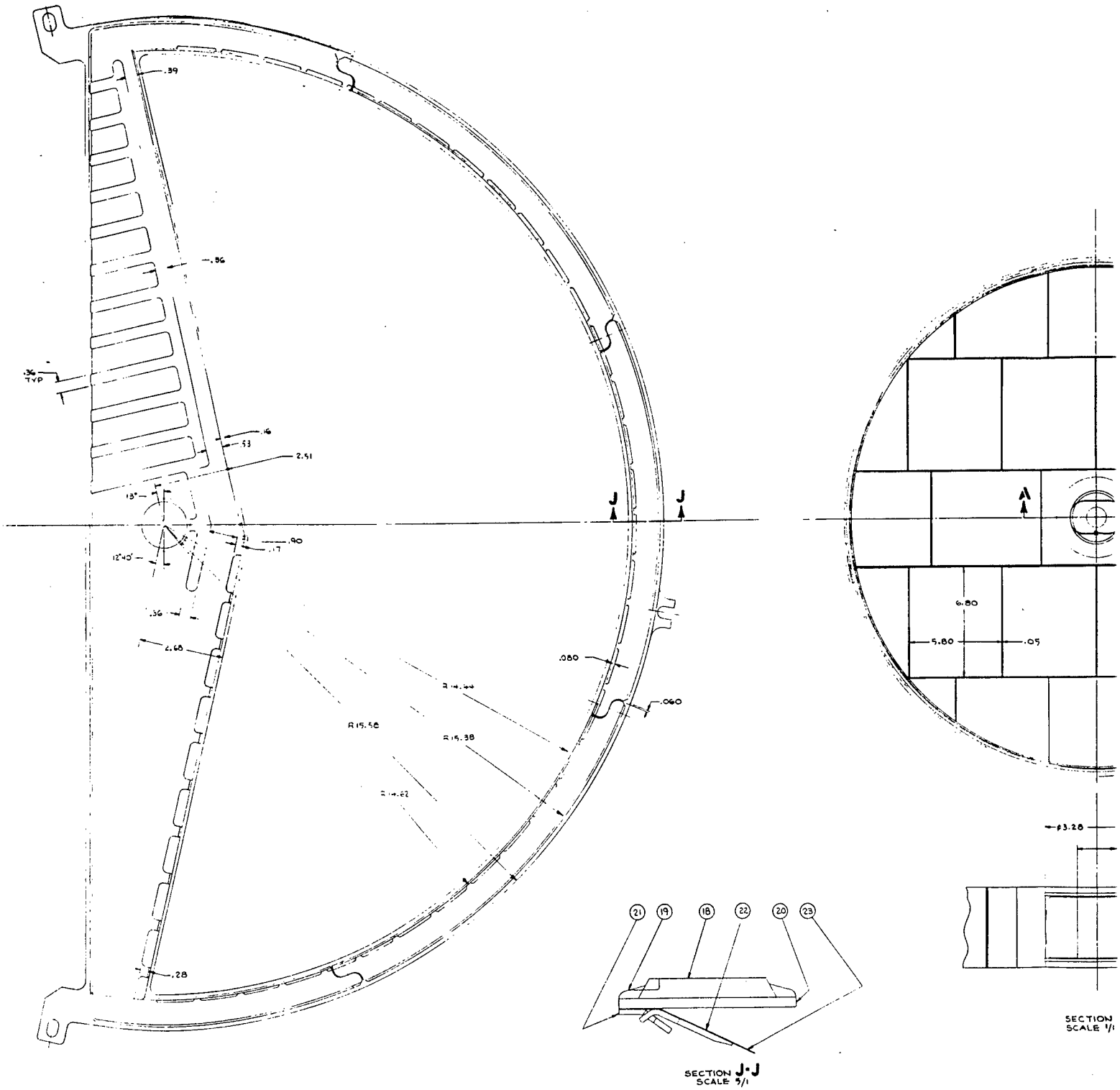
.39
.86
.36 TYP
.16
.53
2.51
13°
12°40'
.31
.90
.17
.36
2.68
.080
.060
R15.58
R15.38
.28
J
J
6.80
5.80
.05
A
A
ø3.28
21
19
18
22
20
23
SECTION J-J
SCALE 5/1
SECTION
SCALE 1/1

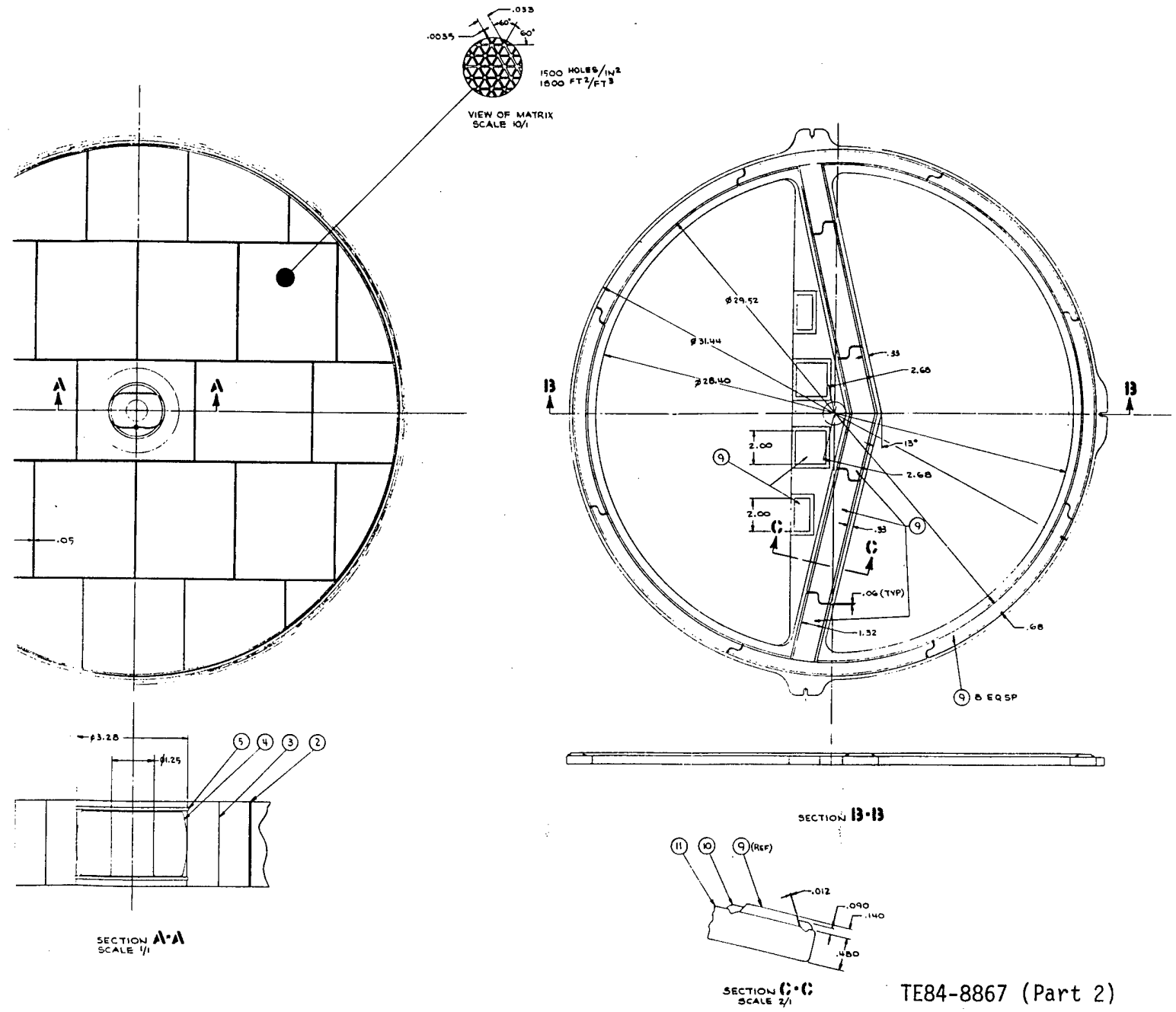

Figure 3-50. Conceptual Layout Drawing of Selected Regenerator Design (Part 2 of 3)

2 of 2

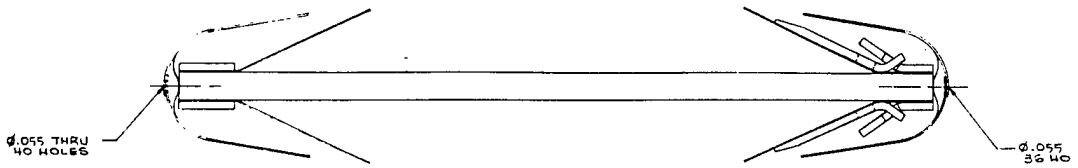

SECTION K-K
SCALE 5/1

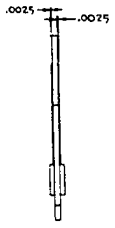

SECTION E-E
SCALE 1/1

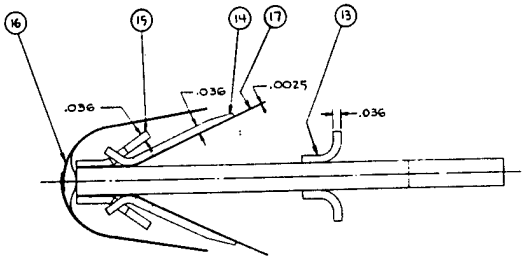

SECTION F-F
SCALE 5/1

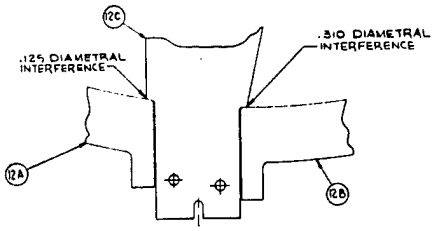

SCALE 1/1

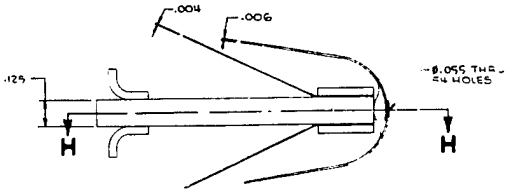

SECTION D-D
SCALE 5/1

SECTION H-H
NO SCALE
TYPICAL FOR SECTIONS F-F & K-K

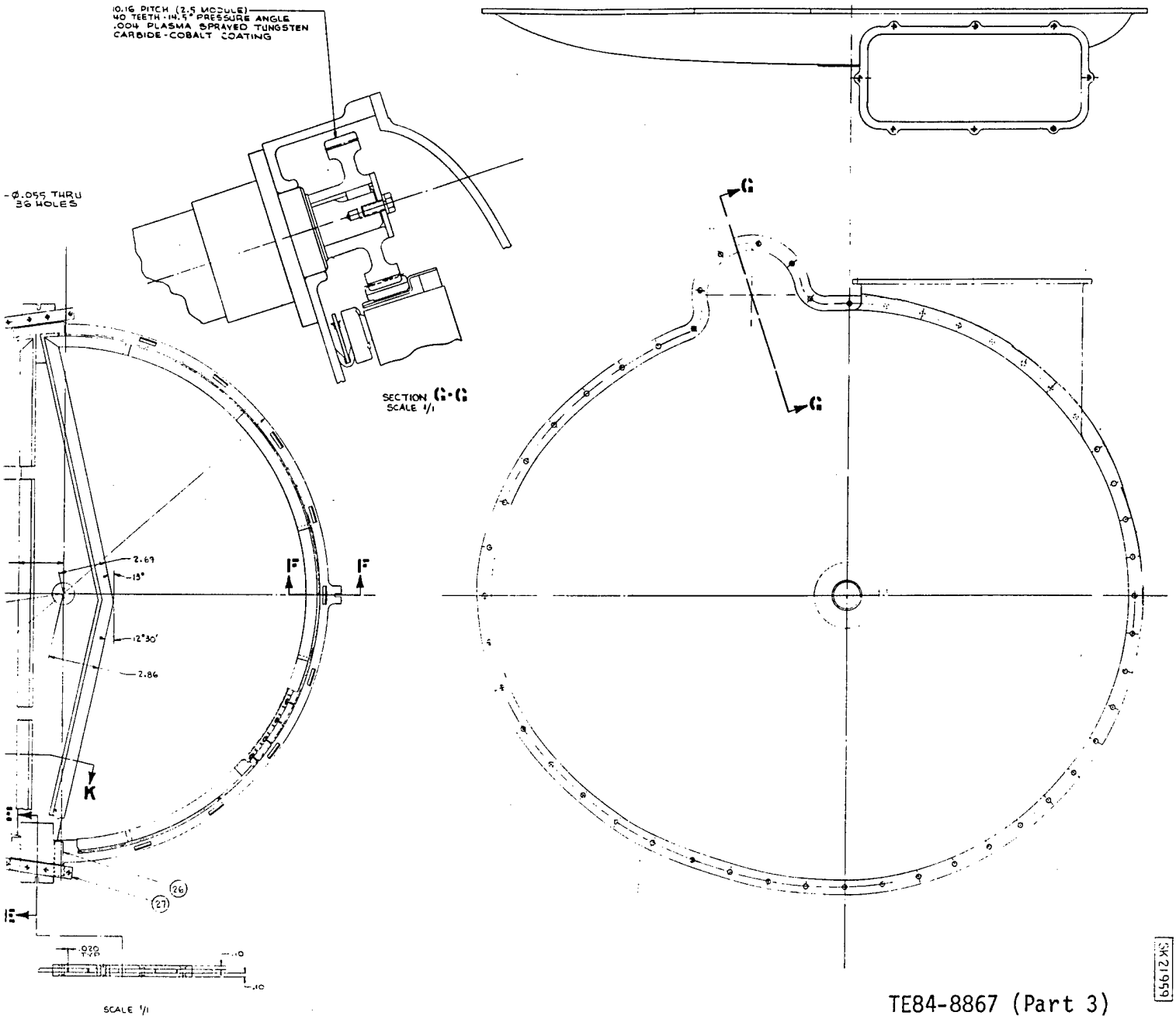

Figure 3-50. Conceptual Layout Drawing of Selected Regenerator Design (Part 3 of 3)

2 of 2

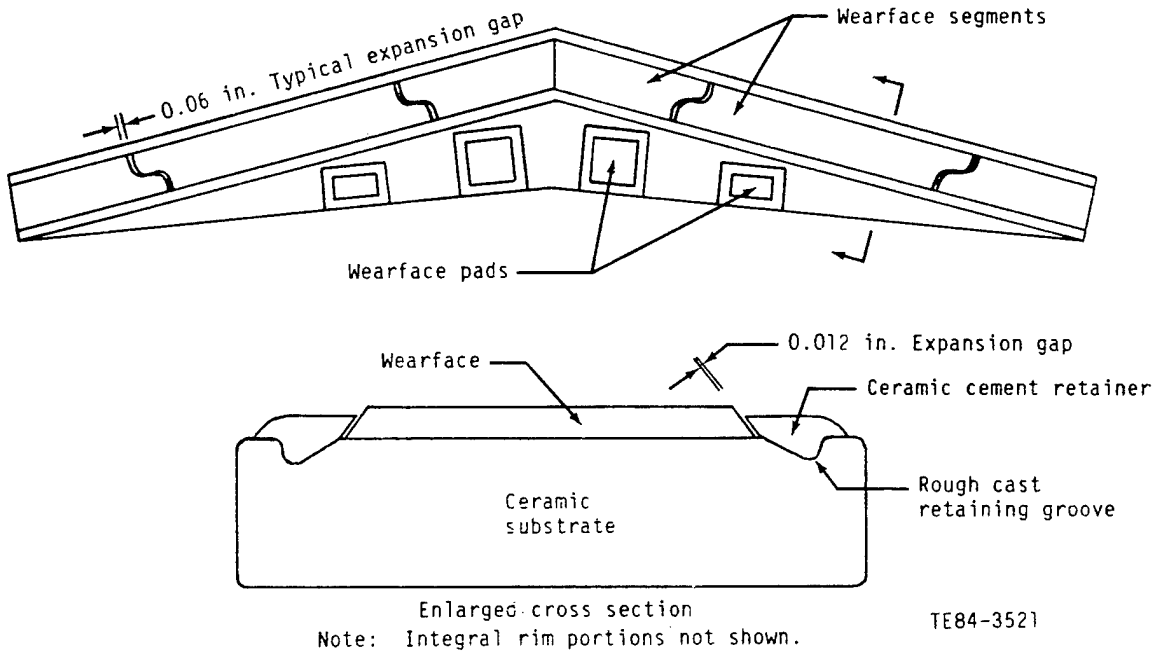

Figure 3-51. Wearface Attachment to Ceramic Seal Crossarm Substrate with Near Zero Expansion

then

$$\frac{L_2}{W_2} \times 100 = \% \text{ leakage}$$

The equation treats the separate sources of seal leakage as shown. For the present we see no more exact way to estimate leakage.

3.3.2. Seal Loading and Wear. Calculations were made to define seal loading grooves in the outboard seal wearface and to locate sealing leaf bearing points to establish the desired seal loading. The seal load was set at 6 lb per lineal inch at a 4:1 pressure ratio, which is typical of the Model 404 engine and ensures adequate low-speed seal loading in the 9:1 pressure ratio design. Seal loads will increase to 17 lb per lineal inch at a 9:1 pressure ratio. Loads of this magnitude have been tested without adverse effects in the Model AGT 100 program. Allison is confident that this load will not result in unacceptable seal wear, because the tank duty cycle has negligible time at higher speeds and pressures. Allison believes that the seals can readily pass the 1,000 hr qualification test, which has 400 hours of full speed full pressure operation. Porting to decrease carryover airflow losses was considered but not included because porting would increase the seal load significantly, undesirably, and unavoidably.

3.3.3. System Size Effects. Table 3-3 compares the effect on total propulsion system size of cooled metal regnerator seals and uncooled ceramic seals for 2000°F operation and a metal seal for 1670°F operation.

All three systems employ the same regenerator disk used for the AIPS Phase II demonstrator enigne. The 2000°F regenerators use the Allison AIPS Phase I engine cycle that requires additional power turbine cooling. Incremental propulsion system compartment length changes in inches that result from the various features are shown with the 1670°F AIPS Phase II demonstrator engine as a base. Volume changes in cubic feet are also shown. The 4.6-in. reduction in compartment size attributed to higher regenerator inlet temperature and higher technology employed in AIPS Phase I includes a reduction due to downsizing the Phase I propulsion system and fuel from 1,500 hp to the same 1,200 hp as the Phase II demonstrator. Restudy of ancillary packaging might provide further size reduction. The 2000°F cooled metal seal provides slightly more reduction in compartment length (3.6 in.) and volume (6.1%) than the uncooled ceramic seal, which provides 2.9 in. length reduction or 4.9% volume reduction. Lower SFC provided by the uncooled ceramic seal is more than offset by its added thickness and blockage. Figure 3-52 shows how the ceramic seal required a thicker ceramic structural substrate together with added blockage from the overhung leaf and an additional static sealing leaf. The overhung leaf results from the leaf location required to maintain proper seal load when the leaf must be mounted on a separate metal structure from the ceramic structure carrying the wearface. Both 2000°F regenerator designs result in small but significant reduction in system volume over the 1670°F AIPS Phase II demonstrator, and both have significant development risks and disadvantages. Table 3-4 lists the advantages, disadvantages, and risks of the cooled metal 2000°F seal versus the uncooled ceramic 2000°F seal.

Table 3-3. Effect of Regenerator Inlet Temperature with Associated Turbine Cooling Technology and Regenerator Seal Material on Total Propulsion System Size

	AIPS Phase II	AIPS Phase I with Phase II regen disk	AIPS Phase I with Phase II regen disk
Maximum regenerator inlet temperature--°F	1670	2000	2000
Seal structural material	Metal	Metal	Ceramic
SFC at 17 mph (719-729 hp)	0.396	0.370	0.345
Seal cooling air lost to turbines--%	0	4	0
Power turbine cooling air--%	2	4	4
Block cooling heat loss to ambient air--Btu/min	310	381	381
Compartment length changes in in. due to the following:			
Higher temp and technology (SFC)	0	-4.6	-4.6
Ceramic seal blockage	0	0	+0.3
Ceramic seal (thickness)	0	0	+1.4
Seal cooling (SFC effect)	0	+1.0	0
Block cooling	0	Negligible	Negligible
Total change	0	-3.6	-2.9
Change in compartment volume			
% (based on length only)	0	-6.1	-4.9
ft^3 (based on length only)	0	-8.6	-6.9
% (based on length, height & width)	0	-11.4	-10.2
ft^3 (based on length, height and width)	0	-16.0	-14.3

Table 3-4. Comparison of Cooled Metal and Uncooled Ceramic 2000°F Seals

	Advantages	Disadvantages and risks
Cooled metal seal	1. less propulsion system volume--but only by 1.3% 2. proven wearface attachment 3. requires 40% less sealing area 4. single static leaf seal	1. complication of cooling fins and shield 2. complication of load control valves 3. complicaion of cooling shut-off valve 4. requires more fuel 5. heavy load on cold seal cross arm at low speed 6. difficult to maintain flatness in manufacture
Uncooled ceramic seal	1. no cooling air required 2. no cooling fins or shield 3. less fuel required 4. no valving required 5. better flatness for sealing 6. no heavier load on cold seal	1. unproven wearface attachment 2. larger propulsion system volume by 1.3% 3. requires 40% more sealing area 4. additional static seal leaf required

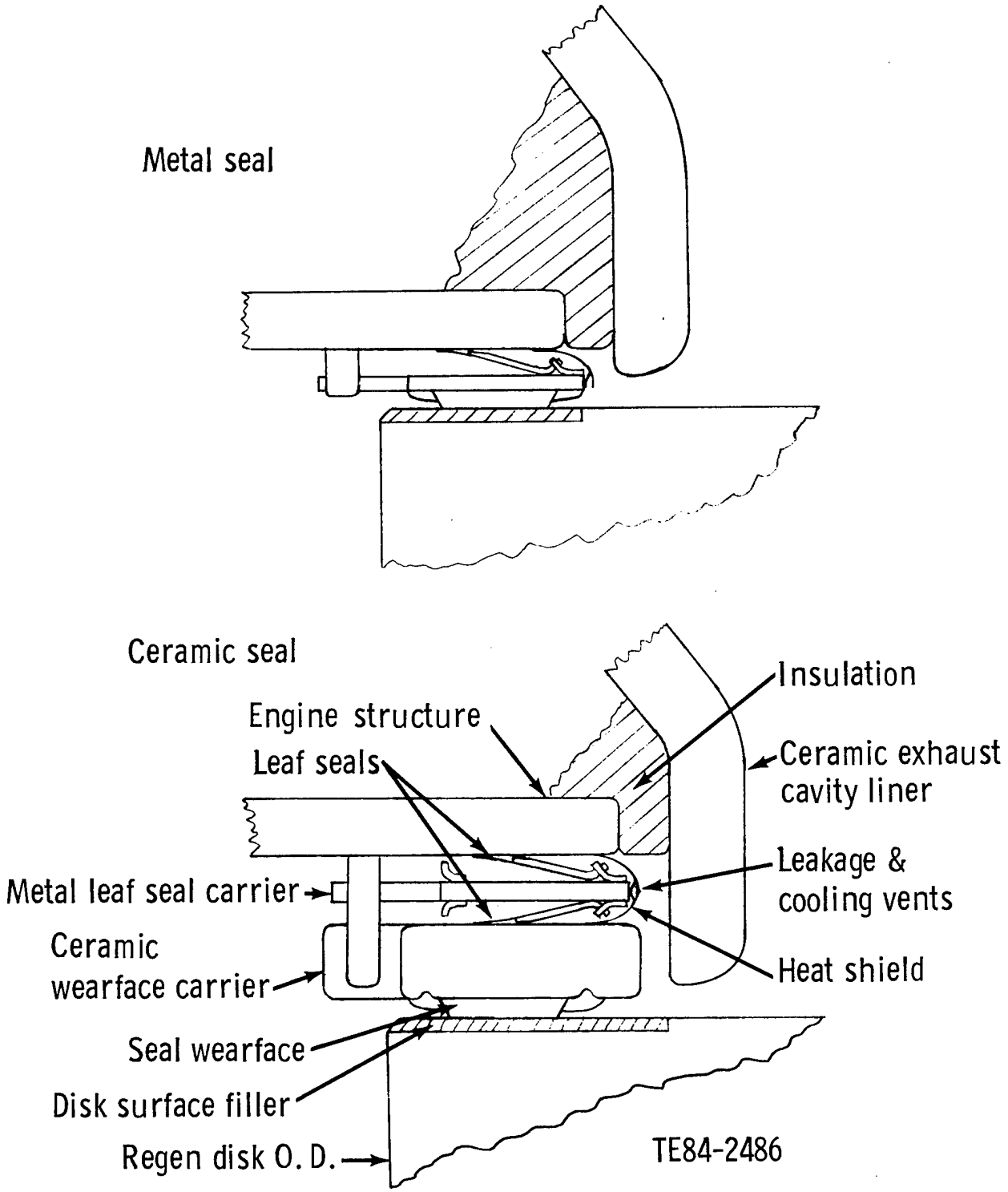

Figure 3-52. Comparison of Rim Cross Sections of Metal and Ceramic Seal Concepts

The cooled metal seal provides slightly more reduction in system volume than the ceramic seal but not sufficient to justify the complication and risk of adding cooling fins, loading groove valves, and cooling shutoff valves. The ceramic seal was selected for the conceptual design for these reasons.

The relatively small 4.9% reduction in volume provided by higher temperature and technology vindicates Allison's selection of the AIPS Phase II demonstrator design.

The foregoing analysis does not consider a last minute unanalyzed cooled seal concept discussed in section 3.1.1.3 that would probably eliminate the requirement for load control valves. It would still be difficult to maintain flatness in manufacture, and the seal might suffer thermal distortion and leakage due to the cooling.

4.0. CONCEPTUAL LAYOUT FEATURES

The conceptual layout drawing, Figure 3-50, shows the selected design with ceramic hot side seals. The regenerator design is shown incorporated into the Allison Model 335-D1 engine, proposed for the TACOM AIPS Phase II program, to depict a typical installation.

Design features are as follows:

- An extruded triangular Corning 9461 aluminum silicate (AS) ceramic disk (item 1 in Figure 3-50) composed of rectangular blocks cemented together with a solid lithium aluminum silicate (LAS) hub. Alternatively, with suitable placement, pie sector blocks might be used. The matrix has 1500 holes/in.^{2} and 3.5 mil thick walls. The AS material would suffice for all steady-state operation and about 1000 accelerations. Further development is required for full cyclic capability. Cyclic life would be adequate if maximum steady-state inlet temperature were 1800°F instead of 2000°F.

- Room temperature vulcanizing silicone rubber General Electric RTV 106 drive gear attachment with 600°F capability for initial development. Improvement for 660°F capability is required and is in process (item 7).

- Ring gear plasma coated with tungsten carbide for wear resistance (item 8).

- Gear tooth size is adequate to maintain engagement under all conditions.

- Oxidation resistant graphite hub bearing (item 4) is barrel shaped to allow disk position to be established by the seals.

- Conventional Allison cold side seal with stainless steel substrate, welded leaf, and oxidation resistant graphite wearface (items 18-23).

- Ceramic substrate hot side seal (LAS) with hot-pressed and sintered zinc oxide wearface and cement retainers (items 9-11). Proven cooled metal seals with plasma sprayed nickle oxide/calcium flouride wearface could be used if inlet temperature was lowered to 1800°F.

- Inco 625 leaf carrier with cobalt alloy L605 leaves (items 12-17).

- o Seals are primarily pressure-loaded to 17 lb per lineal inch at maximum pressure but also experience an initial spring load of 3 lb per inch from the leaves.

- o Seals are positioned and restrained from rotation by pins in the engine block and regenerator covers mating with radial slots in the seals. This leaves the seals free to translate in the axial direction for sealing.

- o The net outboard differential pressure load on the regenerator disk is reacted by the rim of the cold side seal against the cover.

- o Cooling air is ducted to the leaf carrier through the disk support shaft that also supplies cooling to the hub bearing.

- o Even flow distribution of entering air is provided by a baffel in the cover (item 24). Turbine exit vanes provide even flow distribution of exhaust gas.

- o The disks are driven at a constant 12 rpm by hydraulic motors requiring about 2.2 hp maximum for each during startup only. After warmup, power required should not exceed 1.1 hp.

5.0. MATERIALS

The list of materials presented in Table 5-1 is repeated with item numbers in Figure 3-50.

The disk matrix, gear mounting rubber, and seal wearface materials may change during development although the parts listed above should suffice for 50 to 500 hours of typical operation. Anticipated changes include the following:

- o Disk matrix--Allison expects the development of new materials with higher temperature capabilities.

- o Gear mounting rubber--modifications in single-component, room-temperature vulcanizing silicone rubber are underway at the China Lake Naval Weapons Center. The modifications are expected to provide a 780°F intermittent capability in lieu of the current 600°F limit.

- o Inboard seal wearface--test results may show the need for small (5-10%) additions of tin oxide for improved wear and of strontium flouride for lower friction.

6.0. DEVELOPMENT AND TEST PLAN

A follow-on development and test plan for the proposed high pressure ceramic regenerator design is presented in three phases as shown in Figure 6-1. Each phase can be considered a separate entity except for the Corning material and process development work and cost, which is cumulative. Corning fully supports the plan and provided a work statement, schedule, and preliminary cost figures covering their part of the plan.

Table 5-1. Regenerator Materials

Part name	Material
Regenerator disk	
Disk matrix	Extruded Corning 9461 aluminum silicate
Hub cement	Corning foaming cement
Disk hub	Corning 9458 lithium aluminum silicate
Hub bearing	Pure carbon, grade PBH-33
Bearing retaining rings	Inco 718, R_c 36-46
Ring gear adapter	430 stainless steel
Gear mounting rubber	General Electric RTV 106
Ring gear	Ring rolled SAE 1050, tungsten carbide coated
Inboard regenerator seal	
Seal wearface	Hot-pressed and sintered zinc oxide
Wearface cement	Corning foaming cement
Wearface substrate	Corning 9458 lithium aluminum silicate
Leaf substrate and details	Inco 625
Leaf and heat shield and flapper	L-605 cold reduced 17-25% or René 41
Outboard regenerator seal	
Seal wearface	Stackpole graphite 2174
Wearface plasma spray	75 nickel/25 graphite composite
Substrate, leaf and details	430 stainless steel
Regenerator cover	SAE 4130
Disk mounting spindle	SAE 4140

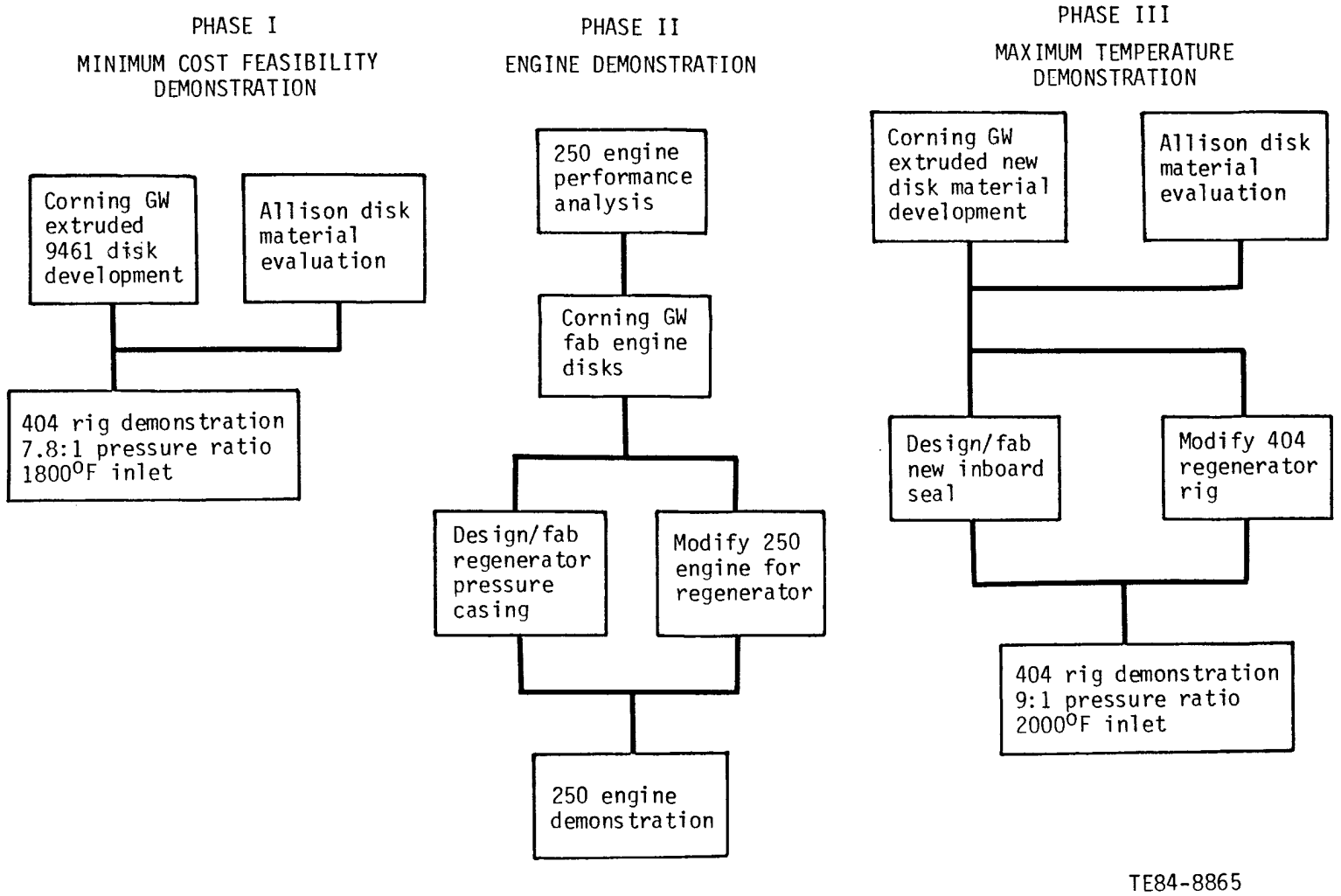

Figure 6-1. Development and Test Plan for Proposed High Pressure Ceramic Regenerator

A 25-in. diameter disk has been selected as the test vehicle over the design study 32-in. disk. This results in a considerable cost saving that is discussed in the following paragraphs. It should be noted that the objective of the development and test plan is "proof of concept." Other longer term objectives are not addressed in this plan. Cost figures are preliminary estimates in 1984 dollars and are not contractually binding.

Principle features of the proposed regenerator development and test plan are summarized in Table 6-1. A schedule is shown in Figure 6-2.

6.1. Phase I

This phase presents the lowest cost and shortest time to demonstrate "proof of concept" of the proposed high pressure regenerator. Two factors make this possible. The first is the availability of Corning 9461 matrix material. This material has been extensively evaluated by Allison--in the laboratory, in test rigs, and in engines--with excellent results. The second factor is the availability of an existing Allison regenerator test rig facility and associated back-up hardware, e.g., seals. The test facility is, however, limited to 7.8:1 pressure ratio and 1800°F regenerator inlet conditions. As can be seen from Table 6-2 and Figure 6-2, Phase I costs an estimated $980,000 and the work will be completed in 21 months from go-ahead. The following work will be undertaken in Phase I.

6.1.1. Corning Disk Development.

Task 1. Demonstrate capability to extrude 1500 cells/in.^{2} and 0.0035 in. thick wall matrix in 9461 material using a small scale die.

Task 2. Demonstrate viability of extruded block bonding technique.

Task 3. Extrude blocks with 1500 cells/in.^{2} and 0.0035 in. thick wall in 9461 material using full size production die.

Task 4. Fabricate two 25-in. diameter x 3-in. wide disks for regenerator rig testing.

6.1.2. Allison Engineering Work. The following work will be coordinated with the Corning disk development and will be conducted in the Allison laboratory:

materials evaluation
- o matrix strength and modulii measurement
- o matrix leakage measurement
- o matrix subscale pressure tests
- o matrix thermal stability tests
- o matrix thermal cyclical tests

Other work that Allison will perform is as follows:

preparation of regenerator test rig
- o determine rig operating conditions and fabricate throttle plate
- o build rig and test fuel, air, control, and safety systems
- o calibrate instrumentation
- o check data transmission, storage, and combustion

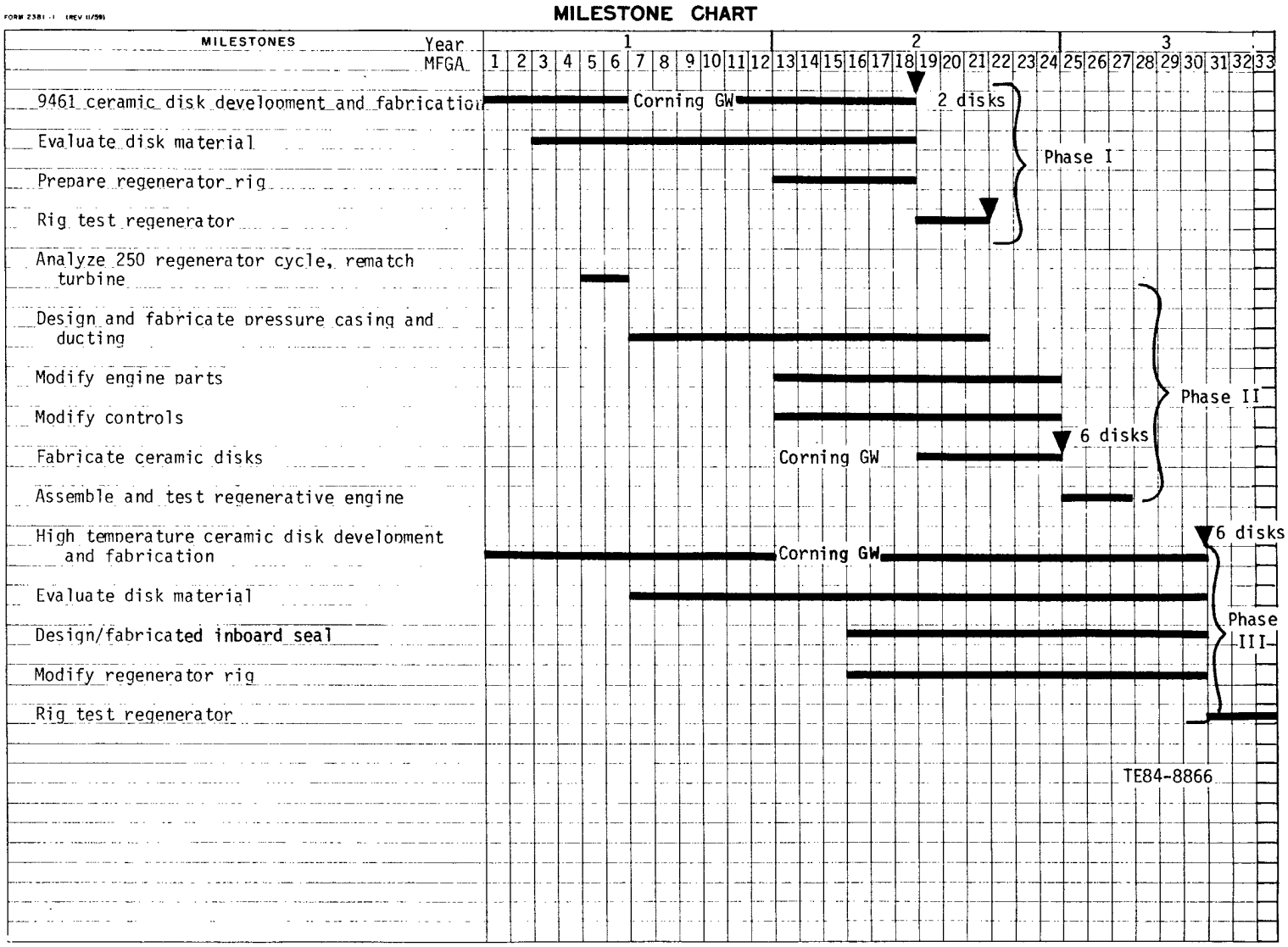

Figure 6-2. Milestone Chart of the Development and Test Plan for the Proposed High Pressure Ceramic Regenerator

Table 6-1. Development of a Regenerator for Military Engine Applications Requiring Minimum Volume and SFC

	Phase I	Phase II	Phase III
Objective	Minimum cost feasibility	Engine demonstration	Maximum temperature
Duration	21 months	26 months	33 months
Test vehicle	Existing CATE regenerator rig	250 engine	Revised CATE rig
Regenerator test conditions	1800°F 7.8:1 R_c	1200°F 8.6:1 R_c	2000°F 9:1 R_c
Features	25-in. diameter	25-in. diameter	25-in. diameter
	Extruded Corning code 9461 AS ceramic	Extruded Corning code 9461 AS ceramic	New extruded ceramic material
	3.5 mil wall 1500 cells/in.^{2} 1800 ft^2/ft^3	3.5 mil wall 1500 cells/in.^{2} 1800 ft^2/ft^3	3.5 mil wall 1500 cells/in.^{2} 1800 ft^2/ft^3
	Existing seals	Existing seals	New hot seal
	2 disks	6 disks	6 disks

Table 6-2. Development of a Regenerator for Military Engine Applications--Preliminary Cost Estimate

	Phase I	Phase II	Phase III
Corning disk development			
Task 1, 2	$390,000		
Task 3, 4	$480,000		
Task 5		$160,000	
Task 6			$230,000
Allison materials evaluation	$ 50,000		$ 30,000
Prepare 1800°F, 7.8:1 pressure ratio rig	$ 30,000		
Rig test 7.8:1 pressure ratio regenerator	$ 30,000		
Analyze 250 regenerative cycle		$ 15,000	
Design/fabricate pressure casing		$204,000 (two sets)	
Modify engine/rework parts		$100,000	
Modify/rework engine controls		$ 25,000	
Assemble/test regenerative engine		$ 40,000	
Modify regenerator rig for 9:1 pressure ratio and 2000°F inlet temperature			$160,000
Design/develop/fabricate 2000°F seal			$160,000
Rig test 9:1 pressure ratio 2000°F regenerator			$ 30,000
Cost/phase	$980,000	$544,000	$610,000

rig test regenerator
- o measure total leakage, thermal effectiveness, pressure loss and friction torque over a range of operating conditions
- o run at maximum disk stress condition to demonstrate mechanical integrity of the disk
- o evaluate results

6.2. Phase II

Phase II is an optional engine demonstration of the high pressure ceramic regenerator using an Allison 250 series engine. Phase II is not considered an alternative to either Phase I or Phase III, but is intended to complement either.

The 250 engine can be adapted to incorporate the rotary regenerator due to the unusual layout of the main components and to the external ducting of high pressure air between the compressor and the combustor. The 25-in. diameter disk used in Phase I is well matched to the 250 engine and is proposed as a twin disk arrangement for the 250-C30 or C34 models. However, a single disk could be used with the 250-C20 model as an alternative arrangement.

In this phase, the regenerator is demonstrated in the engine at a pressure ratio of 8.6:1. However, the 250 engine is not configured with part power temperature control for improved fuel economy, and therefore the regenerator gas inlet temperature will fall with load to a level well below the proposed regenerator maximum design point. The feasibility exists of incorporating power transfer into the 250 engine to improve part power fuel economy (increasing regenerator gas inlet temperatures) at some future date.

The estimated cost and time to complete Phase II is $544,000 and 27 months from go-ahead, as shown in Table 6-2 and Figure 6-2. Work to be undertaken in this phase is as follows.

6.2.1. Corning Disk Development. Task 5. Fabricate six 25-in. diameter x 3-in. wide disks in 9461 material.

6.2.2. Allison Engineering Work. Work to be performed in Phase II is as follows:

analyze engine regenerative cycle
- o develop analytical model
- o determine extent of rematching components

design and fabricate regenerator pressure casing

modify engine to accommodate regenerator and rework parts
- o redesign and rework combustor casing and air inlet ducting
- o redesign and rework turbine exhaust duct
- o design and fabricate regenerator mounting system

modify engine control system

assemble and test regenerative engine
- o measure engine performance over a range of operating conditions
- o measure regenerator thermal effectiveness and pressure loss over engine operating range
- o run temperature transients
- o evaluate results

6.3. Phase III

For this phase, the proposed regenerator design is developed and tested to the maximum pressure ratio of 9:1 and inlet temperature of 2000°F. Several new developments will therefore be required to complete this work. As explained in the feasibility study, a new matrix material with transient temperature capability to 2300°F is required. Development of a material that will meet this requirement is in progress at Corning Glass Works. Funding for this material will be found outside the proposed TACOM regenerator development and test plan although the cost of developing extrusion and block cementation technology and fabrication of disks is a part of the plan.

A new high-temperature wearface for the inboard seal crossarm is also required. Current state-of-the-art materials at Allison are limited to 1800°F. Potential new materials have been researched in the study and promising candidates have been identified. These will be evaluated in laboratory friction and wear rigs before being tested at full scale. Allison inboard (hot) seal technology with an air-cooled Inco 625 substrate is limited to a maximum operating temperature of 1800°F. For 2000°F, a ceramic substrate is required. A 20-in. diameter seal platform has been developed for the AGT 100 from lithium aluminum silicate material. Scaling this design to the larger size of the 25-in. diameter test regenerator is planned. To develop and test the regenerator, modifications to the test rig referred to in the discussion of Phase I will be required. The combustion air heating equipment will be modified to raise the regenerator air inlet and gas inlet temperatures to 660°F and 2000°F, respectively. The hot loop will require additional internal thermal insulation to maintain the pressure piping at a safe temperature level. A new, higher pressure compressed air source will be piped into the rig test cell. Some instrumentation with higher pressure and temperature ratings will also be required. Phase III will cost an estimated $610,000 and will be completed in 33 months from go-ahead. Itemized work to be performed in this phase is as follows.

6.3.1. Corning Disk Development. Task 6. Select optimum Corning new material composition to meet requirements, complete extrusion and block bonding evaluation, and fabricate six 25-in. diameter x 3-in. wide disks for regenerator rig testing.

6.3.2. Allison Engineering Work. The following work will be coordinated with the new Corning matrix material development and will be conducted in the Allison laboratory:

materials evaluation
- o matrix strength and modulii measurement
- o matrix subscale pressure tests
- o matrix leakage measurement
- o matrix thermal stability tests
- o matrix thermal cyclical tests

Other work that Allison will perform is as follows:

design and fabricate a 2000°F seal
- o ceramic substrate design and fabrication
- o develop wearface attachment
- o proof load/deflection test platform
- o leaf design, development, and fabrication
- o wearface hot press and sintering process development
- o laboratory friction and wear testing of wearface samples

modify regenerator test rig for 9:1 pressure ratio and 2000°F inlet temperature
- o install new high pressure air supply in test cell
- o increase insulation to reduce high pressure pipe temperature
- o install instrumentation with higher pressure and temperature ratings
- o modify combustion equipment to give higher air and gas temperatures

rig test regenerator to determine proof of concept
- o measure total leakage, thermal effectiveness, pressure loss and friction torque over a range of operating conditions including maximum temperature and pressure
- o run at maximum disk stress condition to demonstrate mechanical integrity of disk
- o evaluate results

DISTRIBUTION LIST

	Copies
Commander Defense Technical Information Center Bldg. 5, Cameron Station ATTN: DDAC Alexandria, VA 22314	12
Manager Defense Logistics Studies Information Exchange ATTN: DRXMC-D Fort Lee, VA 23801	2
Commander US Army Tank-Automotive Command ATTN: AMSTA-TSL (Technical Library) Warren, MI 48090	2
Commander US Army Tank-Automotive Command ATTN: DRSTA-RGE Warren, MI 48090	15
Commander US Army Tank-Automotive Command ATTN: DRSTA-TSL Warren, MI 48090	14